Mechanisms of adaptive and maladaptive plasticity after spinal cord injury

Sara Goltash

A thesis submitted in partial fulfillment of the requirements for the

Doctorate in Philosophy in Biology

Department of Biology

Faculty of Science

University of Ottawa

Table of Contents

Abstract

Spinal cord injury (SCI) is a debilitating condition that disrupts the communication between the brain and the spinal cord. Several studies have sought to determine how to revive dormant spinal circuits caudal to the lesion to restore movements in paralyzed patients. So far, recovery levels in human patients have been modest at best. In contrast, animal models of SCI exhibit more recovery of lost function. Recovery of lost function could arise from structural changes in spinal circuits following spinal cord injury. Previous work from our lab has identified dI3 interneurons as a spinal neuron population central to the recovery of locomotor function in spinalized mice. We seek to determine the changes in the circuitry of dI3 interneurons and motoneurons following SCI in adult mice. After a complete transection of the spinal cord at T9-T11 level in transgenic Isl1:YFP mice and subsequent treadmill training at various time points of recovery following surgery, we examined changes in three key circuits involving dI3 interneurons and motoneurons: 1) Sensory inputs from proprioceptive and cutaneous afferents, 2) GABAergic inputs onto sensory afferents (GABApre), 3) Central excitatory glutamatergic synapses from spinal neurons onto dI3 INs and motoneurons. Furthermore, we examined the possible role of treadmill training on changes in synaptic connectivity to dI3 interneurons and motoneurons.

Our data suggests that sensory inputs from the periphery labelled by VGLUT1^{+} to dI3 interneurons decrease transiently or only at later stages after injury, whereas levels of VGLUT1^{+} remain the same for motoneurons after injury. Levels of central excitatory inputs labelled by VGLUT2^{+} to dI3 INs and MNs may show transient increases but fall below levels seen in sham-operated mice after a period of time. Levels of GABApre boutons onto the VGLUT1+ sensory afferents that project onto to dI3 INs and MNs can rise shortly after SCI, but those increases do

not persist. However, levels of these GABApre boutons onto VGLUT1^{+} inputs never fell below levels observed in sham-operated mice. For some synaptic inputs studied, levels were higher in spinal cord-injured animals that received treadmill training, but these increases were observed only at some time points.

Changes in spinal circuitry could be maladaptive. For example, spasticity is a common consequence of SCI, disrupting motor function and resulting in significant discomfort. Spasticity may arise from maladaptive changes in spinal circuits. Current models of hindlimb spasticity are lacking, hindering the study of mechanisms or treatments of spasticity. Therefore, we have generated a novel mouse model of SCI-related spasticity that utilizes optogenetics to activate a subset of cutaneous VGLUT2+ sensory afferents to produce reliable incidences of hindlimb spasticity. To examine the efficacy of this optogenetic spasticity model, a T9-T10 complete transection injury was performed in Isl1-Vglut2^{CatCh} mice, followed by the implantation of EMG electrodes into the left and right gastrocnemius and tibialis anterior muscles. Beginning at 9 days post-injury, EMG recordings were performed during episodic optogenetic stimulation. During each recording session, an optic fiber coupled to a 470nm wavelength LED was used to deliver light pulses to the palmar surface of each hindpaw. The results of these recordings demonstrated significant increases in the amplitude of EMG responses to the light stimulus from 2 weeks post-injury to 5 weeks post-injury, indicating hyperreflexia. Interestingly, this hyperreflexia was significantly greater in the female cohort in comparison to the males. Incidences of prolonged involuntary muscle contraction and clonus were also detected through EMG and visual observation during the testing period, supporting the presence of spasticity.

Overall, the results in my thesis suggest remodelling of spinal circuits involving spinal interneurons that have previously been implicated in the recovery of locomotor function after

spinal cord injury in mice. In addition, we have developed an optogenetic mouse model that appears to reliably elicit spasticity in SCI mice and may be valuable for the study of SCI-related limb spasticity mechanisms due to the maladaptive changes within the spinal cord.

Résumé

Les lésions médullaires (LME) sont une maladie débilitante qui perturbe la communication entre le cerveau et la moelle épinière. Plusieurs études ont cherché à déterminer comment raviver les circuits spinaux dormants caudaux par rapport à la lésion pour restaurer les mouvements chez les patients paralysés. Jusqu'à présent, les niveaux de guérison chez les patients humains ont été, au mieux, modestes. En revanche, les modèles animaux de LME présentent une plus grande récupération de la fonction perdue. La récupération de la fonction perdue pourrait résulter de changements structurels dans les circuits spinaux suite à une lésion de la moelle épinière. Des travaux antérieurs de notre laboratoire ont identifié les interneurones dI3 (dI3 IN) comme une population de neurones spinaux essentiels à la récupération de la fonction locomotrice chez les souris médullaires. Nous cherchons à déterminer les changements dans les circuits des interneurones et des motoneurones dI3 suite à une LME chez la souris adulte. Après une section complète de la moelle épinière au niveau T9-T11 chez des souris transgéniques Isl1:YFP et un entraînement ultérieur sur tapis roulant à différents moments de récupération après la chirurgie, nous avons examiné les changements dans trois circuits clés impliquant les dI3 INs et les motoneurones : 1) Les entrées sensorielles de afférents proprioceptifs et cutanés, 2) les entrées GABAergique faisant contact avec des entrées sensorielles (GABApre), 3) synapses glutamatergiques excitatrices centrales des neurones spinaux sur les dI3 INs et les motoneurones. De plus, nous avons examiné le rôle possible de l'entraînement sur tapis roulant sur les modifications de la connectivité synaptique aux dI3 INs et motoneurones.

Nos données suggèrent que les entrées sensorielle provenant de la périphérie et marqué par VGLUT1+ sur les dI3 INs diminuent de manière transitoire ou seulement à des stades ultérieurs

après une blessure, alors que les niveaux de VGLUT1+ restent les mêmes pour les motoneurones après une blessure. Les niveaux d'entrées centrales marquées par VGLUT2+ dans les dI3 INs et MN peuvent présenter des augmentations transitoires, mais tomber en dessous des niveaux observés chez les souris opérées de manière fictive après un certain temps. Les niveaux de boutons GABApre sur les afférences sensorielles marquées par VGLUT1+ sur les dI3 IN et MN peuvent augmenter peu de temps après une LME, mais ces augmentations ne persistent pas. Cependant, les niveaux d'inhibition présynaptique des entrées VGLUT1+ ne sont jamais tombés en dessous des niveaux observés chez les souris opérées de manière fictive. Pour certains apports synaptiques étudiés, les niveaux étaient plus élevés chez les animaux blessés à la moelle épinière ayant reçu un entraînement sur tapis roulant, mais ces augmentations n'ont été observées qu'à certains moments.

Les modifications des circuits spinaux pourraient être inadaptées. Par exemple, la spasticité est une conséquence courante des LME, perturbant la fonction motrice et entraînant un inconfort important. La spasticité peut résulter de modifications inadaptées des circuits spinaux. Les modèles actuels de spasticité des membres postérieurs font défaut, ce qui rend difficile l'étude des mécanismes ou des traitements de la spasticité. Par conséquent, nous avons généré un nouveau modèle murin de spasticité liée aux lésions médullaires qui utilise l'optogénétique pour activer un sous-ensemble d'afférences sensorielles cutanées VGLUT2+ afin de produire des incidences fiables de spasticité des membres postérieurs. Pour examiner l'efficacité de ce modèle de spasticité optogénétique, une lésion de transection complète T9-T10 a été réalisée chez des souris Islet1-Cre+/-;Vglut2-Flp+/-;CreON-FlpON-CatCh+/-, suivie de l'implantation d'électrodes EMG dans le muscles gastrocnémiens gauche et droit et tibial antérieur. À partir de 9 jours après la blessure, des enregistrements EMG ont été réalisés lors d'une stimulation optogénétique épisodique. Au cours de chaque session d'enregistrement, une fibre optique couplée à une LED d'une longueur d'onde

de 470 nm a été utilisée pour délivrer des impulsions lumineuses à la surface palmaire de chaque patte arrière. Les résultats de ces enregistrements ont démontré des augmentations significatives de l'amplitude des réponses EMG au stimulus lumineux de 2 semaines après la blessure à 5 semaines après la blessure, indiquant une hyperréflexie. Il est intéressant de noter que cette hyperréflexie était significativement plus importante dans la cohorte féminine que chez les hommes. Des incidences de contractions musculaires involontaires prolongées et de clonus ont également été détectées par EMG et observation visuelle pendant la période de test, confirmant la présence de spasticité.

Dans l'ensemble, les résultats de ma thèse suggèrent un remodelage des circuits spinaux impliquant des interneurones spinaux qui ont déjà été impliqués dans la récupération de la fonction locomotrice après une lésion de la moelle épinière chez la souris. De plus, nous avons développé un modèle murin optogénétique qui semble provoquer de manière fiable la spasticité chez les souris LME et pourrait être utile pour l'étude des mécanismes de spasticité des membres liés à la LME en raison de changements inadaptés au sein de la moelle épinière.

Acknowledgements

I would like to express my deepest gratitude to my thesis supervisor, Dr. Tuan Bui, for your unwavering support, guidance, and encouragement throughout this research journey. Your expertise, valuable insights, and patience have been invaluable in shaping this thesis. I am truly thankful for the time and effort you invested in helping me refine my ideas and improve my work.

I would also like to extend my heartfelt thanks to my colleagues Dr. Alex Laliberte, Stephanie Gaudreau, Emine Topcu. Their camaraderie, discussions, and shared experiences greatly enriched my research experience. I am grateful for the stimulating conversations, collaborative spirit, and the sense of community that we shared during this time.

I am indebted to the entire members of the Bui lab, past and present, for providing an intellectually stimulating environment that fostered my academic and personal growth. Special thanks to Jonathan Tea, Joshua Lavigne, Tama Davis and Julie Tremblay for excellent animal care; Andrew Ochalski, and Jacky Liang for assistance with microscopy.

Iroshan Hewage, thank you for all the night shifts you've taken care of the animals. Your hard work and reliability do not go unnoticed, and we are fortunate to have you on our team.

I also want to thank my advisory committee, Dr. Emily Standen and Dr. Michael Hildebrand. I am profoundly thankful for the time and effort you invested in reviewing my work, attending committee meetings, and providing thoughtful suggestions. Your commitment to excellence and your genuine interest in my research have motivated me to strive for the highest standards in my academic pursuits.

I am also thankful to my friends and family especially my mom, dad, and my sister for their unwavering belief in me and their constant encouragement. Your moral support kept me motivated and inspired me to overcome challenges.

This research would not have been possible without the support and contributions of all these individuals. I am deeply appreciative of their impact on my academic journey.

Statement of Contributions

I would like to acknowledge that Fariba Sharmin, Phillip Pham and Tarek Jabi have helped with preliminary work to look at the changes in synaptic inputs to dI3 INs and MNs after SCI. Thank you to Shannon Stevens and Emine Topcu for analyzing the videos of the stepping function using DeepLabCut.

For the spasticity project, Alex Laliberte contributed to the conceptualization, data collection, analysis and figure preparation. Riham Khodr helped with data collection and Maude-Sophie Lockman and Émilie Gendron contributed to the data analysis.

Figures 3.1 to 3.8 in this thesis and certain textual segments incorporated within the introduction, methods, results, and discussion sections have been previously published in *Frontiers in Neural circuits* under the title 'Changes in synaptic inputs to dI3 INs and MNs after complete transection in adult mice.'

Goltash S, Stevens SJ, Topcu E, and Bui TV. Changes in synaptic inputs to dI3 INs and MNs after complete transection in adult mice. *Frontiers in Neural Circuits*, 17, https://doi.org/10.3389/fncir.2023.1176310, 2023.

List of Figures

List of Abbreviations

BDNF- Brain Derived Neurotrophic Factor

CatCh – Calcium Translocating Channel Rhodopsin

CGRP – Calcitonin Gene Related Peptides

CST – Corticospinal tract

DRG – Dorsal Root Ganglion

DI3 – Dorsal interneuron 3

EMG – Electromyography

GABA – Gamma Aminobutyric Acid

GAD – Glutamic Acid Decarboxylase

GAD 65 – GAD isoform 65

GAD 67 – GAD isoform 67

IN – Interneuron

Isl1 – Islet Lim Homeobox 1

MN – Motoneuron

PIC – Persistent Inward Current

SCI – Spinal Cord Injury

VGLUT – Vesicular Glutamate Transferase

CHAPTER 1: GENERAL INTRODUCTION

1.1 Spinal Cord Injury

Spinal cord injury (SCI) is one of several neurological injuries without any therapeutic cures in humans. Every year, SCI affects between 250,000 and 500,000 people worldwide (Bennett et al., 2022), and it has many devastating consequences on the physiological and psychological well-being of affected individuals. Symptoms depend on the level and the severity of the injury, resulting in partial or complete loss of motor, sensory or autonomic functions (Barbeau and Rossignol, 1987; Brustein and Rossignol, 1998; Bareyre et al., 2004; Cao et al., 2005; Ballermann and Fouad, 2006; Fink and Cafferty, 2016).

Most cases of SCI are due to physical accidents such as falling or vehicle-related incidents where the bones around the spinal cord are broken or pushed against the spinal cord, severely damaging nervous tissue and non-traumatic SCI accounts for 50% of all the cases (Karamehmetoğlu et al., 1997; Mathur et al., 2014; Živković and Nikolić, 2014). While neurons are readily generated and their axonal processes are highly plastic during embryonic development and postnatal stages of life, the same cannot be said about adulthood (Fink and Cafferty, 2016; Dell'Anno and Strittmatter, 2017). Neurons and their axons have limited capacity to regenerate in the adult due to low availability of intrinsic growth factors and an inhibitory growth environment (Neumann et al., 2005). After SCI, a series of responses occur such as: loss of blood brain barrier, invasion of blood cells into the lesion site and causing inflammation, cell death, demyelination, release of toxin products, and generation of fluid-filled cavity (Ghosh and Hui, 2016). These responses create an inhibitory growth environment where astrocytes transform into reactive astrocytes and produce glial scars around the lesion (Chu et al., 2014). As a result, following injury, damaged axons fail to regenerate and re-establish the original circuits, leading to the irreversible loss of the descending pathways that control movements originating from the brain

and the brainstem descending to the spinal cord (Carmel and Martin, 2014). So far, efforts to induce these descending pathways to regenerate through the injury site have met with limited success at best (Barbeau and Rossignol, 1987; Brus-Ramer et al., 2007; Carmel et al., 2010; Rosenzweig et al., 2010; Carmel and Martin, 2014; Fink and Cafferty, 2016; Martin, 2016), severely limiting the treatment of SCI in humans.

Despite the limited regenerative capacity of the central nervous system, some patients may experience some degree of recovery due to plasticity and sprouting of spared neurons (Nas et al., 2015). This plasticity may, however, also be maladaptive and lead to further complications such as spasticity and increased sensitivity to pain (hyperalgesia). Therefore, despite the presence of some form of regenerative process in the nervous system following SCI, there are currently no effective treatments that provide sustained recovery of lost function. While numerous repair strategies have been developed and tested in experimental settings (Gerasimenko et al., 2007; Kumru et al., 2010; Roy et al., 2010; Harkema et al., 2011; Angeli et al., 2014), none of these elaborated repair strategies have been successfully translated in clinical settings. Similarly, the use of therapeutic approaches such as locomotor training or electrical stimulation have shown some degree of recovery of motor function in animal models of SCI, and recently in a few patients with complete sensory/motor loss (AIS A) and complete motor loss (AIS B) where participants recovered voluntary walking in response to epidural stimulation and motor training via a brain spine interface (Lorach et al., 2023). However, a consistent and sustained recovery from application of similar approaches has yet to be demonstrated in humans. Therefore, a better understanding of the mechanisms of recovery or even secondary complications after SCI in animal models is essential to make breakthroughs in treatment of human patients suffering from SCI.

1.2 Animal models of SCI

Animal models of SCI have been tremendously helpful in understanding the anatomical and biological events involved in SCI and repair. These models provide an opportunity for researchers to determine the characteristic pattern of cell death and sparing and measurement of any demyelination, collateral sprouting, regeneration, neuroprotection and recovery of locomotor or other deficits (reviewed in Sharif-Alhoseini et al., 2017). The pattern of injury in the animal models is selected based on the aim of the researchers. For example, the contusion and/or compression model is preferred when investigating biomechanics and the pathophysiological changes after injury such as inflammation, ischemia, hemorrhagic necrosis, and central cavitation (Smith et al., 2010; Jazayeri et al., 2013; Jalan et al., 2017). On the other hand, transection models that include a partial or a complete transection of the spinal cord are useful to study the effects of scaffolds, biomaterials and neurotrophic factors, regeneration or degeneration and neuroplasticity. Even though transected spinal cords are rarely encountered in clinical practice, this model of injury has also been widely used in rodents and cats to study the role of spared neuronal circuits in recovery of locomotion after SCI (Edgerton et al., 2004; Lavrov et al., 2006; Courtine et al., 2009). In the next section, several plastic changes that take place in the spinal cord have been discussed.

1.3 Morphological changes after SCI and mechanisms of adaptation

1.3.1 Plasticity of supraspinal descending pathways

Possible morphological changes in neural circuitry following SCI that could promote recovery have been widely studied. The plasticity of spinal, brain and peripheral circuits has been observed in mammalian models of SCI after treadmill training, pharmaceutical interventions and epidural stimulations, which has led to partial or full degree of recovery (Ichiyama et al., 2005; Roy et al., 2012; Shah et al., 2013).

The corticospinal tract (CST) originating from the motor cortex is the major pathway involved in controlling voluntary movements (Carmel and Martin, 2014). Following an incomplete SCI in humans or a hemisection in animal models, the descending CST fibers are spared and a combination of pharmacotherapy, treadmill training and epidural stimulation can induce reorganization of spared fibers and improve functional recovery (van den Brand et al., 2012; Angeli et al., 2014b). However, long-distance reorganization of descending fibers is minimal in the absence of any type of intervention (Bradbury et al., 2002; Kim et al., 2004; K. Liu et al., 2010). But the uninjured CST can undergo spontaneous short distance sprouting after incomplete SCI with or without intervention (Thallmair et al., 1998; Cafferty et al., 2010; K. Liu et al., 2010). This sprouting includes increased CST axon crossing of the midline (Ghosh et al., 2009).

When the CST is damaged, the rubrospinal and reticulospinal tracts aid with functional recovery (May et al., 2017; Asboth et al., 2018). The reticulospinal tract descending from the reticular formation in the brainstem and terminating in the spinal cord drives the initiation of locomotion and postural control (May et al., 2017). Their contribution to functional recovery after spinal cord injury may arise from plasticity in these subcortical descending tracts. For example, after a lateral hemisection in adult rats, reorganization of reticulospinal tracts have been observed (Zörner et al., 2014). Using anterograde and retrograde tracings, it was observed that more reticulospinal fibers from the intact side crossed the spinal midline at cervical and lumbar regions.

1.3.2 Plasticity of spinal interneurons

Many populations of spinal interneurons mediate a diverse set of roles including modulation of sensory, motor and autonomic functions (Zholudeva et al., 2021). Amongst these spinal interneurons are propriospinal neurons that are located in the spinal cord and have short or long axon projections, which can span multiple segments of the spinal cord and project onto other

interneurons in the spinal cord (Jankowska et al., 1974, 1983; Cowley et al., 2021). The ascending pathways that they form enable some of these propriospinal neurons to relay information from pain afferents (Szentágothai, 1964) and proprioceptors (Jankowska, 1992) to supraspinal centres. Descending circuits formed by propriospinal neurons transmit descending motor commands from supraspinal and spinal regions. However, propriospinal neurons do not simply transmit information up and down the spinal cord. These neurons are integrated in circuits of central pattern generators, which is associated with rhythmic motor function such as locomotion (Ballion et al., 2001; Jordan and Schmidt, 2002). They also integrate sensory feedback to mediate and coordinate rhythmic motor outputs (Conta and Stelzner, 2004; Cowley et al., 2008, 2021). Recent work where ascending propriospinal neurons in the lumbar cord were inactivated highlights their critical role in the proper synchronous coordination of the hindlimbs and forelimbs in a number of various movements (Pocratsky et al., 2020).

Propriospinal neurons have also been shown to be involved in recovery of respiration (Jensen et al., 2019), autonomic function (Michael et al., 2019), and locomotor function (Laliberte et al., 2019) after SCI. These neurons play a major role in recovery of locomotor function by relaying inputs from spared descending inputs onto locomotor networks or by forming detour circuits that reroute supraspinal commands around the lesion after incomplete SCI (Bareyre et al., 2004). After a midthoracic dorsal transection of CST axons in rats, lesioned CST axons spontaneously sprouted collaterals into the cervical gray matter and made new connections with both short and long propriospinal INs (Bareyre et al., 2004). The CST projections onto short propriospinal INs, which did not bridge the lesion were lost 12 weeks post-injury but the CST contacts that were made with long propriospinal INs crossing the lesion were maintained. Furthermore, the number of direct contacts between long propriospinal axons terminals and

motoneurons were doubled 8 weeks after the hemisection. The maintenance of these intraspinal pathways from cervical to lumbar segments following the dorsal hemisection was verified by pseudorabies virus tracing and their functionality was supported by EMG signals in the hindlimb evoked by intracortical microstimulation. As a result of these new connections made post-injury, improvements in locomotor function were observed in rats (Bareyre et al., 2004; van den Brand et al., 2012).

Using a staggered hemisection paradigm, propriospinal neurons have been shown to form detour circuits around the lesion to provide an alternative flow of motor commands from supraspinal axon collaterals onto lumbar circuits for locomotion (Courtine et al., 2008; Cowley et al., 2008; Martinez and Rossignol, 2013; May et al., 2017). In one adult mouse study, an initial hemisection was made to sever all ipsilateral descending pathways on one side at T12 and another hemisection was made on the contralateral side at T7 to disrupt the spared descending pathways contralateral to the first hemisection (Courtine et al., 2008). Restoration of locomotor function in these mice was associated with evidence of connectivity between spared lumbar circuits with propriospinal INs in the intervening region between the lesions (T8-T10) while showing no direct connectivity between supraspinal locomotor nuclei and lumbar circuits (Courtine et al., 2008).

Functional recovery after incomplete SCI can also be increased by spared descending motor pathways besides the CST. After a complete transection of reticulospinal tract axons in rats using a staggered model where a hemisection at T10 was followed by a contralateral hemisection at T7, it was observed that reticulospinal axons formed new contacts with propriospinal INs and locomotory recovery was observed (May et al., 2017). Similarly, a severe contusion of the spinal cord at T8/T9 (Asboth et al., 2018) or a unilateral cervical hemisection in adult rats was shown to increase reticulo-propriospinal contacts from damaged reticulospinal axons (Filli et al., 2014).

Therefore, remodelling of reticulospinal pathways involving propriospinal INs also play an important role in recovery of locomotion after SCI.

While the above studies have shown a partial or full recovery of locomotion after SCI, the formation of detour circuits around the lesion isn't possible after complete SCI nor axonal regeneration over a long distance. However, animal models of complete SCI have also demonstrated some level of locomotor recovery, which is believed to involve plasticity in spinal circuits below the level of injury and ability of propriospinal neurons to communicate within lumbar segments (Bareyre et al., 2004; Martinez et al., 2009; Rossignol and Frigon, 2011). In the absence of descending inputs in complete SCI models, activation of sensory feedback has been shown to play a great role in recovery of locomotion (Bouyer and Rossignol, 2003; Lavrov et al., 2008; Sławińska et al., 2012; Takeoka et al., 2014; Takeoka and Arber, 2019; Takeoka, 2020). This recovery has been attributed to propriospinal INs (Kathe et al., 2022) that integrate sensory feedback and relay this feedback to the spared locomotor networks across the lumbar spinal cord. One example of these propriospinal INs are dI3 INs, which integrate cutaneous and proprioceptive inputs and have been shown to be involved in recovery of locomotion following complete SCI in mice (Bui et al., 2016).

1.3.3 Changes in intrinsic properties of spinal neurons

Changes in the intrinsic properties of spinal neurons following SCI could change neural activity and possibly motor output. Intrinsic properties of spinal neurons are finely tuned to ensure proper recruitment of muscles by spinal circuits during voluntary contractions (Kernell and Kernell, 2006). Several changes in the intrinsic properties of spinal neurons have been observed after SCI but the results in different animals are contradictory. For example, the resting membrane potential of lumbar motoneurons was observed to be depolarized in chronic SCI rats (Beaumont

et al., 2004) but the membrane potential of motoneurons was unchanged in spinal transected cats (Cope et al., 1986; Munson et al., 1986; Hochman and McCrea, 1994). Motoneuron hyperexcitability in sacral motoneurons due to the activation of large persistent inward currents (PICs) has been reported in rats with acute SCI (Harvey et al., 2006). Other experiments have reported transient increases in input resistance and rheobase current combined with more hyperpolarized resting membrane potential and decreased action potential amplitudes in mouse motoneurons 4 weeks after lateral hemisection of the spinal cord (Rank et al., 2015). However, these intrinsic properties seemed to return to normal values 10 weeks after the injury (Rank et al., 2015). Finally, involuntary muscle contractions have been linked to spasticity or hyperreflexia after SCI and linked to alterations of the excitability of spinal neurons (Nielsen et al., 1995; Carlin et al., 2000; Lee and Heckman, 2001; Li and Bennett, 2003; Bennett et al., 2004; Gorassini et al., 2004 ; Pandyan et al., 2005; Theiss et al., 2007).

Recently, SCI has been demonstrated to trigger plastic changes in both sensory afferent pathways and serotonergic modulation which enhance the activation and excitation of Shox2 interneurons (Garcia-Ramirez et al.,2021). The whole-cell patch-clamp recordings conducted on Shox2 INs indicated minimal changes in their intrinsic excitability properties after a complete transection of T8-T10 cord in adult mice. However, in uninjured mice, afferent stimulation elicited a combination of excitatory and inhibitory input to Shox2 INs, which shifted predominantly towards excitatory signals following SCI. Shox2 INs exhibited varying responses to serotonin in a concentration-dependent manner under uninjured conditions. However, post-SCI, 5-HT primarily induced depolarization in Shox2 INs. While 5-HT7 receptors were found to mediate excitatory effects on Shox2 INs in both uninjured and SCI mice, the activation of 5-HT2B/2C receptors amplified the excitability of Shox2 INs specifically after SCI. These data suggests that

SCI alters the sensory afferent input pathways to Shox2 INs and modifies the modulation of Shox2 INs by 5-HT, resulting in an enhancement of excitatory responses (Garcia Ramirez et al.,2021).

In another experiment, firing characteristics of bursting deep dorsal horn (DDH) neurons were characterized after a complete T10 transection in adult mice (Thaweerattanasinp et al., 2020). During the chronic stage, DDH neurons exhibit an overall increase in excitability and demonstrated varying responses to serotonin and NMDA receptor agonists. During dorsal root stimulation, DDH neurons displayed increased responsiveness with the duration of bursts doubling after chronic injury. Also, application of zolmitriptan, which is a $5HT_{1B/1D}$ receptor agonist, generated a stronger overall suppressive effect, while the facilitative effects of NMDA were comparatively weaker. Furthermore, it was observed that DDH neuron activity commenced before ventral root output, and the firing rates of DDH interneurons were associated with the integrated, sustained ventral root output. These findings indicate the potential contribution of bursting DDH neurons to muscle spasms following spinal cord injury, suggesting a role in modulation by 5-HT inhibition (Thaweerattanasinp et al.,2020). The results of these experiments suggest that changes in intrinsic properties of spinal neurons can have beneficial or detrimental effects on the recovery of motor activity following SCI.

1.3.4 Changes in neurotransmitter function after SCI

1.3.4.1 Glutamate

In addition to structural plasticity that takes place in descending inputs, sensory afferents and neural circuits after SCI, plasticity related to neurotransmitters have also been demonstrated (Kapitza et al., 2012; Khalki et al., 2018; Bertels et al., 2022). In the nervous system, the amino

acid glutamate is considered to be the major excitatory neurotransmitter (Fonnum, 1984; Watkins, 2000) and the nervous system utilizes different transporters such as VGLUT1, VGLUT2 and VGLUT3 to release glutamate at the synaptic cleft. In the spinal cord, VGLUT1 is selectively expressed in central boutons of proprioceptors and low threshold mechanoreceptors while excitatory glutamatergic boutons from central neurons are labelled by VGLUT2 except for corticospinal inputs that are labelled by VGLUT1 (Alvarez et al., 2004).

SCI has been shown to affect the level of VGLUT1 in the spinal cord. Following multiple dorsal rhizotomies (cutting the sensory portion of the nerve) in adult rats, the level of VGLUT1 was significantly decreased in dorsal and ventral laminae of the spinal cord (Alvarez et al., 2004). Several other studies have also observed a decrease in the level of VGLUT1 following SCI. For example, Khalki et al (2018) observed changes in the density of VGLUT1 boutons to some but not all MNs after a complete transection in rats. Kapitza et al. (2012) found that SCI caused a 10-50% decrease in the density of both VGLUT1 and VGLUT2 boutons following a complete S2 sacral transection in adult rats. These prior studies focused mainly on spinal motoneurons, which are the direct interface between the central nervous system and the skeletomuscular system. However, similar changes could hypothetically occur in other spinal interneurons.

1.3.4.2 Inhibitory neurotransmitters and presynaptic inhibition in the spinal cord

The two chief inhibitory neurotransmitters in the central nervous system are GABA and glycine (Shimizu-Okabe et al., 2022). GABA is synthesized by two isoforms of glutamic acid decarboxylase enzyme (GAD 65 and GAD 67) (Esclapez et al., 1994) and binds to two different types of receptors, $GABA_A$ and $GABA_B$, on the postsynaptic membrane (Kuriyama et al., 2000). In the spinal cord, GABAergic, glycinergic and GABA and glycine co-releasing inhibitory neurons play a number of critical roles, for example regulating pain transmission, gating sensorimotor

information, and coordinating the activity of muscles based on their functional relationships (Shimizu-Okabe et al., 2022).

The transmission of sensory information to spinal neurons is under the particular control of a subset of GABAergic neurons, which we will refer to as GABApre neurons, that arise from the dI4 and dIL_A populations of spinal neurons. These neurons are directly under the influence of several supraspinal systems, segmental circuits and sensory afferents. Proprioceptive and cutaneous sensory afferents activate GABApre neurons in a tri-synaptic pathway involving sensory afferents from Aβ, Aδ or C-fibers, GABApre neurons, and excitatory spinal neurons interposed between the two (Rudomin, 1999; Hochman et al., 2010; Zimmerman et al., 2019) (Fig. 1.1). These GABAergic interneurons then release GABA, which was believed to bind to $GABA_A$ receptors on the sensory terminals and cause depolarization of the afferent also known as primary afferent depolarization (PAD) (Rudomin, 2009). Due to high concentration of chloride in primary sensory afferents, PAD causes efflux of chloride ions. For decades, it was believed that PAD was mediated through $GABA_A$ receptors found on Ia afferent terminals. However, recent studies have failed to detect $GABA_A$ receptors on Ia afferent terminals (Alvarez et al., 1996; Lucas-Osma et al., 2018; Hari et al., 2021;) and that instead, GABA binds to metabotropic $GABA_B$ receptors on the presynaptic terminal (Lucas-Osma et al., 2018; Hari et al., 2022, Metz et al., 2023). This binding of $GABA_B$ receptors on the presynaptic terminals of sensory afferents may activate intracellular signalling pathways that reduce glutamate release (such as voltage-dependent Ca^{2+} channels and GIRK channels), and thus sensory input to spinal circuits. PAD may instead originate from the binding of GABA by $GABA_A$ receptors found at or within 100μm of the nodes of Ranvier of many Ia afferents in the dorsal and ventral horn of spinal cord and would act to increase fidelity of sensory transmission, increasing the possible effects of GABApre neuron activity on sensory

transmission (Hari et al., 2022). Thus, GABApre neurons may have multiple, and possibly opposing effects such as facilitatory and inhibitory effect on sensorimotor function depending on what type of receptor they bind to.

After SCI, the loss of supraspinal descending inputs alters inhibitory synaptic transmission within the spinal cord. A number of changes associated with inhibitory transmission following SCI have been reported, including 1) changes in the size and density of presynaptic inhibitory inputs (Khalki et al., 2018) ; 2) changes in expression level of glycine and GABA receptors (Sadlaoud et al., 2020), 3) changes in GAD 65/67 levels (Tillakaratne et al., 2000, 2002) and 4) changes in neurotransmitter phenotype where a conversion of glutamatergic to GABAergic neurotransmitter phenotype was observed amongst many spinal interneurons (Tillakaratne et al., 2000, 2002; Bertels et al., 2022). It is not clear yet how these changes in GABAergic transmission affect motor function after spinal cord injury. One possibility is that the reduction of presynaptic inhibition through reduced activation of $GABA_B$ receptors on synaptic terminals could cause hyperreflexia, perhaps leading to spasticity in patients (Faist et al., 1994). At the same time, loss of PAD in sensory afferents could also reduce fidelity of sensory transmission, which would reduce sensory activation of spinal motor circuits below the lesion site.

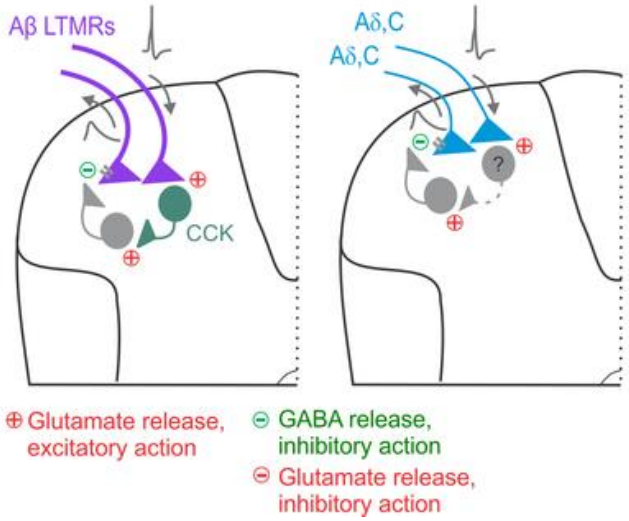

Figure 1.1. Presynaptic inhibition of large and small diameter sensory afferents. (Left panel) Large diameter cutaneous afferents exhibit GABA-dependent Presynaptic Inhibition (PSI). Aβ-Low Threshold Mechanoreceptors (LTMRs) can activate certain excitatory interneurons leading to the activation of GABAergic interneurons. This activation induces GABAAR-dependent primary afferent depolarization (PAD) mainly in other Aβ subtypes. (Right panel) GABAAR-dependent PSI occurs in response to activity in small diameter afferents. Unidentified interneurons, depicted in grey, play a role in this process.

Adapted from Zimmerman et al., 2019

1.3.5 Plasticity of sensory afferents

Perhaps it is not surprising that sensory afferents undergo morphological and functional changes after SCI considering the central role of sensory feedback to recovery of locomotor function after SCI. The role of sensory feedback from the periphery is heightened and more potentiated when the descending inputs are lost after SCI because intact sensory input are still capable of activating spinal motor circuits after the injury. The activation of sensory afferents whether through physical activity (Bouyer and Rossignol, 2003; Reggie Edgerton et al., 2007; Frigon and Rossignol, 2008; Sławińska et al., 2012; Takeoka et al., 2014; Takeoka and Arber, 2019) or electrical stimulation (Gerasimenko et al., 2002; Lavrov et al., 2008; Courtine et al., 2009; van den Brand et al., 2012; Zhang et al., 2021) can generate locomotor activity in SCI animals. On the other hand, silencing or ablating sensory neurons or spinal neurons that integrate sensory inputs can reduce recovery levels in SCI animals (Takeoka et al., 2014; Bui et al., 2016; Takeoka and Arber, 2019).

Proprioception is an important source of sensory information that originates from muscles. Proprioceptive sensory neurons innervate muscle spindles and tendon organs and have direct projections on MNs and spinal interneurons to convey information such as velocity, length of muscles and force to the spinal cord (Rossignol, 2006; Windhorst, 2007; Pearson, 2008). Takeoka et al. (2014) used genetic techniques to demonstrate the importance of proprioceptive afferents to the recovery of locomotion. Mice mutant for Egr3, a zinc finger transcription factor crucial for the survival of muscle spindles, exhibited persistent lack of locomotor control in ladder tasks after a lateral hemisection at thoracic level (T10). In contrast, wild-type mice with the same injury regained basic locomotor function and partially recovered speed dependent adaption but failed to recover precise paw placement (Takeoka et al., 2014). In another elegant study, Takeoka and Arber

(2019) demonstrated that proprioceptive feedback entering spinal segments below but not above the lesion is critical for recovery of locomotor function. Genetically ablating proprioceptive afferents below a lateral hemisection at T10 in adult mice severely restricted recovery of locomotion and reorganization of descending inputs. Even an ablation of proprioceptive afferents that was delayed until later after an injury also caused the loss of recovery. These data suggests that the proprioceptive afferents play an essential role for maintenance of recovery of locomotor function. Moreover, proprioceptive afferents interact with local spinal circuits and this activity dependent reorganization of synaptic connectivity to spinal targets initiates and maintains locomotor output after SCI (Takeoka and Arber, 2019).

In addition to proprioceptive afferents, cutaneous afferents conveying mechanoreceptive information are also activated during locomotion. In intact cats, removal of cutaneous information does not affect the rhythm generation but in spinalized cats, removal of cutaneous feedback severely impairs the recovery of proper foot placement during stepping (Bouyer & Rossignol 2003). Cutaneous inputs from the plantar surface of the paw were also shown to have an influence on locomotion in another study on spinalized rats (Sławińska et al., 2012). The contribution of cutaneous receptors in the foot pad of spinalized rats was tested through medial and lateral injections of lidocaine in the hindpaws to silence cutaneous afferents innervating the foot pad after SCI. Lidocaine altered plantar stepping and decreased intra- and inter-limb coordination of spinalized mice that had shown significant levels of recovery when walking in an upright position. This experiment further supports the conclusion that cutaneous afferents from the surface of the foot may be necessary for recovery of locomotor function in chronic spinal rats (Slawinska et al. 2012).

Quantification of VGLUT1^{+} synapses, which include proprioceptive and low-threshold sensory afferents as well as CST boutons in the spinal cord (Alvarez et al., 2004), suggests changes in the density of sensory afferents to some but not all MNs after complete lumbar spinal transection in rats (Khalki et al., 2018). The prior study focused mainly on spinal motoneurons, which are the direct interface between the central nervous system and the skeletomuscular system. However, many populations of spinal neurons also receive sensory inputs (Brownstone and Bui, 2010), and some of these populations such as dI3s, V0s, V2as,V2bs and others have been implicated in the recovery of locomotor function (Bui et al., 2016; Kathe et al., 2022). Whether there is plasticity in the integration of this sensory feedback by these and other populations of spinal neurons that are crucial to the recovery of locomotor function remains to be determined.

The benefits of targeting sensory feedback in therapeutic strategies such as rehabilitative locomotor training have also been studied in humans. Some improvements have been reported in patients with SCI that have undergone repetitive stepping motion on a treadmill with human or robotic assistance (Field-Fote and Roach, 2011; Nam et al., 2017), since this type of training has been shown to promote plastic changes capable of restoring locomotion in unilaterally transected rodents (van den Brand et al. 2012). Recent experimental trials with human male individuals diagnosed with motor and sensory complete lesions undergoing daily training with weight bearing for standing and stepping using assisted-treadmill walking, in combination with epidural stimulation of sensory afferents led to the expression of some volitional leg movements (Harkema et al., 2011, 2012; Angeli et al., 2014; Behrman et al., 2017; Wagner et al., 2018 ; Rowald et al., 2022 ; Lorach et al., 2023).

While these recent studies in humans are encouraging, the levels of volitional movements are still modest, and they result from extensive amounts of rehabilitation requiring large teams of

rehabilitation therapists. The success of these rehabilitative efforts could be greatly improved with an improved understanding of the spinal circuits that are activated by this kind of training. One target within the spinal cord are dI3 interneurons (dI3 INs), which is a population of spinal neurons that integrate both cutaneous from low-threshold mechanoreceptors and proprioceptive sensory inputs for the control of movement. Silencing these neurons have been shown to reduce the ability of SCI mice to recover rhythmic hindlimb movements during treadmill training (Bui et al., 2016). Therefore, dI3 INs are a promising candidate for future treatments of SCI.

1.4 Characteristics of dI3 INs

The spinal cord contains two structures, the dorsal and ventral horns, whose neurons subserve sensory and motor functions, respectively. Dorsal spinal neurons are mainly responsible for three functions, namely, 1) the processing of sensory information associated with proprioception, touch, pain and heat perceptions, 2) the relay of these sensory afferent information to the brainstem and thalamus and 3) the relay of sensory feedback onto motoneurons to modulate motor control (Müller et al., 2002). The location of the spinal INs that are responsible for the processing of non-noxious, tactile information have been estimated to be located in Rexed laminae I-VIII and X, initially based upon the distribution of the central terminals of low-threshold mechanoreceptors (Rexed, 1952, 1954).

Recently, spinal neurons have been categorized by their molecular characteristics and 6 populations of interneurons named dI1-dI6 have been identified in different layers of the dorsal horn. dI3 INs are excitatory interneurons (glutamatergic) as determined by in situ hybridization for vesicular glutamate transporter 2 (VGLUT2) mRNA (Bui et al. 2013), with ipsilateral projections to MNs (Stepien et al., 2010) (Fig. 1.2).

dI3 INs are characterized by the expression of several transcription factors such as Brn3a/b, Tlx3, Gsh1/2, Ascl1, Olig3, Brn3a, and Isl1 (Mizuguchi et al., 2006; Xu et al., 2008; Avraham et al., 2010). The transcription factor that distinguishes dI3 INs from the rest of the interneurons is Isl1, which is a LIM homeodomain transcription factor found only on dI3 INs, MNs and some sensory neurons (Pfaff and Mendelsohn, 1996; Liem et al., 1997; Bui et al., 2013). Isl1 is essential for determining the axonal projections of dI3 INs during development (Avraham et al., 2010). Since both dI3 and dI5 INs express Tlx3 and PrrxL1 in addition to pain modulatory neuropeptides, it's been hypothesized that dI3 INs belong to nociceptive second order sensory neurons (Qian et al., 2002; Xu et al., 2008). However, there is less evidence for this theory as the expression of Tlx3 and PrrxL1 in dI3 INs is transient and occurs only during embryogenesis compared to dI5 neurons that persists through postgestation. However, the longitudinal axonal trajectory pathways of dI3 neurons, which have been found to be ipsilateral, travelling along two longitudinal fascicules at the ventral lateral and dorsal funiculus, could also strengthen this hypothesis that dI3 INs play a role in relaying pain signals (Avraham et al., 2010).

Recently, the transcription factors of Onecut (OC) family, including hepatocyte nuclear factor 6, OC2 and OC3, have been found to stimulate the expression of Isl1 in MNs during differentiation Roy et al., 2012) and may also regulate the expression levels of Isl1 in dI3 INs (Kabayiza et al., 2017). It was observed that the number of dI3 INs containing OC factors increased from e10.5 to e12.5 in mice and migrated towards the intermediate level of the spinal cord (Kabayiza et al., 2017). However, mutant Hnf6/OC2-/- embryos also expressed Isl1 in dI3 INs in the absence of Onecut transcription factors. Therefore, these data suggest that the Onecut transcription factors regulate the distribution of dI3 INs in the spinal cord during development but are not required for their differentiation (Kabayiza et al., 2017)

The final location of dI3 INs in the spinal cord has been determined by driving expression of a yellow reporter fluorescent protein by the Isl1 promoter. Thus, dI3 INs were found to be predominantly located in cervical and lumbar segments of the spinal cord, at similar densities, within laminae V-VII (Bui et al., 2013). Due to their location, immunohistochemical labelling of VGLUT1 has shown that dI3 INs are contacted by primary sensory afferents (Alvarez et al., 2004) and electrophysiological experiments have confirmed the observation that dI3 INs received monosynaptic input from proprioceptive and low threshold cutaneous afferents (Bui et al. 2013). However, it was observed that sensory information is mainly transmitted from cutaneous as opposed to proprioceptive afferent and this was characterized by less abundance of parvalbumin expression in many $VGLUT1^{+}$ sensory contacts (Bui et al. 2013). Furthermore, electrophysiological and immunohistochemical techniques in addition to genetic manipulations have demonstrated that dI3 INs play a role in motor control (Stepien et al., 2010; Bui et al., 2013; Pivetta et al., 2014).

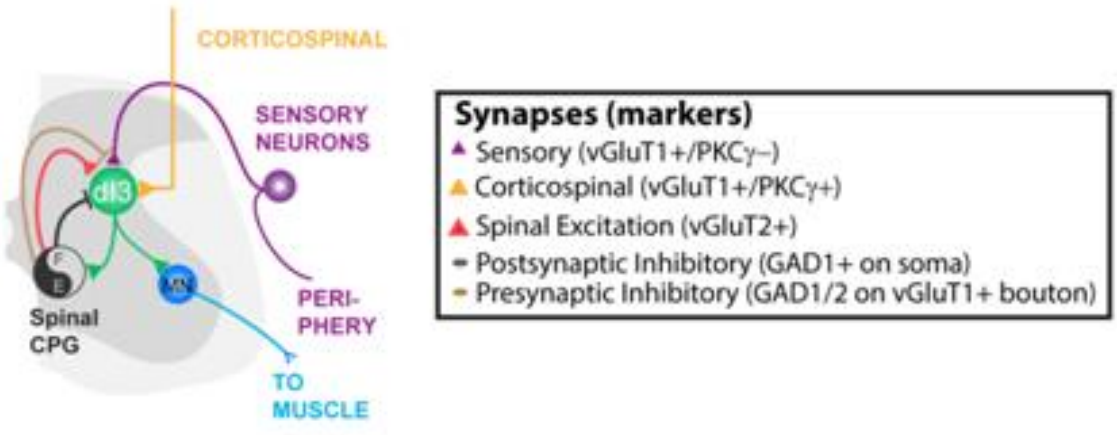

Figure 1.2. Connectivity of dI3 INs within the context of locomotor control. dI3 INs receive descending supraspinal inputs as well as cutaneous and proprioceptive sensory inputs. In turn, they have glutamatergic inputs, which projects onto CPG networks and MNs.

1.5 Role of dI3 INs in locomotion and recovery

Considering the importance of cutaneous inputs to locomotor recovery after SCI in both cat (Bouyer and Rossignol, 2003) and rats (Sławińska et al., 2012), the role of dI3 INs in locomotor recovery was investigated. Neurotransmission of dI3 INs was genetically silenced by Isl1-driven conditional ablation of the VGLUT2 protein, a protein important for glutamatergic neurotransmission in most spinal neurons, including dI3 INs (Bui et al. 2013). These mice were named dI3^{OFF} mice. In-vitro electrophysiological experiments where the spinal cord of control mice was isolated with the predominantly cutaneous sural nerve left in continuity showed that sural nerve stimulation was capable of eliciting locomotor activity in the isolated neonatal mouse spinal cord. However, when the same experiments were repeated in dI3^{OFF} animals only 6 of 12 dI3^{OFF} mice showed locomotor activity and in those spinal cord where locomotor activity was elicited, a higher amount of current stimulation was necessary to elicit locomotion. Therefore, these results suggested that dI3 INs are capable of activating the spinal locomotor circuits induced by stimulation of low threshold cutaneous afferents (Bui et al., 2016).

Despite this access to spinal locomotor networks, gait analysis in intact adult dI3^{OFF} animals suggest that dI3 INs play an accessory rather than necessary role (Bui et al. 2016). However, as described beforehand, cutaneous inputs are important for recovery of locomotor function and dI3 INs have been shown to integrate cutaneous inputs at the spinal level. This and their access to spinal locomotor networks would make them ideally positioned to play important roles in recovery of locomotor function following SCI when the spinal cord is deprived of descending motor commands to activate locomotor activity. Bui et al. (2016) tested this hypothesis. Following lower thoracic spinal cord transections in control and dI3^{OFF} mice, mice were subjected to treadmill training in order to recover locomotor activity. Functional recovery was quantified as

forelimb/hindlimb step ratios with steps being defined as any forward excursion of the toes. In both groups, there was a gradual increase during treadmill training following SCI but the step ratios plateaued by 50 days following transection. More interestingly, the number of forward toe excursions in $dI3^{OFF}$ spinal cord injured mice was observed to be about half that of control SCI mice leading to the conclusion that these $dI3^{OFF}$ mice showed a greatly reduced capacity of motor recovery following spinal transection (Figure 1.3). These experiments point to dI3 INs as being central players in the process of recovering locomotor activity following SCI. How dI3 INs contribute to locomotor recovery after SCI remains to be determined. Considering the evidence for plasticity in spinal circuits after SCI, there may be associated changes in circuits of dI3 INs during the recovery of locomotor function.

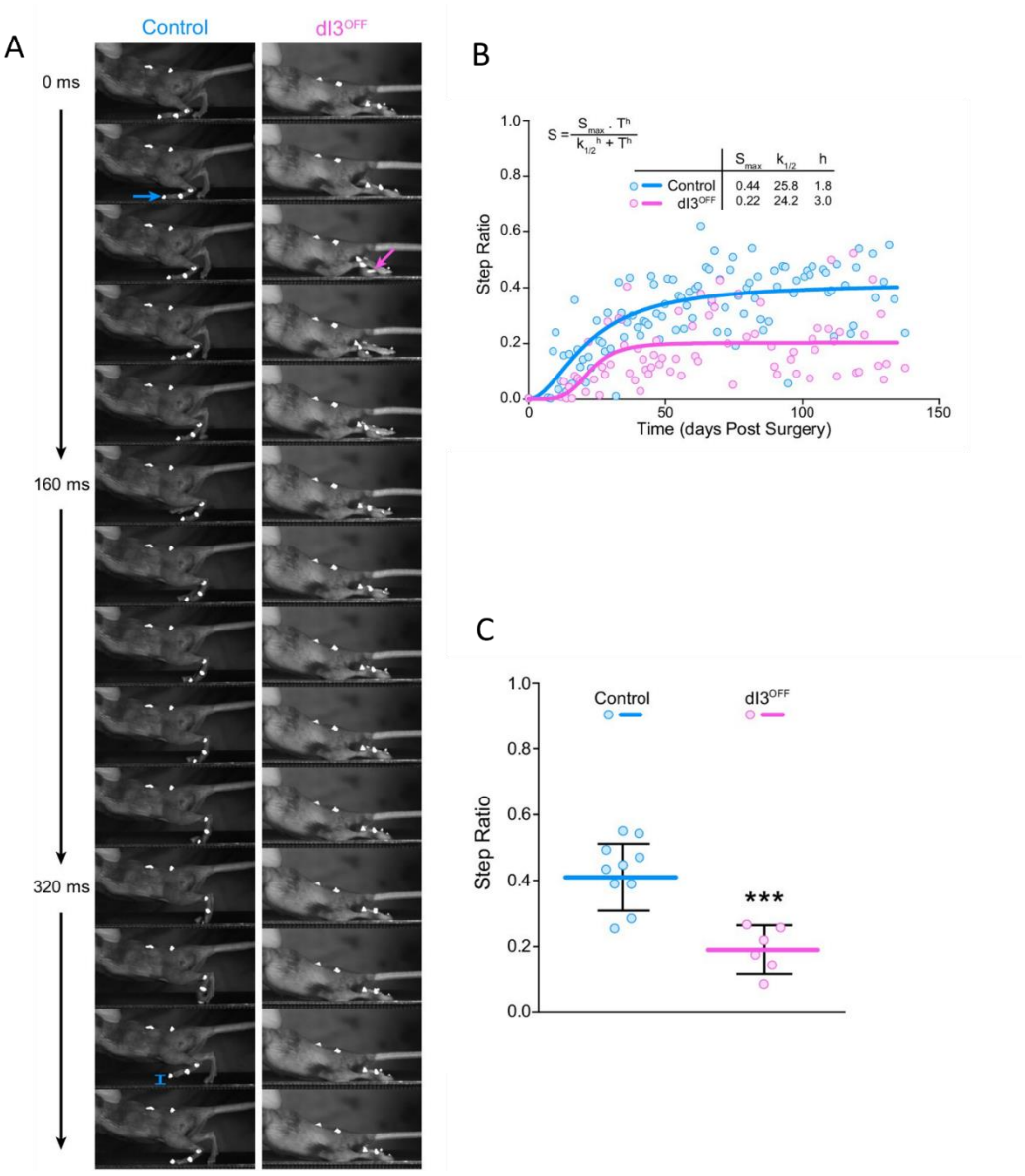

Figure 1.3. DI3 INs play a role in recovery of locomotion following SCI
(**A**) Kinematic recordings at 32 ms intervals in control and dI3^{OFF} mice 50 days following complete spinal transection. Blue arrow at 32 ms portrays proper paw dorsiflexion in control mice but dI3^{OFF} mice show abnormal plantarflexion during stance (magenta arrow at 64 ms). Cyan segment at t = 384 ms indicates toe elevation in control, which is absent in dI3^{OFF} during the swing phase. (**B**) Hindlimb/Forelimb step ratio as a function of time following complete spinal transection in control and dI3^{OFF} animals (**C**) Hindlimb/Forelimb step ratio 30 days following complete spinal transection in control and dI3^{OFF} animals. Mean +/− Standard Deviation. Two-tailed Student's t-test (***p<0.0001).

Adapted from Bui et al.,2016

1.6 Maladaptive changes after SCI

Neuroplasticity that occurs after SCI, can also become maladaptive and cause secondary complications such as pain and spasticity in the patients suffering from SCI. Spasticity is one of the major symptoms manifested after spinal cord injury and is characterized as a velocity dependent increase in muscle tone due to the exaggeration of stretch reflexes (Lance, 1990). It's been reported that over 65% of individuals develop spasticity a few months after SCI and over 35% have problematic spasticity where medical treatments are required (Holtz et al., 2017; Maynard et al., 1990). In these patients, spasticity is often observed as involuntary muscle activity such as muscle spasms, augmented tendon reflex activity (hyperreflexia) and involuntary rhythmic muscle contractions also known as clonus (Nielsen et al., 1995; Pandyan et al., 2005). Spasticity impacts the daily activities of SCI patients by limiting joint mobility, causing postural abnormalities, and disturbing sleep (Adriaansen et al., 2016; Lundström et al., 2017; Widerstrom-Noga et al., 2001).

1.7 Underlying neural mechanisms

The neural mechanisms underlying the development of spasticity after SCI are not well understood. Three types of changes have been observed after SCI that could lead to spasticity. First, disinhibition of spinal networks could be implicated. In both cats and humans, Golgi tendon organs, which are sensitive to muscle tension, project via large diameter fibres (Ib afferent fibres) onto the motoneuron of the muscle from which they originate to inhibit them. This activation is mediated through glycinergic Ib interneurons and results in a postsynaptic short-lasting inhibition (Ib inhibition). The inhibitory effect of Ib interneurons on motoneurons was tested in in both legs of six hemiplegic patients (Delwaide and Oliver, 1988), by using a technique proposed by Pierrot Deseilligny et al,1970. It was found that the Ib inhibitory effect was functionally absent in the

spastic leg and reduction in Ib inhibition could contribute to the hyperexcitability of the myotatic reflex, which is the putative basis of spasticity (Lance, 1990). This reflex could be the basis of spasticity, but spasticity could involve polysynaptic reflexes involving muscle and cutaneous receptors (mechanoreceptive and nociceptive).

Another malfunction in spinal inhibitory networks after SCI can be seen in the Renshaw cell mediated recurrent inhibitory pathway for regulation of synergic muscles during movement. A lesion interrupting the reticulospinal projections onto the inhibitory Renshaw cells, could lower the level of excitability of these interneurons (Katz and Pierrot-deseilligny, 1982) and could contribute to the development of extreme limb stiffness (Mazzocchio and Rossi, 1997). Recurrent inhibition of soleus motoneurons was compared in healthy control subjects and spastic patients with progressive paraparesis due to a spinal cord or cerebral lesion. Recurrent inhibition was found to be normal in 50% of the patients at rest while in the other half there was evidence of reduced or absent inhibitory activity at rest. Oral administration of L-acetylcarnitine increased activity of Renshaw cells and consequently the hyperexcitability of H reflexes was reduced and as a result reduction in flexor spasms and clonus was observed (Mazzocchio and Rossi, 1997).

Sprouting of sensory afferents following SCI could be a second means by which spasticity could arise due to increased spinal reflexes such as nociceptive hyperreflexia (Fig. 1.4). After SCI, pain pathways are reorganized and development of mechanical and thermal allodynia has been observed at the level of injury and in rostral and caudal segments of the lesion site (Ondarza et al., 2003a). Calcitonin gene related peptide (CGRP) is a putative nociceptive neurotransmitter found in peripheral projections (Hokfelt et al., 1992) that is implicated in the transmission of pain, temperature and noxious and non-noxious mechanical stimuli (Coggeshall et al., 1991; Yu et al., 1994) and also in inflammations during SCI (Christensen and Hulsebosch, 1997). After a unilateral

lesion at thoracic T13 level of the spinal cord in rats (Ondarza et al., 2003), increased sprouting of CGRP containing afferents was observed near the lesions site and in segments above and below the lesion. The segments rostral to the lesion (C8-T13) contain sensory fibers from glabrous skin of the forepaw whereas segments caudal to the lesion (T13-L5) contain sensory fibers from the glabrous skin of the hindpaw. Colocalization of CGRP was observed along with GAP-43, which is a marker of neurite sprouting (Neve et al., 1988; Aigner et al., 1995), and upregulation of GAP-43 was most robust near the T13 lesion site (Ondarza et al., 2003). Therefore, sprouting in CGPR pathways may lead to allodynia following spinal injury (Ondarza et al., 2003).

In a similar study, it was observed that a T10 hemisection in rats produced cutaneously evoked nociceptive hyperreflexia (Lee et al., 2019). Central projections of cutaneous nociceptive afferents were significantly increased in segments above and below the lesion and increased synaptic terminations in the dorsal horn was observed (Lee et al., 2019).

Downregulation of mechanisms that gate the sensory afferents may also cause the development of spasticity (Fig.1.4). Gating of sensory information by presynaptic inhibition of Ia terminals is mediated by axo-axonal GABAergic synapses by activation of $GABA_B$ receptors on the Ia afferent. In a healthy subject, the GABAergic spinal interneurons that mediate presynaptic inhibition are under the control of descending tracts (Rudomin et al., 1983; Rudomin and Schmidt, 1999). A number of studies suggest that the Ia pathways are no longer inhibited by presynaptic inhibition after lesions to the spinal cord. This downregulation of presynaptic inhibition could contribute to the hyperexcitability of the stretch reflex seen in spastic patients. In 18 paraplegic patients with bilateral spinal cord lesion, facilitation of the soleus H-reflex was investigated (Faist et al., 1994). It was observed that in these patients, upon femoral nerve stimulation, the heteronymous Ia facilitation was significantly larger compared to the control healthy subjects. A

decrease in presynaptic inhibition upon binding of GABA to $GABA_B$ receptors on Ia afferents after SCI could explain this facilitation of the Ia reflex (Faist et al., 1994).

Finally, changes in motoneuron excitability could very well promote spasticity (Fig. 1.4). There are voltage-dependent persistent inward currents in motoneurons mediated by calcium currents from low threshold L-type calcium channels (Cav1.3 type) (Carlin et al., 2000). When activated, PICs produce a sustained depolarization called plateau potentials. These plateau potentials amplify and sustain the output of motoneurons (Hounsgaard et al., 1988; Lee and Heckman, 1996; Bennett et al., 1998). After an acute spinal transection in the rat sacral cord, plateau potentials are eliminated in motoneurons but a few months post-injury, motoneurons regain their ability to produce plateaus (Eken et al., 1989; Bennett et al., 2001). These plateau potentials were accompanied by large PICs and enhanced the intrinsic excitability of motoneurons, which led to spasms in the muscles of the tails (Bennett et al., 2002, 2004).

The mechanisms underlying this spontaneous emergence of plateau potentials in chronic spinal rats may be due to loss of control of descending inputs on synaptic transmission below the level of injury (Baldissera et al., 1982; Jankowska, 1992), increased neurotransmitter release from sensory afferent or interneurons (Thor et al., 1994), receptor upregulation after chronic SCI (Mills and Hulsebosch, 2002) and metabotropic receptor facilitating PICs becoming supersensitive to the released neurotransmitters (Hains et al., 2002). This enhanced action of metabotropic receptors by glutamate or constitutive activity of $5\text{-}HT_{2B/C}$ receptors can contribute to exaggerated PICs and increased plateaus after chronic spinal cord injury (Murray et al., 2010).

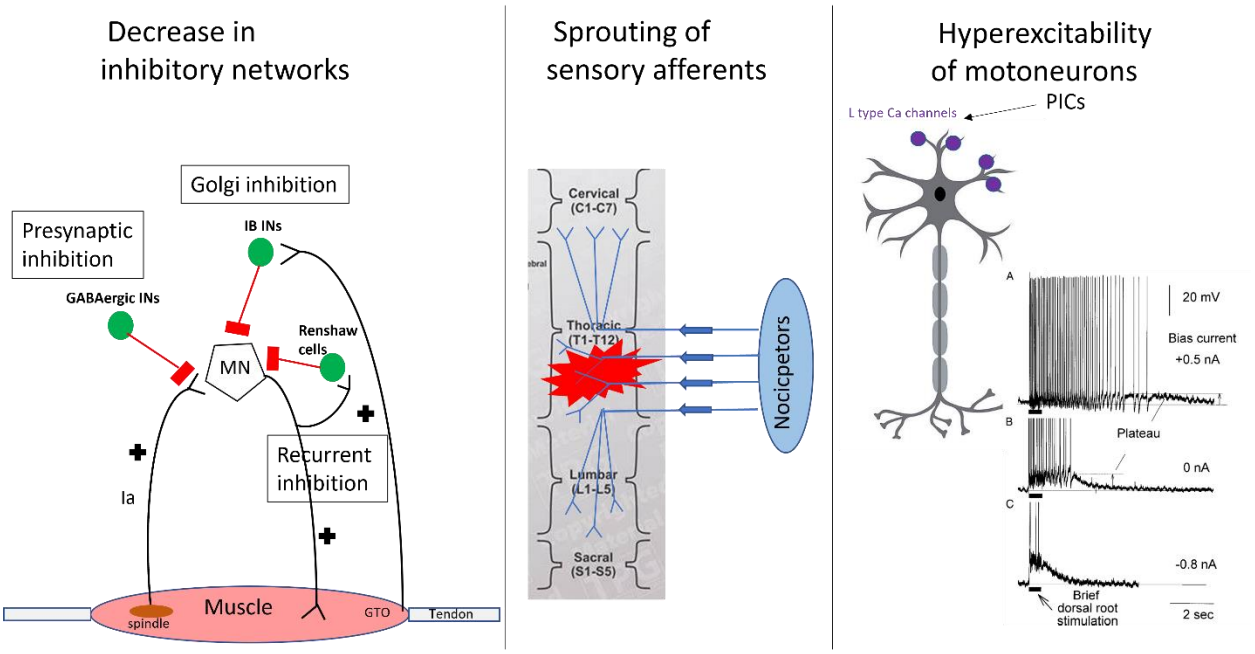

Figure 1.4. Neural mechanisms underlying spasticity following SCI. Several mechanisms can lead to emergence of spasticity. (Left panel) Downregulation of spinal inhibitory networks that gate the sensory afferents. (Middle panel) Sprouting of sensory afferents (Right panel) Changes in motoneuron excitability.

1.8 Treatments of spasticity

Current treatments for spasticity include blocking synaptic transmission by intramuscular injections of the neurotoxin botulinum toxin (Ward et al., 2003), intrathecal targeting of the GABAergic receptors using the $GABA_B$ receptor agonist baclofen (Heetla et al., 2014), blocking calcium channels (Cav1.3) by nimodipine as tested in animal models (Marcantoni et al.,2020), and neuromodulatory approaches such as transcranial magnetic stimulation in combination with conventional therapies such as physiotherapy (Leo et al., 2017). These treatments have major secondary side effects such as sedation and muscle weakness (Chang et al., 2013), which is why the discovery of new treatments with less side effects are crucial for the effective treatment of spasticity. Our lack of understanding of the pathophysiology of spasticity hinders our ability to completely reverse the symptoms of spasticity and develop effective antispastics. One of the major challenges to completely elucidating the pathophysiology of spasticity and the development of more effective antispastic treatments is the lack of animal models where spasticity in the hindlimbs can be easily and reliably elicited in awake behaving animals (Yoshizaki et al.,2020).

1.9 Current animal models of spasticity

Despite the prevalence of spasticity after injury or disease to the nervous system, few if any animal models are available to reliably study limb spasticity. Experimental models of spasticity in rodents often rely on electrophysiological recordings of the Hoffman reflex in anesthetized animals (Yates et al., 2008, 2011) or manual scoring of limb spasticity (Craven and Morris, 2010). A complicating factor in observing limb spasticity after SCI is the variability in the onset and frequency of spastic events. The rat spastic tail model was developed by David Bennett and colleagues to circumvent this variability. This model of spasticity has revealed changes in intrinsic and network properties of neurons as possible mechanisms underlying spasticity after SCI

(Bennett et al., 2004, 2001, Hari et al., 2021, Metz et al., 2023). Another spastic tail model after a sacral S2 transection has been investigated in adult mice based on the previous rat spastic tail models (Kapitza et al., 2012). While the spastic tail model has been well developed such that tail spasticity is reliably induced after SCI, there are not many models of limb spasticity available. Another recent study has investigated the generation of limb spasticity after an incomplete transection of the spinal cord at T8 level. However, the severity of spasticity in this model suffered from variability, which might be inherent to spontaneously appearing spasticity (Yoshizaki et al., 2020). Electrophysiological measure of spasticity has mostly relied on the loss of rate-dependent depression of the H-reflex, a measure of muscle-spindle excitation of motoneurons. The causal relationship of rate-dependent depression and its attenuation with spasticity remains to be fully established, and the technical demands of electrophysiology pose hurdles to relying on these measurements for the evaluation of potential treatments of spasticity. There is, therefore, a need for animal models where hindlimb spasticity can be more reliably elicited, particularly in the context of SCI.

1.10 Thesis overview

Restoring the activity of spinal circuits after spinal cord injury is essential for recovery of lost locomotor function after spinal cord injury. The adaptive changes within spared neuronal circuits can be beneficial for restoring sensorimotor function. In parallel, adverse, and maladaptive changes can happen during cortical and intraspinal circuit reorganization after SCI. As a result of increased neuronal sprouting of sensory afferents and formation of new intraspinal connections or strengthening of existing connections, an imbalance of inhibitory and excitatory signaling can cause spasticity.

Now that it has been demonstrated that dI3 INs are important for recovery of locomotor function, I first seek to determine the mechanisms by which they could potentially reconfigure the spinal cord to improve locomotor function following SCI. The first step in identifying these mechanisms is to understand the plasticity of their connectivity during the recovery of locomotor function following SCI. To reach this goal, I have 3 sub-aims to investigate:

A) Changes in sensory inputs onto MNs and dI3 INs

B) Changes in GABAergic inputs onto central terminals of sensory inputs

C) Changes in central excitation of MNs and dI3 INs, putatively through VGLUT2+ inputs

In the second half of my thesis, I will turn my focus on maladaptive plasticity after SCI, namely spasticity. I will investigate a possible mouse model for maladaptive hindlimb spasticity based on photoactivation of sensory afferents innervating the skin via transgenic conditional expression of the light-sensitive ion channel calcium translocating channel rhodopsin (CatCh) in subpopulations of sensory neurons of dorsal root ganglia. I will first characterize the conditional expression of transgenes of the fluorescent reporter tdTomato in the DRGs and the spinal cord to determine the expression pattern of CatCh in our transgenic animals. I will then study the spasticity response induced by light stimulation of the hindlimbs of our transgenic animals after SCI to establish the value of these animals as possible models of hindlimb spasticity after SCI.

CHAPTER 2: MATERIALS AND METHODS

2.1 Animals

All animal procedures were approved by the University of Ottawa Animal Care Committee and conform to the guidelines put forth by the Canadian Council for Animal Care. For our study investigating the changes in connectivity to dI3 interneurons and motoneurons after spinal cord injury (see sections 3.1.1 to 3.1.6), we used Isl1-Cre; Rosa26-YFP transgenic line of mice, herein referred to as Isl1:YFP mice, which allowed us to visualize dI3 INs through the expression of yellow fluorescent protein (YFP). Animals used in experiments ranged in age from adult 3-6 months old. Both male and female mice were used in this study.

For our study investigating a novel model of hindlimb spasticity (see sections 3.2.1 to 3.2.5), we used Isl1^{CRE}; Vglut2^{FLP}; Ai80(RCFL- CatCh)-D transgenic strain of mice. For simplicity, these mice will be referred as Isl1-Vglut2^{CatCh} herein. These mice conditionally express the blue light-sensitive CatCh channels only in cells that are Isl1+ and VGLUT2+. This conditional expression limits the expression of CatCh to a population of spinal dI3 interneurons (dI3 INs) (Bui et al,2013) and a subset of sensory neurons involved in mechanical nociception and thermoception (Lagerström et al., 2010). Animals used in these experiments ranged in age from 2-3 months and N =5 male and N=10 female mice were used.

2.2 Surgical details of spinal cord injury

Complete transections were performed at T9-T10 under isoflurane anesthesia. This injury interrupts all descending supraspinal pathways, as well as all ascending sensory tracts – preventing the perception of potentially noxious stimuli in the mice. Sterile surgical foam (Surgifoam, Johnson & Johnson Medtech) was placed in the spinal space to prevent any re-growth of the axons across the lesion. Animals were individually housed, given analgesic (Buprenorphine, 0.1mg/kg

subcutaneous injection, Ceva Animal Health) for three days, and allowed to recover for at least one week prior to treadmill training. Sham animals received a sham surgery where the skin and muscle were opened and the T8 vertebrae was removed but the cord was not transected. The skin and muscle were immediately closed after the vertebrae was removed. Animals were monitored thrice daily, and bladders were expressed manually thrice daily. Humane endpoints were defined as self-mutilation, improper feeding, decreased grooming, ataxia, or loss of body weight >20%.

For the group of animals used for the spasticity project, complete transections of the spinal cords were performed at T9-T10 and following a one-week recovery period, mice were anesthetized with isoflurane and custom-built fine wire EMG electrodes were implanted into the tibialis anterior and gastrocnemius muscles as previously described (Akay et al., 2008, 2006). After shaving the neck and hindlimbs of the mice, small incisions were made into the skin at the neck area and at the hindlimbs. The electrodes were led under the skin from the neck to the leg incisions and implanted into the left and right ankle flexor tibialis anterior and ankle extensor gastrocnemius muscles using an attached 27 G needle. Following insertion into the muscle, the electrodes were anchored in place by knotting the paired wires at the distal end of the muscle and removing the attached needle. The incisions on the hindlimbs were closed with 7-0 polypropylene sutures (Ethicon) and the headpiece was stitched to the skin near the neck incision by 5-0 silk sutures (Ethicon) and mice were given analgesic and allowed to recover for 3 days.

2.3 Treadmill training

Locomotor training on a custom-made treadmill was provided twice a week, with an additional testing session per week. Animals were allowed to habituate to the treadmill environment before training and then trained on the treadmill (belt speed of 10 cm/s) with minimal weight support to ensure continual contact with the treadmill belt. On the testing day, mice walking

on the treadmill were filmed from the side using a Basler ace acA640 – 750 μm camera to record at 60 frames per second for 3 minutes. Views of the mice from the side and the bottom were captured as the treadmill was equipped with a transparent belt and a mirror below. In addition to the session walking with no weight support, a subset of mice also had a session walking in a more upright position by providing manual body weight support during the weekly testing. We previously observed that recovery of rhythmic hindlimb movements plateaus after about two months (Bui et al., 2016a). Based upon these data, we collected the lumbar spinal cord in mice after 6 days post-injury (dpi), 2-3 weeks post-injury (wpi), 4-6 wpi and 10-12 wpi of locomotor training. SCI mice were sacrificed at these time points, and spinal cords were removed for immunohistochemistry.

2.4 Perfusion and Immunohistochemistry

Mice were injected with 120 mg/kg pentobarbital sodium and, after sedation, checked for the presence of a toe pinch reflex. Following complete anesthesia, animals were cut open and transcardially perfused with PBS for five minutes and then with ice-cold 4% paraformaldehyde for another five minutes or until the liver was clear of blood. Next, the spinal cord was removed and post-fixed in fresh 4% PFA overnight. The next day, the spinal cord was stored in 30% sucrose for cryoprotection and, after a few days, embedded in OCT cryostat sectioning medium and stored at -80 °C. When ready for sectioning, the spinal cord was cut in transverse sections on a cryostat (40-50 μm) and collected as free-floating sections. Sections were washed three times with PBS, blocked for one hour in PBS with 0.3% triton-X100 (PBST) and 5% normal goat serum, and then incubated overnight at 4°C with primary antibodies in PBST plus 5% serum. The following day, sections were washed three times with PBS, incubated with Alexa Fluor-conjugated secondary antibodies for three hours at room temperature and washed three final times in PBS. Antibodies

used for fluorescent immunohistochemistry were as follows: chicken anti-GFP (1:1000; Abcam; RRID: AB 300798), guinea-pig anti-VGLUT1 (1:2500; EMD Millipore; RRID: AB 262185), guinea-pig anti-VGLUT2 (1:2500; EMD Millipore; RRID: AB 2251) and mouse anti-GAD65/67 (3 μg/ml; Developmental Studies Hybridoma Bank; RRID: AB 2314499). TRPV1 and IB4 staining was done using a rabbit anti-TRPV1 (1:500, #PA1-748, Invitrogen). The secondary antibody used was a goat anti-rabbit conjugated to Alexa 488 (1:500, ab150077, Abcam). IB4 staining was performed using IB4 conjugated to Alexa 647(1:200, I32450, Invitrogen). Sections were mounted onto Superfrost (Fisher Scientific) slides with Immu-Mount (Fisher Scientific), and a coverslip was applied.

2.5 Microscopy and Synaptic Quantification

Olympus FV1000 BX61 confocal laser scanning microscope (RRID: SCR_020337) was used to acquire the images and optical sections were collected in z-stacks. Fluoview software (Olympus) was used to analyze the images. From each mouse, 20 dI3 INs and 20 MNs were selected, and the number of VGLUT1, VGLUT2 and GABApre boutons was quantified manually using orthogonal views to confirm apposition onto the cell body. For quantification of sensory synapses on dI3 INs and MNs, $VGLUT1^+$ boutons were counted manually on the entire soma and proximal dendrites (100 μm from the soma) on confocal images. Boutons were characterized as circular or elliptical structures appearing larger than the smaller dots that are characteristic of background noise frequently seen in immunostained images. Similarly, $VGLUT2^+$ boutons on the surface of soma were counted to estimate the number of central excitatory synapses onto dI3 INs and MNs. In addition, $GAD65^+/67^+$ boutons contacting $VGLUT1^+$ terminals were counted, and the fraction of $VGLUT1^+$ boutons with $GAD65^+/67^+$ boutons was calculated to estimate GABAergic inputs onto sensory afferents to dI3 INs and MNs.

For images taken after RNAscope experiments, Zeiss Axio Imager was used to acquire the images. Zen Blue software was used to analyze the images. From each mouse, 6 DRGs were selected to count the number of cells within each DRG.

2.6 RNAscope *in situ* hybridization

A RNAscope multiplex fluorescent v2 assay combined with immunofluorescence was performed as instructed by Advanced Cell Diagnostics (ACD). Mice were perfused with fresh 4% PFA in 1X PBS and then the spinal cord tissues were dissected and stored in 4% PFA for 24 hr. Next, the tissues were immersed in 10%, 20%, 30% sucrose in 1X PBS until the tissues sank to the bottom of the container. The tissues were embedded in optimal cutting temperature (OCT) media and stored in -80°C. The tissue blocks were then cut at a thickness of 12 um on Superfrost plus slides in a cryostat and air dried for 60-120 minutes at -20°C. After removing the slides from the cryostat, they were washed with 1X PBS to remove the OCT. Next, the slides were placed in a pre-warmed humidity control tray containing dampened filter paper and placed in a HybEZ oven (ACD) for 30 min at 40°C. The slides were post fixed in 4% PFA for 15 min at 4°C. Next, the slides were dehydrated in 50%, 70% and 100% ethanol for 5 min at room temperature. The slides were then baked for 30 minutes at 60°C in the oven. About 5 drops of hydrogen peroxide was added to each slide to cover the entire section and then washed with distilled water and baked for 1 hour at 60°C. Next, the slides were submerged into hot 1X Co-Detection target retrieval solution for 5 minutes using the steamer method and then washed in distilled water and 1X PBST by moving the rack of slides up and down. The slides were dried in the oven at 60°C and then boundaries were drawn around each section using a hydrophobic pen (ImmEdfe PAP pen; Vector Labs). When hydrophobic boundaries had dried, 200 µl of rabbit anti-RFP (1:500, 600-401-379,

Rockland Immunochemical,) was added to cover each slide and incubated at 4°C overnight. On the second day, another post-primary fixation was performed and then after washing the slides, 4 drops of RNAscope Protease Plus was added to each slide. After incubating the slides at 40°C for 30 minutes, the slides were washed in distilled water. The slides were then placed in a pre-warmed humidity control tray containing dampened filter paper and 4-6 drops from a mixture of Channel 1 and Channel 2 probes (50:1 dilution) was added to each slide. Our target of interest in channel 1 was VGLUT1 and in channel 2 was VGLUT2. The humidity control tray was placed in the HybEZ oven for 2 hours at 40°C. Following probe incubation and washing in 1X RNAscope wash buffer, the three amplification steps were performed using AMP-1, AMP-2 and AMP-3 reagents with a 15-, 30-, and 15-minute incubations periods, respectively. In the following steps, the C1 and C2 channels were developed, and Opal 520 dye (FP1487001KT, Akoya Biosciences) was assigned to the C1 channel and Opal 690 dye (FP1497001KT, Akoya Biosciences) was assigned to the C2 channel. In the final step, fluorophore conjugated secondary antibody (goat anti-rabbit conjugated to Alexa 555, 1:500, #A-21428, Invitrogen) was added to the slides and incubated for 30 minutes at room temperature. Slides were then washed twice in PBST and then a few drops of DAPI were added to each slide. After removal of DAPI, slides were cover slipped with Prolong Gold Antifade mounting medium (Invitrogen).

2.7 Automated detection of stepping function

Videos of stepping function during weekly testing sessions were analyzed using DeepLabCut (Version:2.2.0.6, RRID:SCR_021391) (Mathis et al., 2018). The training of the network involved using the graphical interface provided by DLC to label various body parts. Several body parts from the side and bottom view were labelled, though for the purpose of this study, only the following body parts were analyzed: nose, ear, left knee, left hind toes, left ankle,

and tail base. For the training of the network, one video from each mouse filmed at the 2-3 wpi, 4-6 wpi and 10-12 wpi time points were chosen per time point. Around 20-40 frames were labelled per video, and the label diameter was set to 5 pixels. Training the network was done with Google Colab using the ResNet-50 network with the number of iterations set to 200,000 and an accepted range of error set to 3 pixels.

The trained network was then used to analyze all the testing videos to estimate the horizontal and vertical coordinates of each body part detected. The validity of the calculated coordinate was based on a likelihood probability with a threshold of 0.5 for SCI mice and 0.8 for sham mice. For sham mice, video frames where mice were sitting or standing up were excluded if they did not meet the following criteria: 1) The difference between the vertical coordinates of the nose and ear to the tails was between the median value ± two standard deviations for the video analyzed. 2) The horizontal coordinates of both the nose and ear are more forward than the tail base.

The left ankle angle was calculated as the angle between the left knee, left ankle, and left hind toe using custom-made python code. The left ankle was used as it faced the camera. The number of steps was then calculated. The ankle angle for SCI mice on a treadmill without weight support was frequently extended between 90° and 180°. Stepping motions of their limbs flexed the ankle resulting in a rapid decrease of the ankle angle below 90°. Thus, we detected minimum peak angles using a 30-frame-long moving time window (0.5 second). The occurrences of local minima below 90° were identified as steps. For sham mice, local minima and maxima of ankle angles were determined using a 10-frame-long moving time window. Due to the occasional presence of consecutive minima without an interposed maximum or vice-versa, the number of steps was calculated as the arithmetic mean of the number of local minima and maxima in each video.

2.8 Chronic in-vivo EMG recordings

For the EMG experiments, the electrodes were made using multi-stranded, Teflon coated annealed stainless-steel wire (#793200, A-M systems). Four pairs of electrodes were prepared for each mouse. For each electrode pair, two pieces of wires were cut about 15 cm in length and twisted together to make a knot. On the first strand, 1mm distal to the knot, 1mm section of the Teflon coating was stripped off. On the second strand, 3mm distal to the knot, 1 mm of the insulation was stripped off so that the bare regions from each wire were separated by about 2 mm. Next, about 8-9 mm of coating was removed from one end of the wires, dipped in glue to prevent the exposed wires from fraying and crimpled into the shaft of a 27-gauge needle. The opposite ends of the wires were cut about 8 cm from the knot, stripped of their insulation, and soldered to an eight-pin miniature connector (SamTech). The underside of the connector was covered with epoxy (Devcon 5 min Epoxy Gel) to electrically insulate the wire insertions that were made into the connector and the epoxy was extended about 2 mm beyond the edges of the connector. Small holes were drilled into the edges of the epoxy to suture the connector into the skin.

2.9 EMG recordings and optical stimulation of the hindlimbs

We started electrophysiological recordings 1 week after implanting the EMG electrodes. Recordings were made over the course of 5 consecutive weeks. Mice were placed in a transparent, open field chamber. A lightweight cable of 50 cm was attached to the connector of the electrode array. A blue light source (100 ms pulse) from a 470 nm LED was positioned below the chamber to deliver stimulation of the right and left paws from below. We measured the motor responses through the implanted EMG electrodes in the tibialis anterior and gastrocnemius muscles of the hindlimbs. Each EMG recording involved 9 stimulation episodes per paw and 2 control episodes, where the light pulse was directed away from the mouse. Signals were recorded using a Digidata

series 1550b digitizer (Molecular Devices) and amplified by a Model 1700 differential amplifier (A-M systems). EMG data collected were rectified and binned in one-second long epochs starting one second before the stimulus was applied and until 5 seconds after the stimulus. A single 5-10 second post-stimulus epoch was also analyzed. The mean EMG amplitude within each epoch was calculated.

2.10 Statistical Analysis

GraphPad Prism 9.2.0 (RRID:SCR_002798) was used to perform all statistical analyses. Data are reported as mean ± S.D. For all tests, the level of statistical significance was set at $p < 0.05$ and indicated by asterisks in the figures. Comparisons involving all means within a group were made using one-way ANOVA followed by comparisons between pairs of groups using Tukey's multiple comparison test. Comparisons involving only a subset of all possible pairs (trained versus untrained at each time point) within a group were performed using paired t-tests with Bonferroni's multiple-comparisons correction. Correlations between synaptic inputs and stepping function were analyzed using the non-parametric Spearman Correlation test. In the second half of the thesis related to spasticity project, comparisons were made using Mixed effects analysis followed by comparison between pairs of groups using Tukey's or Sidak's multiple comparison test.

CHAPTER 3: RESULTS

3.1.1 Changes in sensory inputs to dI3 INs and MNs

We first sought to determine changes in sensory inputs to dI3 INs and MNs. dI3 INs and MNs (both expressing Isl1) were identified by yellow fluorescent protein (YFP) expression in Isl1:YFP transgenic mice. Thirty-eight transgenic Isl1:YFP mice, 21 in the trained group (Sex: 8 M, 13 F, Average weight = 22.09 +/- 2.37 g) and 17 in the untrained group (Sex: 9M, 8 F, Average weight = 21.5 +/- 2.4 g) underwent a complete transection of the spinal cord at T9-T10. The transection occurred at age 3.62 +/- 0.76 months. Data from 3 mice were not included due to incomplete lesions of the spinal cord or walking performance on the treadmill that was very close to sham levels shortly after the injury.

To characterize sensory terminals onto dI3 INs and MNs, we used an antibody against VGLUT1$^+$ (Fig. 3.1A, D), a vesicular glutamate transporter selectively expressed in central boutons of proprioceptors and low-threshold mechanoreceptors (Alvarez et al., 2004). VGLUT1$^+$ sensory boutons on the surface of dI3 INs and MNs were quantified at different time points post-injury in two groups of mice with and without treadmill training.

The number of VGLUT1$^+$ boutons contacting per dI3 INs changed after SCI in the untrained and trained animals (Fig. 3.1B; N = 17 untrained animals and N = 21 trained animals; one-factor ANOVA, p = 0.0089 for untrained animals, p = 0. 0079 for trained animals). In the untrained group, differences were limited to the 2-3 wpi time point, which was significantly decreased compared to sham and the 6 dpi time point (Fig. 3.1B left panel; N = 10 sham animals, N = 4 at 6 dpi and 2-3 wpi, Tukey's multiple comparison test: p = 0.0416 and p = 0.0124, respectively). In dI3 INs from trained animals, the number of VGLUT1$^+$ boutons was significantly decreased at 10-12 wpi compared to 6 dpi, 2-3 wpi and 4-6 wpi (Fig. 3.1B right panel; N = 4 at 6 dpi, N = 6 at 2-3 wpi and 4-6 wpi, N = 5 at 10-12 wpi, Tukey's multiple comparison test: p =

0.0245, p = 0.008, p = 0.01498 respectively). Pairwise comparisons between the untrained and trained groups suggest a greater number of VGLUT1$^+$ boutons at 2-3 wpi in the trained mice compared to untrained mice (Fig. 3.1E; N = 4 untrained animals, N = 6 trained animals, t-tests with Bonferroni's multiple-comparisons correction: p = 0.0007).

We then normalized the number of VGLUT1$^+$ boutons by an estimate of soma area and calculated the number of boutons per area and found changes only in untrained animals (Fig. 3.1C; N = 17 untrained animals and N = 18 trained animals; one-factor ANOVA, p = 0.003 for untrained animals, p = 0. 4525 for trained animals). In the untrained group, bouton density was decreased between sham and the longer-term injury time points 2-3, 4-6, and 10-12 wpi (Fig. 3.1.1 C left panel; N = 5 sham and at 10-12 wpi, N = 4 at 2-3 wpi and 4-6 wpi, Tukey's multiple comparison test: p = 0.0004, p = 0.0421, and p = 0.0160, respectively). Pairwise comparisons of VGLUT1$^+$ bouton density on dI3 INs from trained versus untrained mice failed to show any differences (Fig. 3.1F; N = 4-5 untrained and trained animals, t-tests with Bonferroni's multiple-comparisons correction).

We also measured the size of VGLUT1$^+$ boutons to dI3 INs by measuring the maximum diameter of each bouton at different time points after injury. We found very small but statistically significant differences in the size of boutons in the untrained and trained animals (Fig. 3.1D; n = 273-388 boutons in untrained animals and n = 346-459 boutons in trained animals; one-factor ANOVA, p < 0.0001 for untrained and trained animals). The VGLUT1$^+$ boutons to dI3 INs in sham (mean = 2.0 ± 0.4 μm) was similar or larger than VGLUT1$^+$ boutons to dI3 INs in SCI mice, which ranged in average from 1.6 to 1.9 μm. Pairwise comparisons of VGLUT1$^+$ bouton size on dI3 INs from trained versus untrained mice suggest differences at 2-3 dpi (Fig. 3.1G; n = 273 synapses in untrained animals and 459 synapses in trained animals, t-tests with Bonferroni's

multiple-comparisons correction, $p < 0.0001$) and at 10-12 wpi (Fig. 3.1G; n = 375 synapses in untrained animals and 346 synapses in trained animals, t-tests with Bonferroni's multiple-comparisons correction, $p < 0.0001$).

No changes were observed in the number of VGLUT1$^+$ boutons on motoneurons in either of the trained and untrained animals (Fig. 3.1I; N = 17 untrained animals and N = 21 trained animals; one-factor ANOVA, $p = 0.54$ for untrained animals, $p = 0.26$ for trained animals). Pairwise comparisons between the untrained and trained groups at different time points failed to reveal any differences in VGLUT1$^+$ boutons to motoneurons due to training (Fig. 3.1L, t-tests with Bonferroni's multiple-comparisons correction). On the other hand, differences were revealed when analyzing the density of VGLUT1$^+$ bouton on motoneurons. VGLUT1$^+$ bouton density on motoneurons was higher at the longer-term injury time points 2-3, 4-6, and 10-12 wpi than 6 dpi in untrained animals (Fig. 3.1J left panel; N = 4 at 6 dpi, 2-3 wpi, and 4-6 wpi, N = 5 dpi at 10-12 wpi, Tukey's multiple comparison test: $p < 0.0001$, $p < 0.0001$, and p = 0.0208, respectively). Similarly, VGLUT1$^+$ bouton density on motoneurons was higher at the longer-term injury time points 2-3, 4-6, and 10-12 wpi than both sham and 6 dpi in trained animals (Fig. 3.1J right panel; N = 4 at 6 dpi, 2-3 wpi, and 4-6 wpi, N = 5 dpi sham and at 10-12 wpi, Tukey's multiple comparison test: $p < 0.0001$, p – 0.0004, and p = 0.0021, respectively in comparison to sham, $p < 0.0001$ for all comparisons between 2-3, 4-6, and 10-12 wpi and 6 dpi). Pairwise comparisons of VGLUT1$^+$ bouton density on MNs from trained versus untrained mice failed to show any differences (Fig. 3.1.1 M; t-tests with Bonferroni's multiple-comparisons correction).

An analysis of the size of VGLUT1$^+$ boutons to MNs at different time points after injury revealed similar findings to dI3 INs. We found very small but statistically significant differences in the size of boutons in the untrained and trained animals (Fig. 3.1K; n = 912-1110 boutons in

untrained animals and n = 912-1248 boutons in trained animals; one-factor ANOVA, $p < 0.0001$ for untrained and trained animals). The VGLUT1$^+$ boutons to MNs in sham (mean = 2.0 ± 0.5 μm) was larger than VGLUT1$^+$ boutons to MNs in SCI mice, where the average VGLUT1$^+$ boutons ranged from 1.6 to 1.9 μm. Pairwise comparisons of VGLUT1$^+$ bouton size on MNs from trained versus untrained mice revealed a difference at 2-3 wpi (Fig. 3.1N; n = 916 synapses in untrained animals and 1216 synapses in trained animals, t-tests with Bonferroni's multiple-comparisons correction, $p < 0.0001$).

Overall, our data suggest that changes in the number of sensory inputs were limited to dI3 INs and not motoneurons. The changes in the number of VGLUT1$^+$ boutons to dI3 INs were only observed at specific time points; the timing depended on whether the animal received treadmill training. A difference in the number of VGLUT1$^+$ inputs between trained and untrained animals was only seen in dI3 INs and only at 2-3 wpi. When accounting for soma size, MNs showed an increase in VGLUT1$^+$ bouton density at longer time points after SCI, whereas untrained dI3 INs showed a decrease in VGLUT1$^+$ bouton density at longer time points after SCI. An analysis of bouton size suggests that VGLUT1$^+$ boutons to dI3 INs and MNs are smaller at many time points after injury compared to sham.

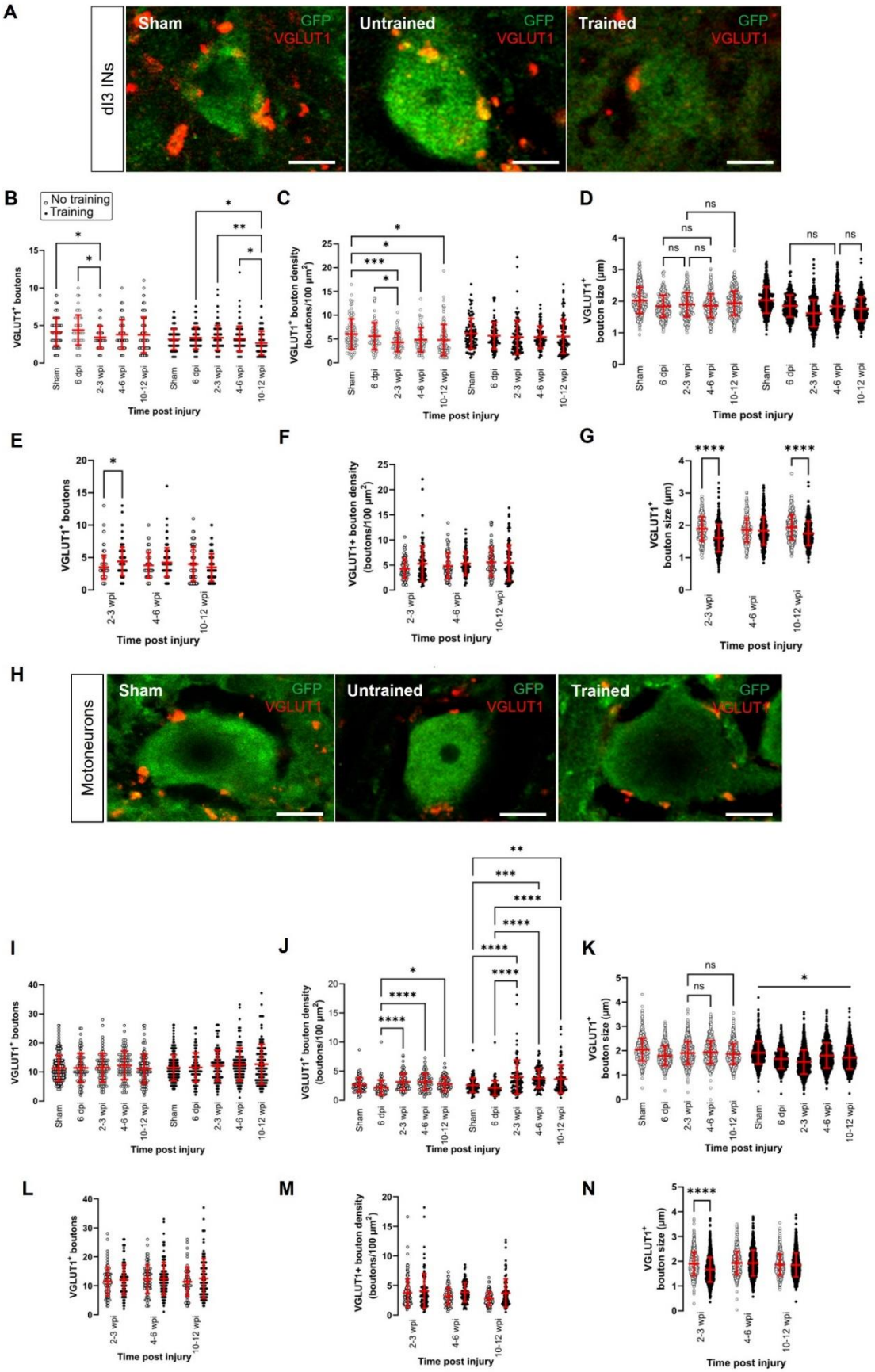
A
dI3 INs
Sham
Untrained
Trained
GFP
VGLUT1
B
No training
Training
VGLUT1+ boutons
C
VGLUT1+ bouton density (boutons/100 µm²)
D
VGLUT1+ bouton size (µm)
ns
Sham
6 dpi
2-3 wpi
4-6 wpi
10-12 wpi
Time post injury
E
F
G
H
Motoneurons
I
J
K
L
M
N

Figure 3.1 Changes in VGLUT1$^+$ sensory inputs to dI3 INs and MNs following SCI. Immunostaining of sensory boutons from proprioceptive and mechanoreceptive afferents onto **(A)** dI3 INs and **(H)** MNs from 10 to 12 wpi animals (except for sham). Number of VGLUT1$^+$ boutons per lumbar **(B)** dI3 IN and **(I)** MNs; VGLUT1$^+$ bouton density per lumbar **(C)** dI3 IN and **(J)** MNs; and size of VGLUT1$^+$ boutons to **(D)** dI3 INs and **(K)** MNs in mice that did not receive (left) and received treadmill training (right). The data in left and right panels of **(B–D,I–K)** for sham and 6 dpi are the same as neither group underwent training post-surgery. Comparing the effect of locomotor training on the number of VGLUT1$^+$ boutons, their density, and their size, respectively, for **(E–G)** dI3 INs and **(L–N)** MNs at different time points post-injury. Circles denote counts for individual cells. Red lines denote ± SD. $^{*}p \leq 0.05$, $^{**}p \leq 0.01$, $^{***}p \leq 0.001$, $^{****}p \leq 0.0001$ (Tukey's multiple comparison test following one-factor ANOVA for **(B-D, I-K)**; *t*-tests with Bonferroni's multiple-comparisons correction for **(E-G, L–N)**. In all of **(D)** and just **(K)** left, all pairwise comparisons are significant unless noted by ns. In **(K)** right, all pairwise comparisons are statistically significant. Scale bar in images = 10 μm. N=38 mice.

3.1.2 Changes in central excitatory inputs

Next, we investigated whether there were changes in central excitatory inputs to dI3 INs and MNs after SCI. While sensory boutons in the spinal cord are labelled by VGLUT1$^+$, excitatory glutamatergic boutons from central neurons are labelled exclusively by VGLUT2$^+$ (Fig. 3.2A, D) except for corticospinal inputs that are labelled by VGLUT1$^+$ (Persson et al., 2006). We observed several changes in the dI3 INs (Fig. 3.2B; N = 15 untrained animals and N = 21 trained animals; one-factor ANOVA, $p < 0.0001$ for untrained animals, $p < 0.0001$ for trained animals) and MNs of both untrained and trained animals (Fig. 3.2E; N = 15 untrained animals and N = 21 trained animals; one-factor ANOVA, $p < 0.0001$ for untrained animals, $p < 0.0001$ for trained animals).

In the untrained animals, there were no changes in VGLUT2$^+$ inputs to dI3 INs until 4-6 wpi where there was a significant decrease compared to sham, 6 dpi and 2-3 wpi (Fig. 3.2B left panel; N = 10 sham and N = 4 at 6 dpi, 2-3 wpi and 4-6 wpi, Tukey's multiple comparison test: $p = 0.0003$, $p < 0.0001$, $p = 0.0009$ respectively) and a further decrease at 10-12 wpi (Fig. 3.2B left panel; N = 3, Tukey's multiple comparison test: $p = 0.026$).

On the other hand, in the trained animals, there was an initial increase in VGLUT2$^+$ inputs to dI3 INs at 2-3 wpi compared to sham (Fig. 3.2B right panel; N = 10 sham and N = 6 animals at 2-3 wpi, Tukey's multiple comparison test: $p = 0.0005$) but this increased excitatory inputs did not last long and was decreased at 4-6 wpi (Fig. 3.2B right panel; N = 6 animals, $p < 0.0001$) and further decreased at 10-12 wpi (Fig. 3.2 B right panel; N = 5 animals, $p < 0.0001$). A pairwise comparison between the untrained and trained groups showed that there was a significant increase in the level of VGLUT2$^+$ boutons to dI3 INs in the mice that received treadmill training at 2-3 wpi (Fig. 3.2C; N = 4 untrained animals, N = 6 trained animals, t-tests with Bonferroni's multiple-comparisons correction: $p = 0.0119$).

In the motoneurons of both untrained and trained mice, we observed an initial decrease in the level of VGLUT2^{+} boutons at 6 dpi compared to sham (Fig. 3.2E; N = 10 sham and N = 4 animals at 6 dpi, Tukey's multiple comparison test: $p = 0.0115$ untrained and $p = 0.0193$ trained), which later increased in both groups at 2-3 wpi (Fig. 3.2E; N = 4 untrained and N = 6 trained animals, Tukey's multiple comparison test: $p = 0.0393$ untrained and $p < 0.0001$ trained) but then decreased at 10-12 wpi (Fig. 3.2E; N = 3 untrained and N = 5 trained animals, Tukey's multiple comparison test: $p = 0.0016$ untrained and $p < 0.0001$ trained). A pairwise comparison between the untrained and trained groups showed that there was a significant increase in the level of VGLUT2^{+} boutons to MNs at 2-3 wpi in the mice that received treadmill training (Fig. 3.2F; N = 4 untrained and N = 6 trained animals, t-tests with Bonferroni's multiple-comparisons correction: $p = 0.0007$).

Overall, VGLUT2^{+} inputs to dI3 INs and MNs showed either an increase or decrease shortly after the injury, but at 10-12 wpi, VGLUT2^{+} levels to both types of neurons were lower when compared to sham animals in both trained and untrained animals.

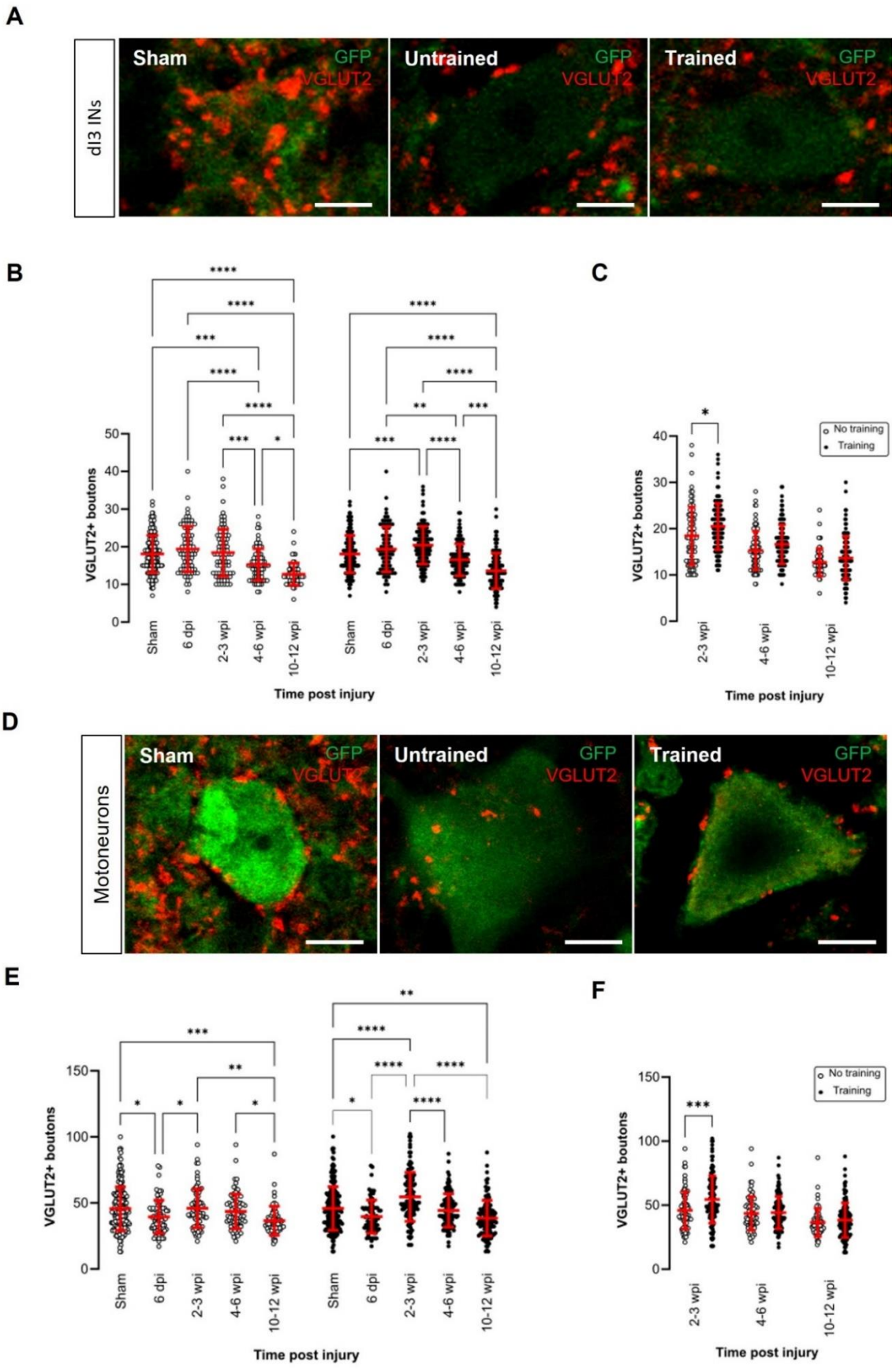
A
dI3 INs
Sham
Untrained
Trained
GFP
VGLUT2
B
VGLUT2+ boutons
Sham
6 dpi
2-3 wpi
4-6 wpi
10-12 wpi
Time post injury
C
No training
Training
VGLUT2+ boutons
2-3 wpi
4-6 wpi
10-12 wpi
Time post injury
D
Motoneurons
Sham
Untrained
Trained
GFP
VGLUT2
E
VGLUT2+ boutons
Sham
6 dpi
2-3 wpi
4-6 wpi
10-12 wpi
Time post injury
F
No training
Training
VGLUT2+ boutons
2-3 wpi
4-6 wpi
10-12 wpi
Time post injury

Figure 3.2 Changes in VGLUT2^{+} central excitatory inputs to dI3 INs and MNs following SCI. Immunostaining of excitatory boutons from spinal neurons onto **(A)** dI3 INs and **(D)** MNs from 10 to 12 wpi animals (except for sham). **(B)** Number of VGLUT2 + boutons per lumbar dI3 IN and **€** MNs in the mice that did not receive (left) and received treadmill training (right). The data in left and right halves of **(B,E)** for sham and 6 dpi are the same as neither group underwent training post-surgery. **(C)** Comparing the effect of locomotor training in dI3 INs and **(F)** in MNs at different time points post-injury. Circles denote counts for individual cells. Red lines denote ± SD. $^{*}p \leq 0.05$, $^{**}p \leq 0.01$, $^{***}p \leq 0.001$; $^{****}p \leq 0.0001$ (Tukey's multiple comparison test following one-factor ANOVA for **(B,E)**; *t*-tests with Bonferroni's multiple-comparisons correction for **(C,F)**). Scale bar in images = 10 μm.

3.1.3 Changes in GABApre inputs onto sensory afferents

Excitatory inputs are important in reactivating the dormant circuits after SCI. However, inhibitory inputs gating the sensory afferents may also play a critical role in keeping a proper balance between excitation and inhibition within the spinal cord (Bertels et al., 2022). A prominent circuit that can gate the excitation of dI3 INs and MNs is formed by the spinal GABAergic neurons (referred to herein as GABApre neurons) that mediate presynaptic inhibition of VGLUT1-expressing central proprioceptive sensory terminals and cutaneous sensory afferents (Betley et al., 2009; Hughes et al., 2005). Therefore, we next looked at changes in presynaptic inhibition of sensory afferents onto dI3 INs and MNs after SCI.

GABApre terminals are distinguished from postsynaptic GABAergic terminals in the spinal cord by the dual expression of the two GAD isoforms, GAD65 and GAD67 (Erlander and Tobin, 1991). Thus, we used antibodies against GAD65/67 as molecular markers for terminals mediating presynaptic inhibition in the spinal cord and sought GAD65/67^{+} terminals in contact with VGLUT1^{+} sensory boutons (Fig. 3.3A, D). In contrast, postsynaptic GABAergic inhibitory neurons directly target the cell body or dendrites of spinal neurons and are identified by GAD67 staining. Therefore, we quantified the percentage of VGLUT1^{+} boutons with GAD65/67^{+} boutons.

In the dI3 INs, changes in GABApre boutons were only observed in the untrained animals (Fig. 3.3B; N = 17 untrained animals and N = 21 trained animals; one-factor ANOVA, $p = 0.0035$ for untrained animals, $p = 0.077$ for trained animals). There was a significant increase in the level of GABApre boutons onto VGLUT1^{+} sensory inputs to dI3 INs from untrained animals at 2-3 wpi compared to sham (Fig. 3.3B left panel; N = 10 in sham and N = 4 at 2-3 wpi, Tukey's multiple comparison test: $p = 0.0153$), which later was reduced at 10-12 wpi to levels similar to sham levels (Fig. 3.3B left panel; N = 5 at 10-12 wpi, Tukey's multiple comparison test: $p = 0.0225$ for test

between 2-3 wpi and 10-12 wpi; p = 0.9982 for test between sham and 10-12 wpi). A pairwise comparison between the trained and untrained animals at different time points failed to reveal any differences between the groups (Fig. 3.3D; t-tests with Bonferroni's multiple-comparisons correction).

On the other hand, we observed several changes in the MNs of both untrained and trained animals (Fig. 3.3G; N = 17 untrained animals and N = 21 trained animals; one-factor ANOVA, p = 0.0005 for untrained animals, p = 0.0032 for trained animals). In the untrained group, there was an initial increase in the level of GABApre boutons at 6 dpi compared to sham (Fig. 3.1.3 G left panel, N = 10 sham, N = 4 animals at 6 dpi, Tukey's multiple comparison test: p = 0.0143), which then decreased at 2-3 wpi (Fig. 3.3G left panel; N = 4 animals, Tukey's multiple comparison test: p = 0.0079) and further decreased at 10-12 wpi (Fig. 3.3G left panel; N = 5 animals, Tukey's multiple comparison test: p = 0.0002). The same pattern was observed in the trained animals where there was an increase at 6 dpi compared to sham (Fig. 3.3G right panel; N = 10 in sham and N = 4 animals at 6 dpi, Tukey's multiple comparison test: p = 0.0059) and then later decreased at 4-6 wpi (Fig. 3.3G right panel; N = 6 animals, Tukey's multiple comparison test: p = 0.0103). A pairwise comparison between the untrained and trained groups showed a significant increase in the level of presynaptic inhibition at 2-3 wpi in the mice that received treadmill training (Fig. 3.3I; t-tests with Bonferroni's multiple-comparisons correction: p = 0.014).

The size of GABApre terminals was measured in dI3 INs (Fig. 3.3H; n = 359-521 boutons in untrained animals and n = 453-636 boutons in trained animals; one-factor ANOVA, $p < 0.0001$ for untrained and trained animals) and MNs (Fig. 3.3H; n = 1071-1326 boutons in untrained animals and n = 1301-1719 boutons in trained animals; one-factor ANOVA, $p < 0.0001$ for untrained and trained animals). The GABApre terminals on VGLUT1$^+$ inputs to dI3 INs or MNs

in sham (dI3 INs: mean = 0.8 ± 0.2 μm; MNs: mean = 0.8 ± 0.2 μm) were smaller in SCI mice, where the mean ranged between 0.6 to 0.7 μm for both dI3 INs and MNs. Pairwise comparisons of GABApre terminal size on VGLUT1$^+$ boutons in dI3 INs and MNs from trained versus untrained mice showed differences at all injury time points (Fig. 3.3J; t-tests with Bonferroni's multiple-comparisons correction, $p < 0.0001$ for all time points).

Overall, levels of GABApre boutons onto VGLUT1$^+$ inputs to dI3 INs in untrained animals and MNs in untrained and trained animals showed a pattern of short-term increases compared to sham levels, followed by decreases though never to levels below sham levels. There were no detectable changes in presynaptic inhibition to VGLUT1$^+$ inputs to dI3 INs in trained animals. Training increased presynaptic inhibition to VGLUT1$^+$ inputs to MNs at 2-3 wpi.

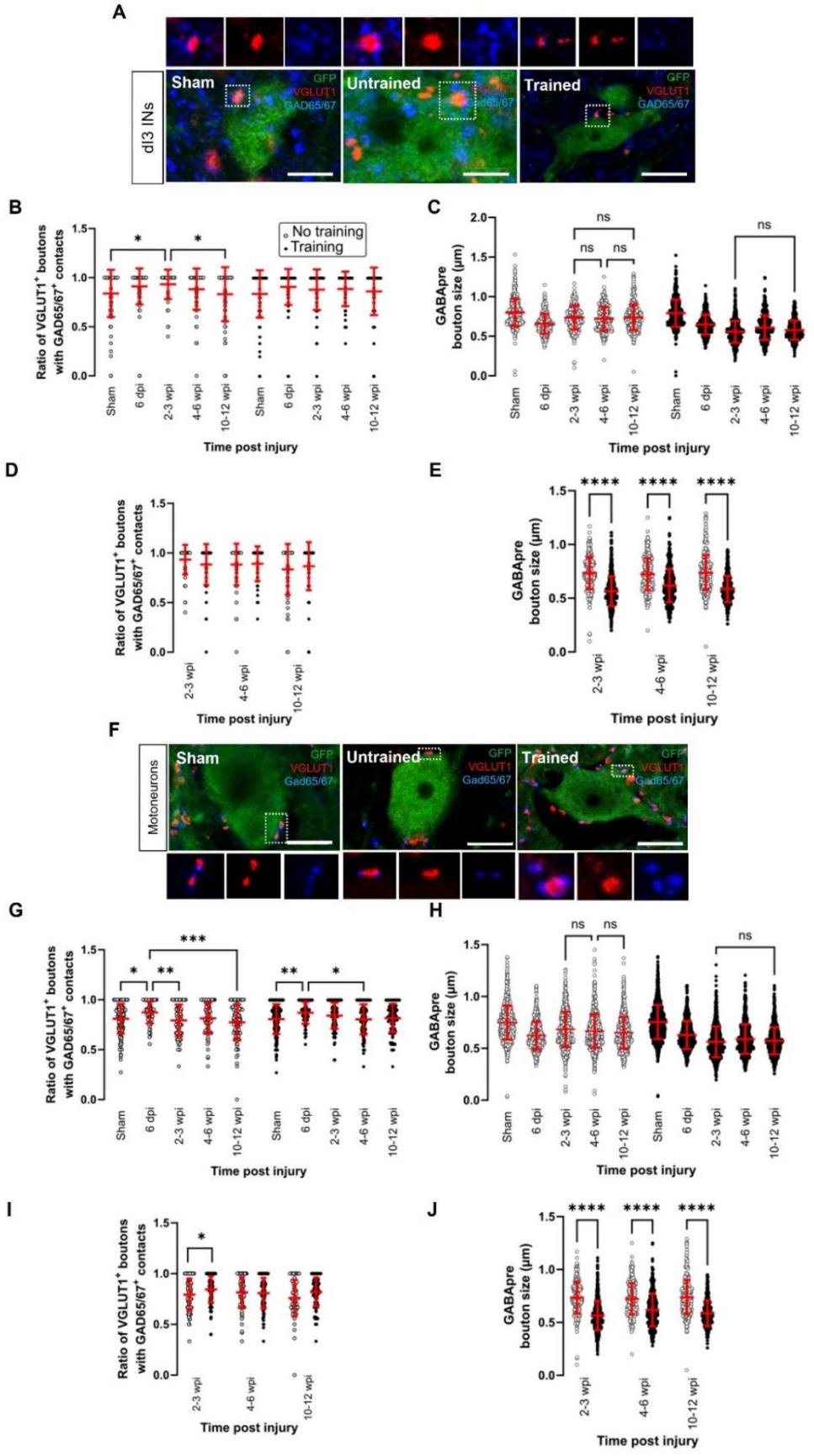
A
dI3 INs
Sham
Untrained
Trained
GFP
VGLUT1
GAD65/67
B
Ratio of VGLUT1+ boutons with GAD65/67+ contacts
No training
Training
Sham
6 dpi
2-3 wpi
4-6 wpi
10-12 wpi
Time post injury
C
GABApre bouton size (µm)
ns
D
E
****
F
Motoneurons
Gad65/67
G
***
**
*
H
I
J

Figure 3.3. Changes in the level of GABA pre boutons onto VGLUT1 + boutons onto dI3 INs and MNs following SCI. Presynaptic inhibition of sensory boutons is stained by GAD65/67^{+} and found on VGLUT1 + terminals to (**A**) dI3 INs and (F) MNs from 10 to 12 wpi animals (except for sham). Percent of VGLUT1 + inputs with GAD65^{+} contacts per lumbar (**B**) dI3 IN and (**G**) MN, and size of GAD65/67^{+} contacts on VGLUT1^{+} inputs to (**C**) dI3 INs and (**H**) MNs in the mice that did not receive (left panel) and received treadmill training (right panel). The data in left and right halves of (**B,C,G,H**) for sham and 6 dpi are the same as neither group underwent training post-surgery. Comparing the effect of locomotor training on the percentage of VGLUT1^{+} inputs with GAD65/67^{+} contacts and the size of GAD65/67^{+} contacts on VGLUT1^{+} inputs, respectively, to (**D,E**) dI3 INs and (**I,J**) MNs at different time points post-injury. Circles denote counts for individual cells. Red lines denote ± SD. $^{*}p \leq 0.05$, $^{**}p \leq 0.01$, $^{***}p \leq 0.001$, $^{****}p \leq 0.0001$ (Tukey's multiple comparison test following one-factor ANOVA for (**B,C,G,H**); *t*-tests with Bonferroni's multiple-comparisons correction for (**D,E,I,J)**. (C,H) All pairwise comparisons are significant unless noted by ns. Scale bar in images = 10 μm.

3.1.4 Between upper and lumbar dI3 INs and MNs

We compared changes in synaptic inputs to upper (L1-L3) versus lower (L4-L6) lumbar dI3 INs and MNs (Figs. 3.4 and 3.5). Most of the changes observed in the overall population of lumbar dI3 INs and MNs were observed in the upper and lower lumbar subsets of dI3 INs and MNs. We did notice that changes in the number of VGLUT1^{+} boutons after SCI were only observed in lower lumbar dI3 INs. At the same time, the decrease in presynaptic inhibition after SCI that was seen in all MNs was absent in lower lumbar MNs.

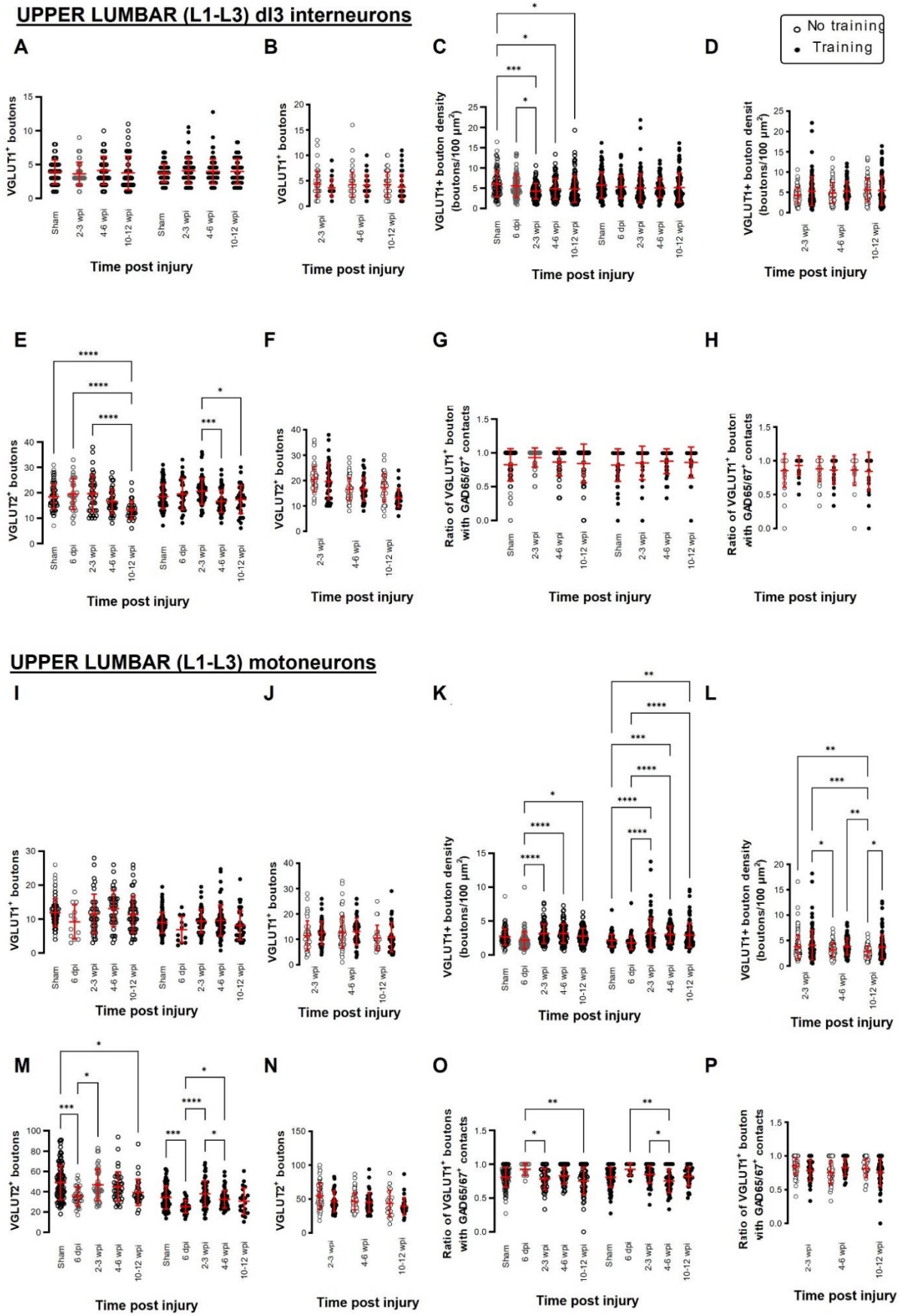
UPPER LUMBAR (L1-L3) dI3 interneurons
A
B
C
D
No training
Training
VGLUT1+ boutons
VGLUT1+ bouton density (boutons/100 µm²)
Time post injury
Sham
6 dpi
2-3 wpi
4-6 wpi
10-12 wpi
E
F
G
H
VGLUT2+ boutons
Ratio of VGLUT1+ boutons with GAD65/67+ contacts
UPPER LUMBAR (L1-L3) motoneurons
I
J
K
L
M
N
O
P

Figure 3.4. Changes in the number of VGLUT1$^+$ boutons, VGLUT1$^+$ bouton density, the number of VGLUT2$^+$ boutons, and levels of GABApre boutons to upper lumbar dI3 INs (**A-D**) and MNs (**I-L**) after spinal cord injury at different time points. Differences in spinal cord from animals with or without training after spinal cord injury in upper lumbar dI3 INs (**E-H**) and MNs (**M-P**). Circles denote counts for individual cells. Red lines denote +/- SD. *: $p \leq 0.05$, **: $p \leq 0.01$, ***: $p \leq 0.001$ (Tukey's multiple comparison test following one-factor ANOVA for A-D and E-H; paired t-t-tests with Bonferroni's multiple-comparisons correction for E-H and M-P).

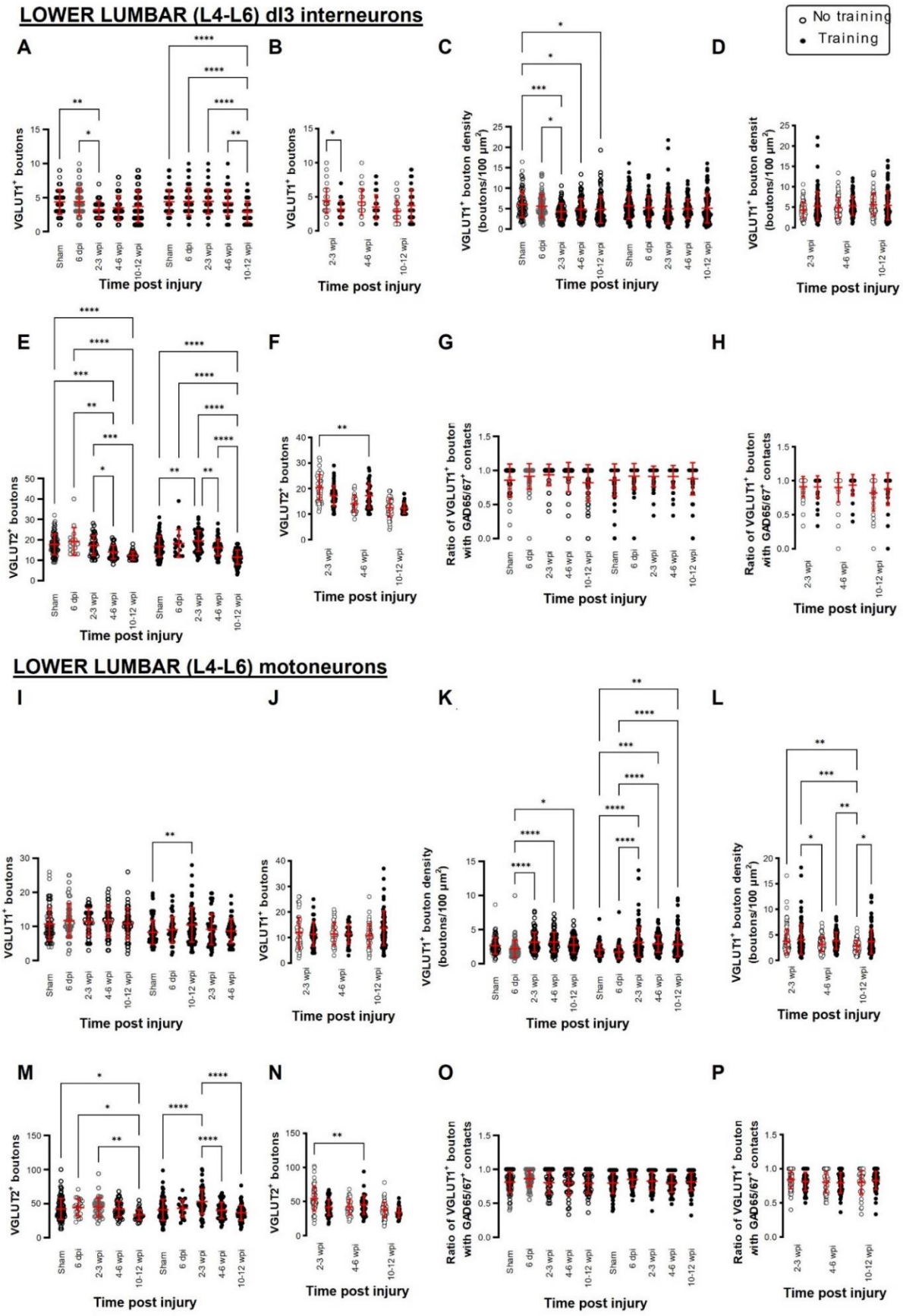
LOWER LUMBAR (L4-L6) dI3 interneurons
No training
Training
A
B
C
D
E
F
G
H
LOWER LUMBAR (L4-L6) motoneurons
I
J
K
L
M
N
O
P
VGLUT1+ boutons
VGLUT2+ boutons
VGLUT1+ bouton density (boutons/100 µm2)
Ratio of VGLUT1+ bouton with GAD65/67+ contacts
Time post injury
Sham
6 dpi
2-3 wpi
4-6 wpi
10-12 wpi

Figure 3.5. Changes in the number of VGLUT1$^+$ boutons, VGLUT1$^+$ bouton density, the number of VGLUT2$^+$ boutons, and levels of GABApre boutons to lower lumbar dI3 INs (**A-D**) and MNs (**I-L**) after spinal cord injury at different time points. Differences in spinal cord from animals with or without training after spinal cord injury in lower lumbar dI3 INs (**E-H**) and MNs (**M-P**). Circles denote counts for individual cells. Red lines denote +/- SD. *: $p \leq 0.05$, **: $p \leq 0.01$, ***: $p \leq 0.001$ (Tukey's multiple comparison test following one-factor ANOVA for A-D and E-H; paired t-t-tests with Bonferroni's multiple-comparisons correction for E-H and M-P).

3.1.5 Sex-related differences in the changes in synaptic inputs to dI3 INs and MNs after SCI

We have also performed an analysis of possible sex-related differences in the changes in synaptic inputs to dI3 INs and MNs after SCI. A two-way ANOVA for injury time-point and sex was performed for all of the changes in synaptic inputs to dI3 INs and MNs described above. Sex was a factor for the number of VGLUT2^{+} inputs to dI3 INs, the size of VGLUT1^{+} boutons to dI3 INs and MNs, and the size of GABApre terminals contacting VGLUT1^{+} inputs to dI3 INs (Fig. 3.6).

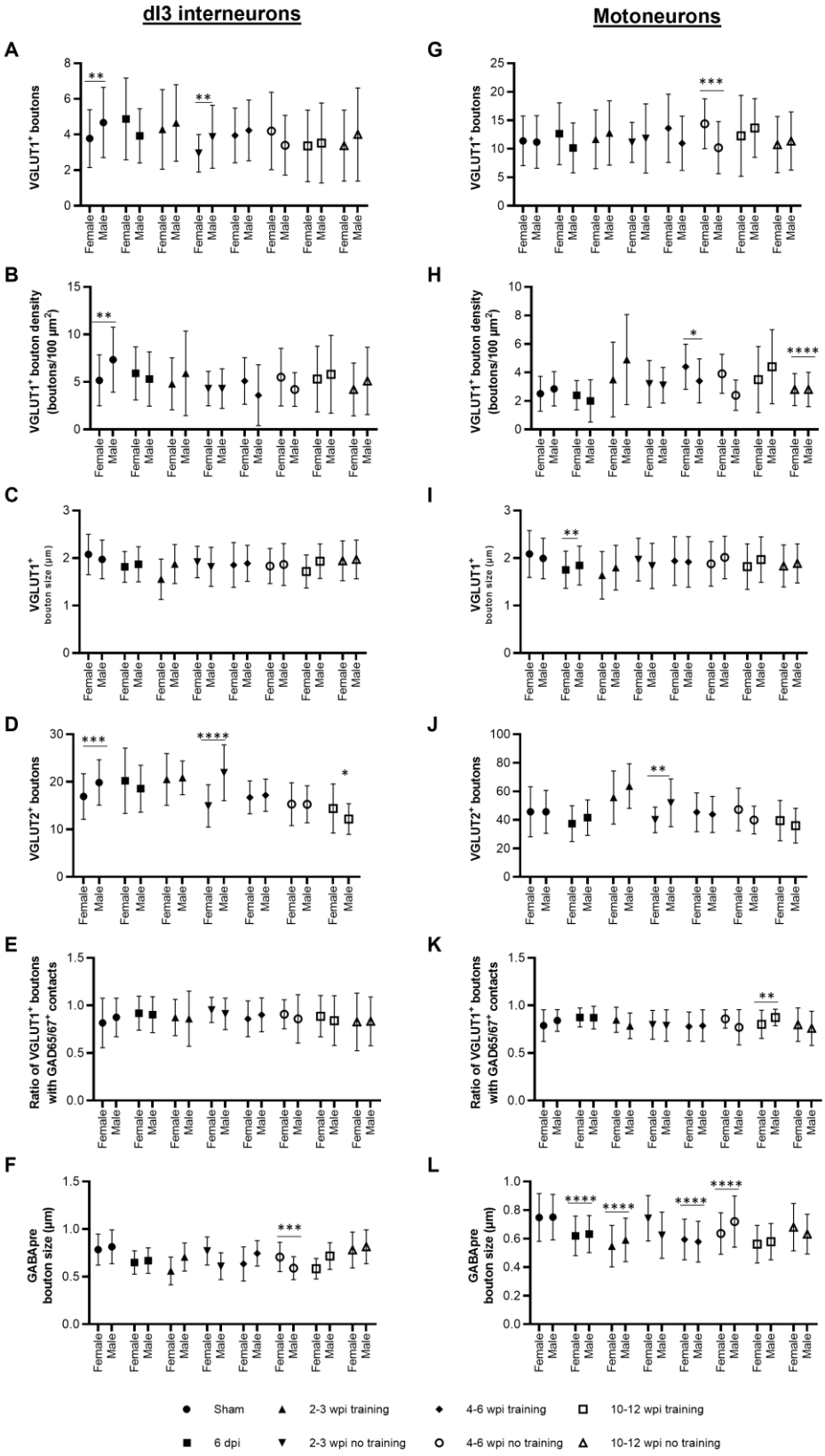
dI3 interneurons
Motoneurons
A
B
C
D
E
F
G
H
I
J
K
L
VGLUT1+ boutons
VGLUT1+ bouton density (boutons/100 µm2)
VGLUT1+ bouton size (µm)
VGLUT2+ boutons
Ratio of VGLUT1+ boutons with GAD65/67+ contacts
GABApre bouton size (µm)
Female
Male
Sham
6 dpi
2-3 wpi training
2-3 wpi no training
4-6 wpi training
4-6 wpi no training
10-12 wpi training
10-12 wpi no training

Figure 3.6. Sex-based analysis of changes in the number of VGLUT1$^+$ boutons, VGLUT1$^+$ bouton density, VGLUT1$^+$ bouton size, the number of VGLUT2$^+$ boutons, levels of presynaptic inhibition and GABApre bouton size to dI3 INs (A-F) and MNs (G-L). *: $p \leq 0.05$, **: $p \leq 0.01$, ***: $p \leq 0.001$ (Dunnett's T3 multiple comparison test following two-way ANOVA).

3.1.6 Effects of stepping function on levels of synaptic inputs to dI3 INs and MNs

Each animal in our experimental cohort underwent weekly testing for stepping function on a treadmill without any weight support provided. The number of steps performed per minute was estimated using DeepLabCut for automated hindlimb joint detection. We found no differences in the number of steps between trained and untrained animals at their experimental endpoints (Fig. 3.7A; one-factor ANOVA, $p = 0.1950$). Trained and untrained SCI animals made fewer steps than sham animals at their respective experimental endpoints (Fig. 3.7A; Tukey's multiple comparison test: $p < 0.0001$). To determine whether there was any improvement in stepping function with time post-injury, we compared the stepping function at different time points in animals whose experimental endpoint was 10-12 wpi. While some animals had their highest stepping function between 7-10 wpi, statistical testing failed to detect any differences in stepping function between the different time points (Fig. 3.7B; one-factor ANOVA, $p = 0.1395$ for untrained animals, $p = 0.2885$ for trained animals).

To determine whether there was any correlation between stepping function and levels of synaptic inputs, we performed a correlation analysis between the number of various synaptic inputs with the number of steps per minute of mice at the experimental endpoint using the non-parametric Spearman Correlation test. Correlations could not be detected between the number of VGLUT1$^+$ inputs, or presynaptic inhibition of VGLUT1$^+$ inputs to dI3 INs (Fig. 3.7D, M) or MNs (Fig. 3.7G, N) and stepping function. On the other hand, there was a negative correlation between the number of VGLUT2$^+$ inputs to dI3 INs (Fig. 3.7E) and MNs (Fig. 3.7 G) and stepping function. There were no correlations between VGLUT1$^+$ bouton density on dI3 INs or MNs and stepping function (Fig. 3.7H, J). We also tested for possible correlations with VGLUT1$^+$ bouton size and stepping function and found weak positive correlations for both dI3 INs and MNs (Fig. 3.7L, N). Weak

positive correlations for both dI3 INs and MNs was also found between GABApre bouton size and stepping function (Fig. 3.7M, O).

Animals with experiment endpoints at 10-12 wpi also had an additional testing session where they walked with manual body weight support. We compared the stepping function with body weight support at different time points. Stepping function with body weight support improved with time post-injury in untrained animals (Fig. 3.8A; N = 5 animals; one-factor ANOVA, $p < 0.001$) from 4-6 wpi to 7-10 wpi (Fig. 3.8A; Tukey's multiple comparison test: $p = 0.0186$) such that stepping function between 1-3 and 7-10 wpi was also significantly different (Fig. 3.8A; Tukey's multiple comparison test: $p < 0.0001$). Due to lighting issues, the number of steps with body weight support for the trained animals was counted manually rather than using DeepLabCut. In the trained animals, stepping function did not improve with time post-injury (Fig. 3.8B; N = 5 animals; one-factor ANOVA, $p = 0.1869$). Correlations could not be detected between levels of VGLUT1$^+$ inputs or presynaptic inhibition of VGLUT1$^+$ inputs to dI3 INs (Fig. 3.8C, H) or MNs (Fig. 3.8E, J) and stepping function in animals with body weight support. While there was a negative correlation between VGLUT2$^+$ inputs to dI3 INs and stepping function in animals with body weight support (Fig. 3.8D), no correlation was detected for VGLUT2$^+$ inputs to MNs (Fig. 3.8F). There was a negative correlation between VGLUT1$^+$ bouton density in dI3 INs and stepping function with body weight support (Fig. 3.8G). In contrast, there was a positive correlation VGLUT1$^+$ bouton density in MNs and stepping function with body weight support was found (Fig. 3.8I). Just as for stepping without weight support, we found weak positive correlations with VGLUT1$^+$ bouton size as well as GABApre bouton size and stepping function with body weight support for dI3 INs (Fig. 3.8K-L), and between GABApre bouton size and stepping function with body weight support for MNs (Fig. 3.8M-N). Since two of the mice showed relatively much greater

stepping function, we tested the effects of removing these two animals on the correlations. No changes in correlations were observed (Data not shown).

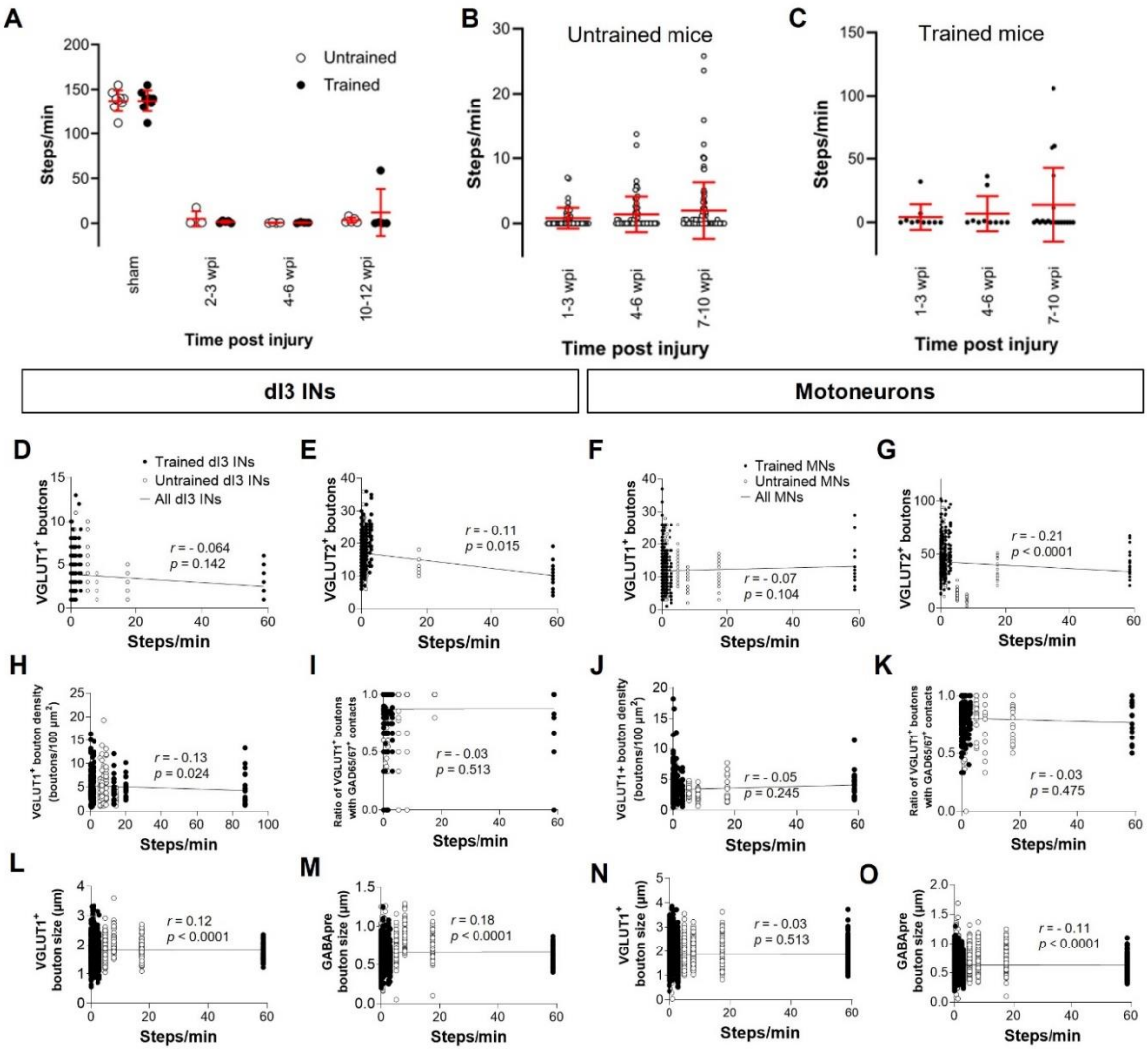

Figure 3.7. Analysis of stepping function without weight support after SCI and levels of synaptic inputs (A) Number of steps per minute at the experimental endpoint or in sham animals. (**B**) The number of steps per minute at different time points in untrained or in (**C**) trained animals with 10-12 wpi experimental endpoint. **(D)** Number of VGLUT1$^+$, (**F**) VGLUT2$^+$, and (**H**) percent of VGLUT1$^+$ boutons with GAD65/67$^+$ contacts per lumbar dI3 INs in relation to the number of steps per minute made by the SCI mice from which each neuron came from in their last testing session. **(E)** Number of VGLUT1$^+$, (**G**) VGLUT2$^+$, and (**I**) percent of VGLUT1$^+$ boutons with GAD65/67$^+$ contacts per lumbar MNs in relation to the number of steps per minute made without weight support by the SCI animal from which each neuron came from in their last testing session. Circles denote counts for individual cells. Red lines denote +/- SD.

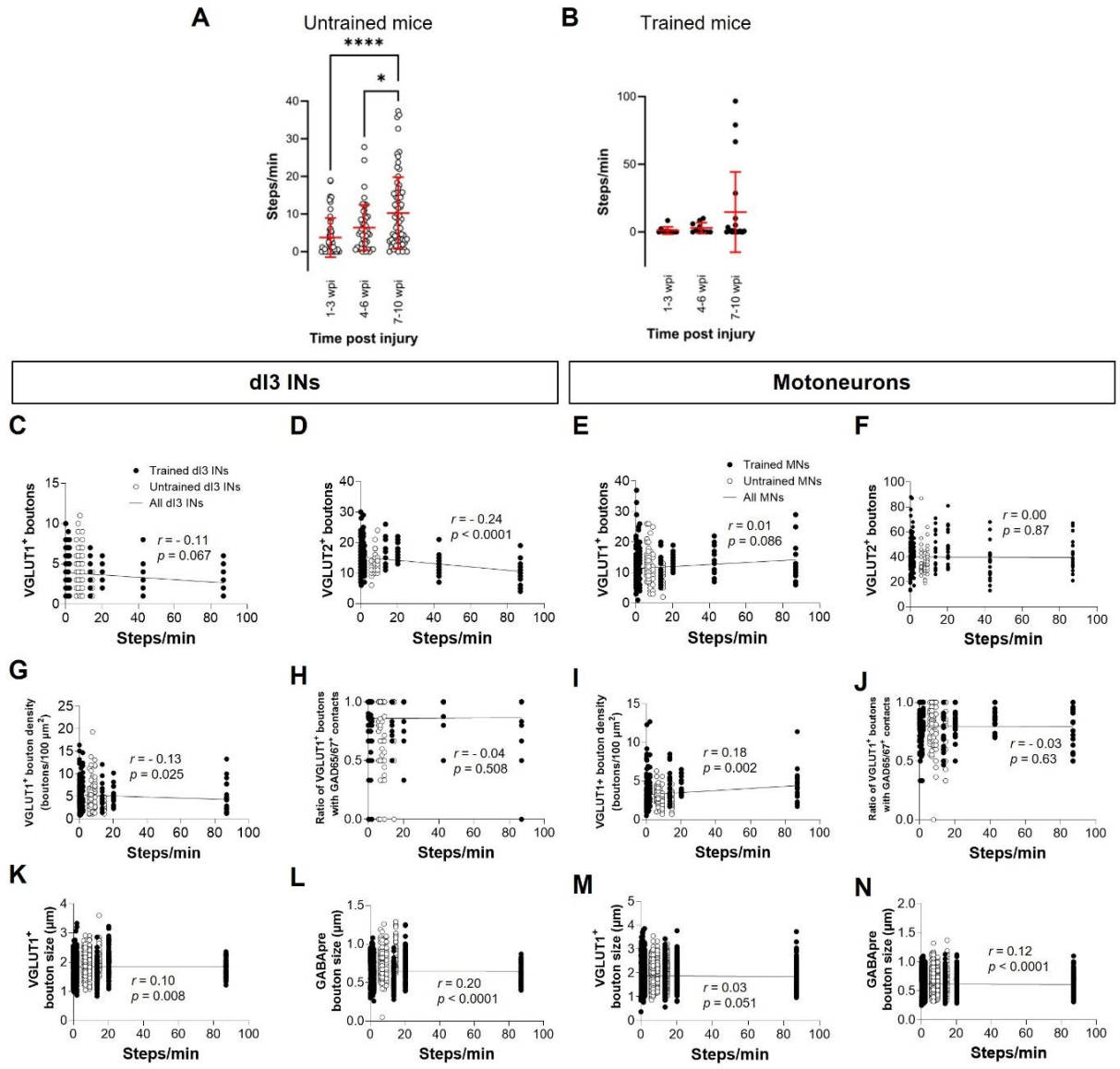

Figure 3.8. Analysis of stepping function with body weight support after SCI and levels of synaptic inputs (**A**) The number of steps per minute at different time points in untrained or in (**B**) trained animals with 10-12 wpi experimental endpoint. **(C)** Number of VGLUT1$^+$, (**E**) VGLUT2$^+$, and (**G**) percent of VGLUT1$^+$ boutons with GAD65/67$^+$ contacts per lumbar dI3 INs in relation to the number of steps per minute made by the SCI mice from which each neuron came from in their last testing session. **(D)** Number of VGLUT1$^+$, (**F**) VGLUT2$^+$, and (**H**) percent of VGLUT1$^+$ boutons with GAD65/67$^+$ contacts per lumbar MNs in relation to the number of steps per minute made with body weight support by the SCI mice from which each neuron came from in their last testing session. Circles denote counts for individual cells. Red lines denote +/- SD. *: $p \leq 0.05$, ****: $p \leq 0.0001$ (Tukey's multiple comparison test following one-factor ANOVA).

3.2.1 A new model of limb spasticity after SCI in Isl1-Vglut2^{CatCh}

My previous results provide support to a growing body of literature demonstrating plasticity of spinal circuits after SCI. However, plasticity after injury can be maladaptive and could cause secondary complications such as spasticity (Brown and Weaver, 2012). Current treatments for spasticity can be ineffective and have secondary complications (Ward et al., 2003; Marcantoni et al., 2020). Currently, there is no mouse model where hindlimb spasticity can be reliably induced in awake mice and this absence of a reliable model could hinder the development of new treatments. This study was designed to establish a new model of hindlimb spasticity where spasticity could be reliably induced as a tool that could facilitate the understanding of the mechanisms that contribute to spasticity and the development of better treatments for patients suffering from spasticity.

We have generated a transgenic strain of mice where sensory afferents innervating the skin of the hindlimbs can be stimulated by blue light illumination and induce spasticity after SCI. Our transgenic mice Isl1-Vglut2^{CatCh} conditionally express the light sensitive ion channel Calcium translocating Channelrhodopsin (CatCH) in Isl1+/VGLUT2+ cells. Expression of CatCH in this line of mice requires concurrent CRE and FLP expression. This approach was taken as Isl1 is more widely expressed in the nervous system, including motoneurons, dI3 interneurons and sensory neurons (Pfaff and Mendelsohn, 1996; A. Roy et al., 2012). To restrict the expression of any transgenes to sensory neurons, an additional constraint of requiring VGLUT2 expression restricts the expression of CatCh to sensory neurons and dI3 INs. Since dI3 INs can't be directly activated through illumination of the body due to their location within the spinal cord, in contrast, Isl1+/VGLUT2+ sensory neurons can be activated through the illumination of the hindlimbs.

First, we sought to determine which populations of sensory neurons in the lumbar dorsal root ganglions (DRGs) express the transgene CatCh in our Isl1-Vglut2^{CatCh} mice. The DRGs contain the cell bodies of primary sensory neurons including large diameter proprioceptive and mechanoreceptive neurons whose axons make up low threshold, fast conducting and myelinated Aα and Aβ fibers, as well as small diameter nociceptors that transmit pain through thinly myelinated medium velocity Aδ fibers or unmyelinated slow conducting C fibers. The population of nociceptive neurons are further divided into peptidergic (Calcitonin gene related peptide; CGRP and Transient receptor vanilloid 1; TRPV1) and non-peptidergic (the P2x3R and/or isolectin B4-binding) sub populations. The capsaicin-sensitive TRPV1 receptors are activated by thermal (Eid, 2011), mechanical (Cui et al., 2014) or both stimuli (Walder et al., 2012). They are the largest receptors that mediate pain in the DRG neurons and highly expressed in nociceptors.

To delineate between the expression in proprioceptors/mechanoreceptors and nociceptors, we looked at expression of the vesicular glutamate transporters, VGLUT1 and VGLUT2, with tdTomato. In the spinal cord, VGLUT1 is selectively expressed in central boutons of proprioceptors and low threshold mechanoreceptors while excitatory glutamatergic boutons from nociceptors and central neurons are labelled by VGLUT2 except for corticospinal inputs that are labelled by VGLUT1 (Alvarez et al., 2004). We used multiplexed RNAscope *in situ* hybridization to assess mRNA expression of VGLUT1 and VGLUT2 in the lumbar DRGs (Fig. 3.9A).

20 lumbar DRGs were selected from 3 mice for analysis. We observed that 1.0 ± 1.5 (mean ± SD) tdTomato cells expressed VGLUT1 only and 65.83 ± 37.66 tdTomato cells expressed VGLUT2 only, while 4.61 ± 3.35 cells co-expressed both VGLUT1 and VGLUT2 (one-factor ANOVA, $p < 0.0001$) (Fig. 3.9B). This represents 1.0% ± 1.49%, 77.1% ± 12.8% and 5.7% ± 4.0% of the overall tdTomato+ population, respectively (one-factor ANOVA, $p < 0.0001$) (Fig.

3.9E). Our results show that the majority of the tdTomato+ cells both in terms of number and percentage were VGLUT2+ compared to VGLUT1 (Tukey's multiple comparison test: $p < 0.0001$) (Fig. 3.9B) and VGLUT1+/VGLUT2+ (Tukey's multiple comparison test: $p < 0.0001$) (Fig. 3.9E).

In the population of VGLUT2+ cells in the sampled DRGs, 65.8 ± 37.7 cells expressed tdTomato only (i.e. VGLUT2-) and 10.7 ± 6.0 cells expressed VGLUT1 only, while 4.6 ± 3.4 cells expressed both tdTomato and VGLUT1 (one-factor ANOVA, $p < 0.0001$) (Fig. 3.9C). This represents 71.7% ± 13.7%, 15.6% ± 8.9% and 5.0% ± 3.0% of all VGLUT2+ cells, respectively (one-factor ANOVA, $p < 0.0001$) (Fig. 3.9F). There were more tdTomato+ only cells compared to VGLUT1+ only cells (Tukey's multiple comparison test: $p < 0.0001$) and compared to tdTomato+/VGLUT1+ cells (Tukey's multiple comparison test: $p < 0.0001$). As a percentage of VGLUT2+ cells, there were more tdTomato+ only cells compared to VGLUT1+ only cells (Tukey's multiple comparison test: $p < 0.0001$) and compared to tdTomato+/VGLUT1+ cells. There were also more VGLUT1+ only cells compared to tdTomato+/VGLUT1+ cells within the VGLUT2+ population (Tukey's multiple comparison test: $p = 0.0046$).

In the VGLUT1+ cell population in the sampled DRGs, 1.0 ± 1.5 cells expressed tdTomato only and 10.7 ± 6.0 cells expressed VGLUT2 only (i.e., VGLUT1-), while 4.6 ± 3.4 cells expressed both (one-factor ANOVA, $p < 0.0001$) (Fig 3.9D). Tukey's multiple comparison test suggests that within the VGLUT1+ population, there were more VGLUT2+ only cells compared to tdTomato+ only cells ($p < 0.0001$) and more VGLUT2+ cells compared to td/Tomato/VGLUT2+ cells ($p = 0.0001$) and there were more tdTomato+/VGLUT2+ cells compared to tdTomato+ cells ($p = 0.0277$). The percentage of VGLUT1+ neurons that were only tdTomato+, only VGLUT2+ and tdTomato+/VGLUT2+ was 4.6% ± 7.4%, 49.1% ± 12.0% and 18.9% ± 11.0%, respectively (one-

factor ANOVA, $p < 0.0001$) (Fig. 3.9G). Tukey's multiple comparison test confirmed that the percentage of VGLUT1+ neurons that were VGLUT2+ only was greater than those that were tdTomato+ only ($p < 0.0001$), there more VGLUT2+ only neurons compared to tdTomato+/VGLUT2+ neurons ($p < 0.0001$), and there were more tdTomato+/VGLUT2+ neurons compared to tdTomato+ cells $p = 0.0004$.

Our data indicates a higher expression of our transgene in the population of VGLUT2+ cells. Therefore, next we looked at the expression in different subpopulations of nociceptors. To look at the expression of tdTomato amongst peptidergic and non-peptidergic neurons in the DRGs of our transgenic mice, we chose TRPV1 and IB4 as markers and used immunohistochemistry to label TRPV1, IB4 and tdTomato cells (Fig. 3.10A). DRGs from lumbar segments L1-L6 of 3 mice were immunostained with primary antibodies against TRPV1, IB4 and tdTomato. Our results showed that amongst tdTomato+ cells of the DRG, 108.4 ± 74.7 cells per DRG expressed TRPV1 and 58.2 ± 37.6 cells were IB4-bound ($p = 0.0129$, Mann-Whitney t-test) (Fig. 3.10B) which corresponds to 67.7% ± 16.5% and 38.7± 13.2% of the tdTomato+ cells, respectively ($p < 0.0001$, Mann-Whitney t-test) (Fig. 3.10E). In the population of TRPV1+ cells of DRGs, 108.4 ± 74.7 cells were tdTomato+ (68.1% ± 18.6%; Fig. 3.10C, F). As expected, no TRPV1+ cells co-expressed IB4. On the other hand, 58.2 ± 37.6 IB4+ cells colocalized with tdTomato+ cells (72.0% ± 15.3%; Fig. 3.10D, G) with a complete absence of colocalization with TRPV1. Our data suggests that our transgene is expressed in both peptidergic and non-peptidergic populations of nociceptors in Isl1-Vglut2^{CatCh} animals.

TRPV1 represents a subset of peptidergic nociceptors. The neuropeptide CGRP can also be used to label peptidergic nociceptors. Figure 3.11 shows expression of CGRP and tdTomato cells in the lumbar DRG of Isl1-Vglut2^{CatCh} expressing mice. In the tdTomato+ cell population,

1.9 ± 1.6 cells expressed CGRP (4.8% ± 3.4 of the tdTomato population), while 35.3 ± 15.8 cells did not express CGRP (95.2% ± 3.4 of the tdTomato population) (Figure 3.11B, C). tdTomato expression was seen in 9.14% ± 7.5 of the CGRP+ population (Figure 3.11D). Therefore, there was relatively low colocalization levels of tdTomato and CGRP.

In spinal transverse sections, immunostaining for tdTomato+ showed expression constrained to axonal processes and synapses in the superficial layers of the dorsal horn (Fig. 3.12A) and sometimes in the deeper layers of the dorsal horn in lumbar segments (Fig. 3.12B). This expression pattern in the spinal cord is consistent with the predominant expression of tdTomato in nociceptors of the DRGs.

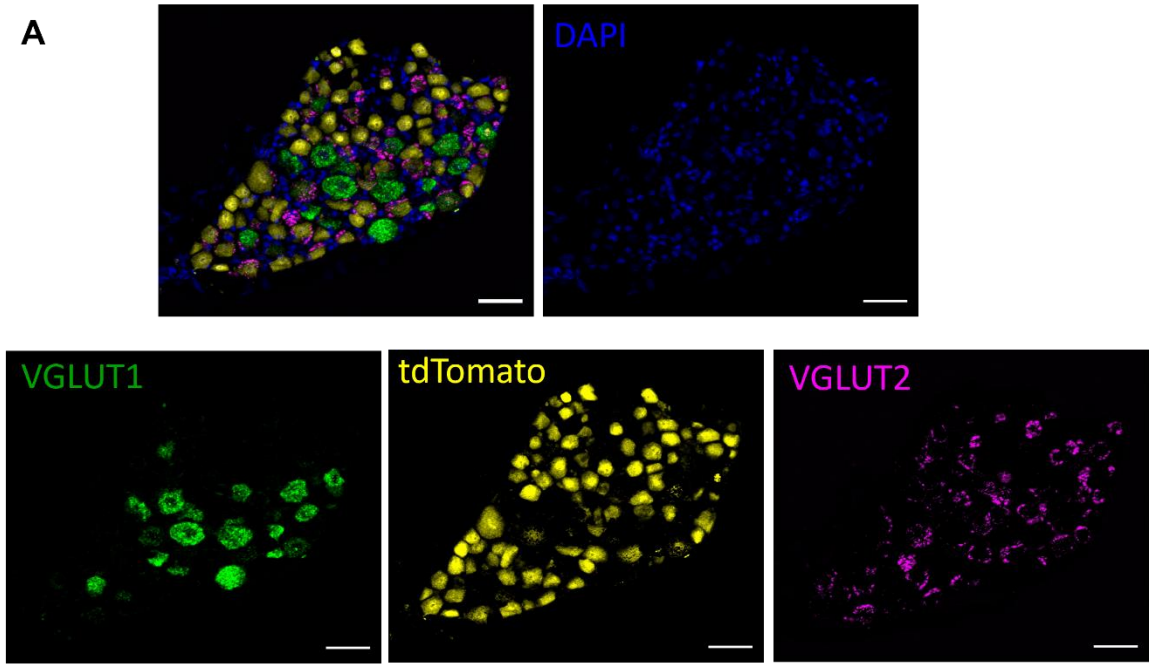
A
DAPI
VGLUT1
tdTomato
VGLUT2

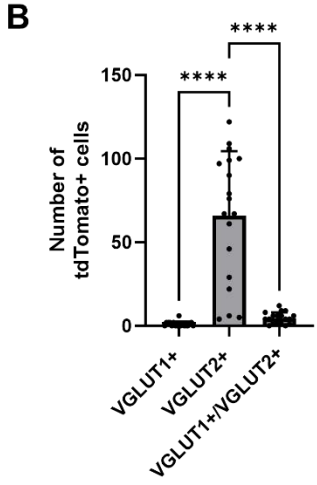
B
Number of tdTomato+ cells
150
100
50
0
****
****
VGLUT1+
VGLUT2+
VGLUT1+/VGLUT2+

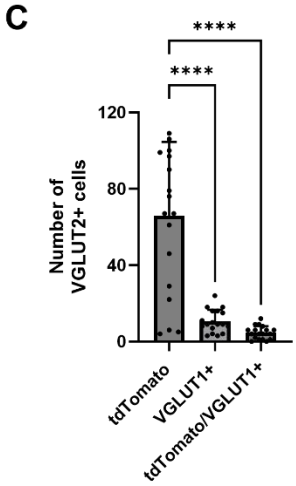
C
Number of VGLUT2+ cells
120
80
40
0
****
****
tdTomato
VGLUT1+
tdTomato/VGLUT1+

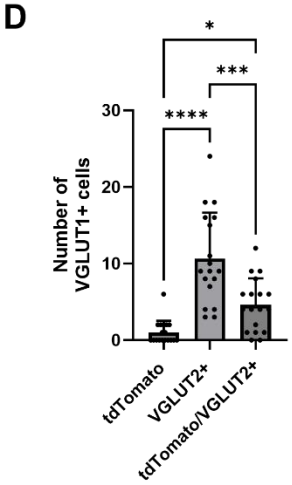
D
Number of VGLUT1+ cells
30
20
10
0
*
***
****
tdTomato
VGLUT2+
tdTomato/VGLUT2+

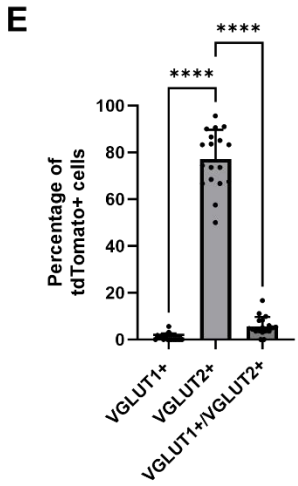
E
Percentage of tdTomato+ cells
100
80
60
40
20
0
****
****
VGLUT1+
VGLUT2+
VGLUT1+/VGLUT2+

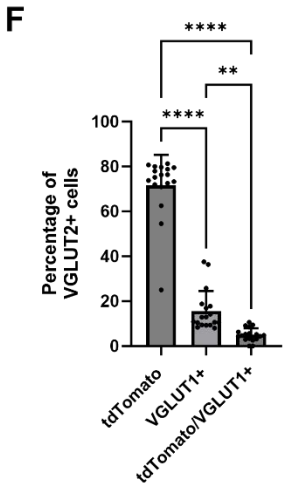
F
Percentage of VGLUT2+ cells
100
80
60
40
20
0
****
**
****
tdTomato
VGLUT1+
tdTomato/VGLUT1+

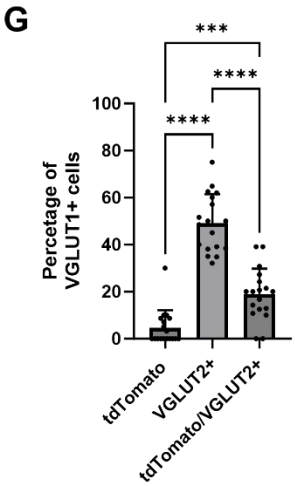
G
Percetage of VGLUT1+ cells
100
80
60
40
20
0
***
****
****
tdTomato
VGLUT2+
tdTomato/VGLUT2+

Figure 3.9 VGLUT1 and VGLUT2 expression in lumbar DRG of Isl1-Vglut2^{CatCh} mice. (A) Immunostaining of VGLUT1 and VGLUT2 mRNA in tdTomato+ cells. Scale bar = 50μm. **(B-G)** Distribution of VGLUT1 mRNA, VGLUT2 mRNA and tdTomato positive cells. Data are presented as Mean ± SD. $^{*}p \leq 0.05$, $^{**}p \leq 0.01$, $^{***}p \leq 0.001$, $^{****}p \leq 0.0001$ (Tukey's multiple comparison test following one-factor ANOVA).

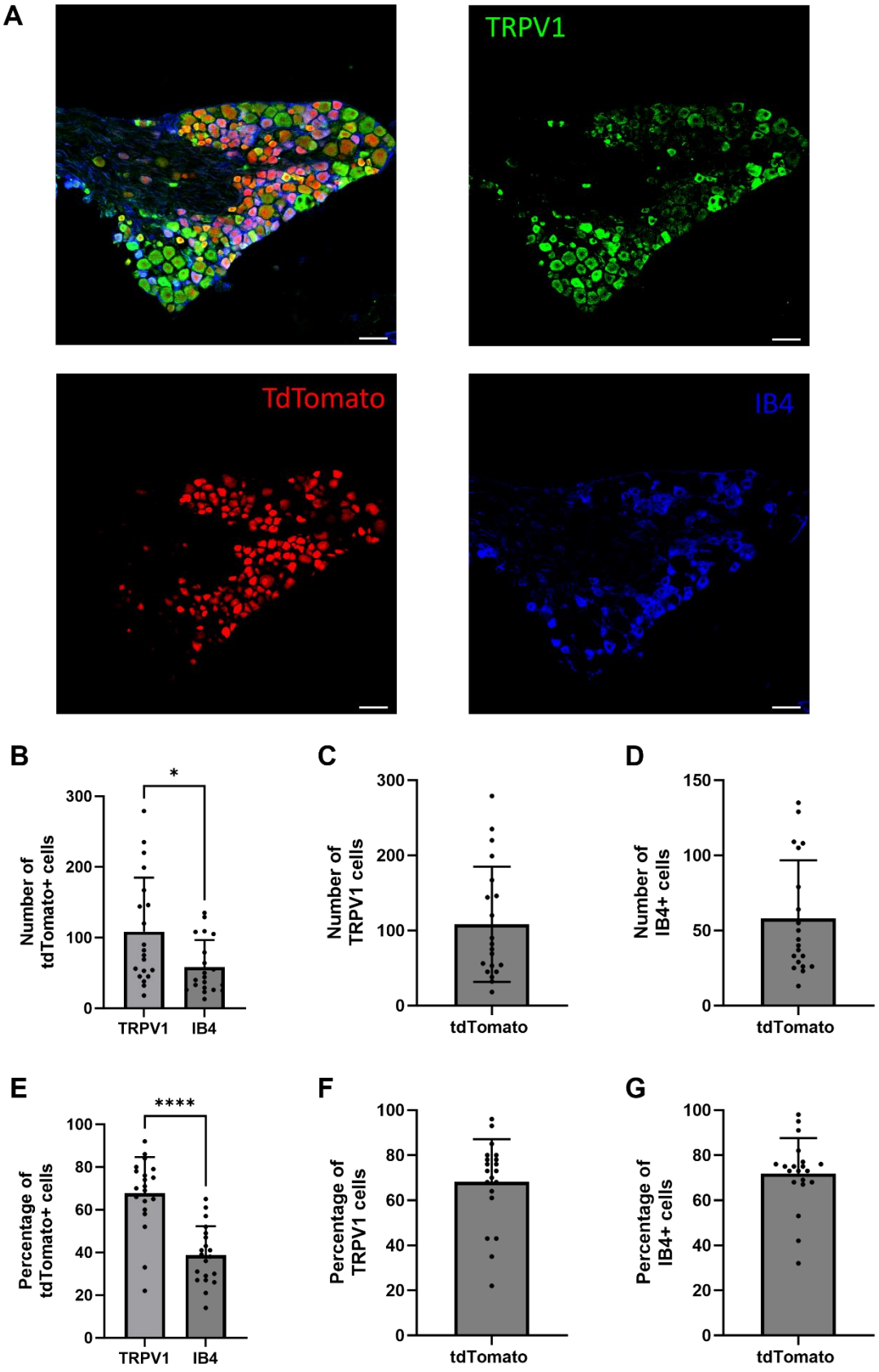
A
TRPV1
TdTomato
IB4
B
Number of tdTomato+ cells
300
200
100
0
*
TRPV1
IB4
C
Number of TRPV1 cells
300
200
100
0
tdTomato
D
Number of IB4+ cells
150
100
50
0
tdTomato
E
Percentage of tdTomato+ cells
100
80
60
40
20
0
****
TRPV1
IB4
F
Percentage of TRPV1 cells
100
80
60
40
20
0
tdTomato
G
Percentage of IB4+ cells
100
80
60
40
20
0
tdTomato

Figure 3.10 TRPV1 and IB4 expression in lumbar DRG of Isl1-Vglut2^{CatCh} mice. (A) Immunostaining of TRPV1 and IB4 In tdTomato+ cells. Scale bar = 50µm **(B-G)** Distribution of TRPV1, IB4, and tdTomato positive cells. Data are presented as Mean ± SD. $^{*}p \leq 0.05$, $^{****}p \leq 0.0001$ (Mann-Whitney t-test).

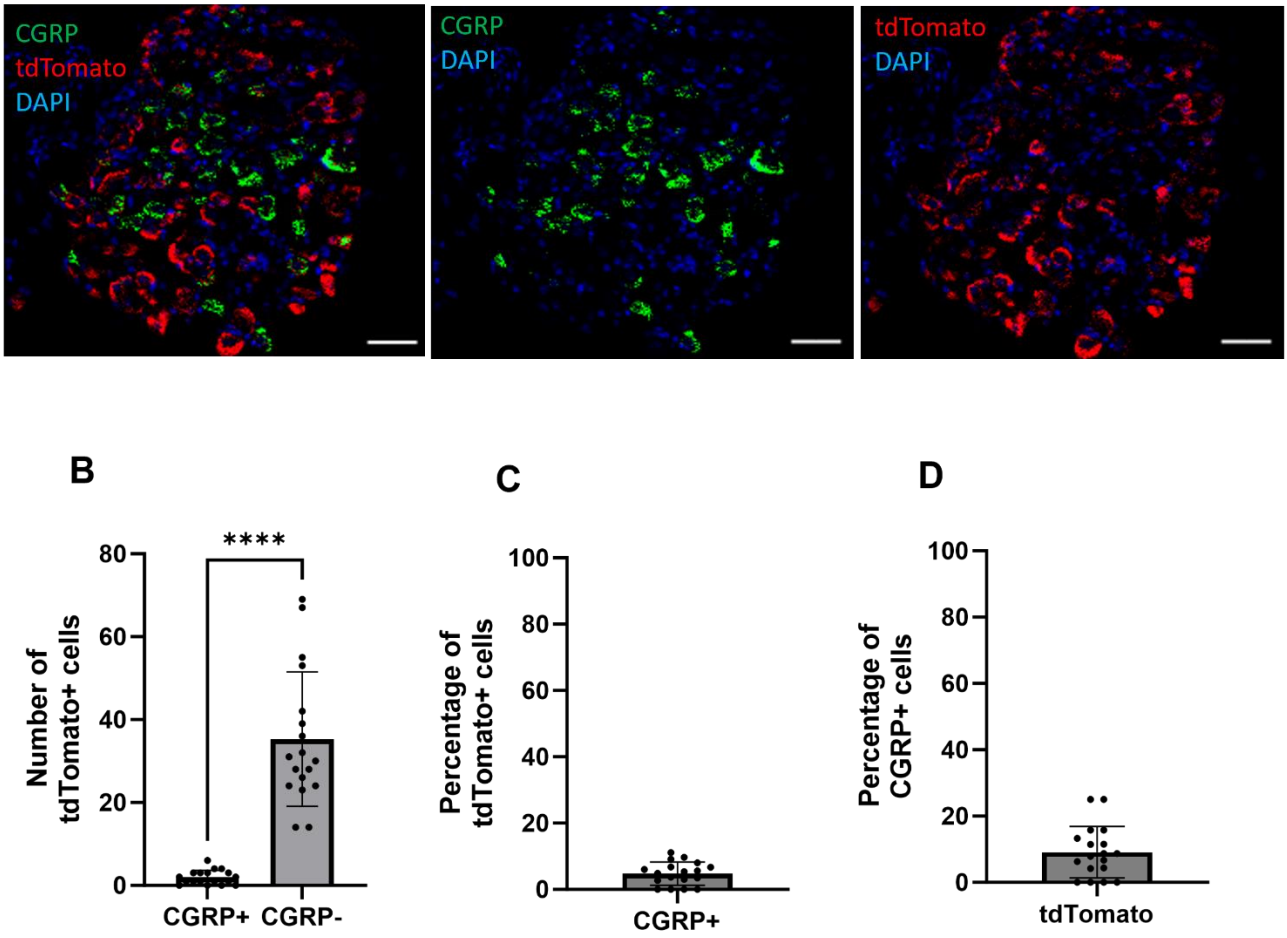

Figure 3.11 CGRP and tdTomato expression in lumbar DRG of Isl1-Vglut2^{CatCh} mice. (A) Immunostaining of CGRP mRNA in tdTomato+ cells. Scale bar = 50µm **(B)** Number of CGRP+ and CGRP- cells within the tdTomato+ population. **(C)** Percentage of tdTomato+ cells that were CGRP+. **(D)** Percentage of CGRP+ cells that were tdTomato+. Data are presented as Mean ± SD. $^{****}p \leq 0.0001$ (Mann-Whitney t- test).

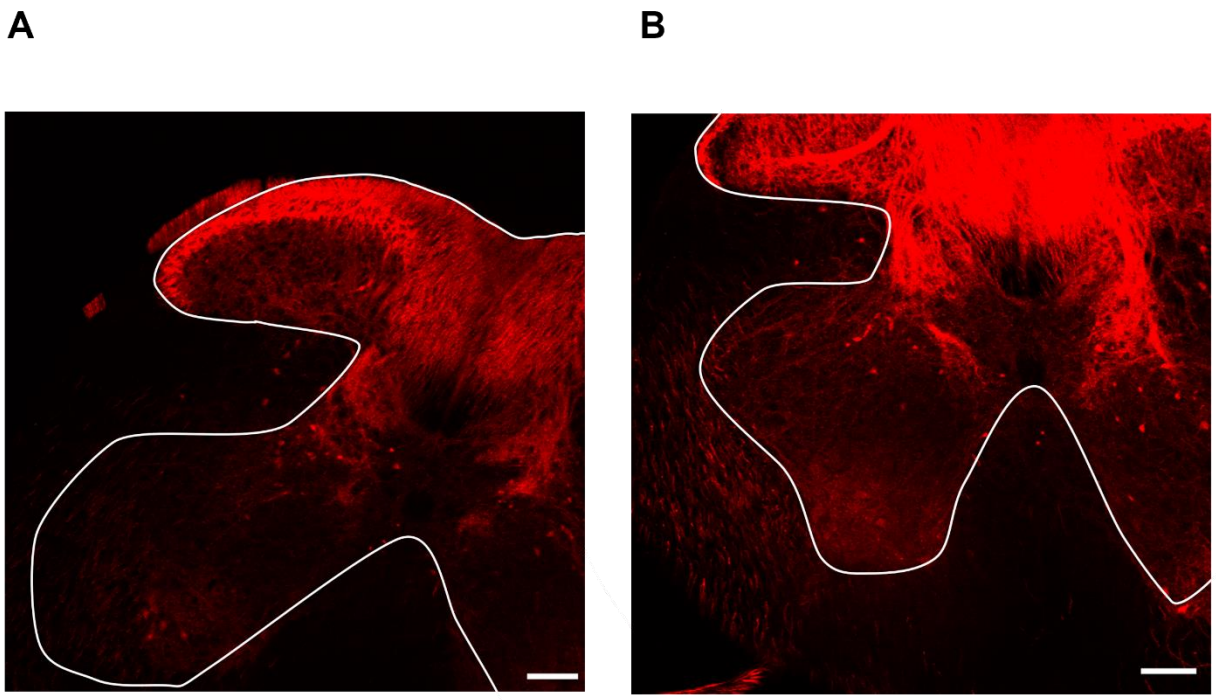

Figure 3.12 Distribution of tdTomato in the spinal cord of Isl1-Vglut2^{CatCh} mice.
Immunostaining of tdTomato+ cells in the superficial (A) and deep (B) dorsal horn layers of the grey matter of the spinal cord where nociceptive afferents are usually found. Thin white lines demarcate the gray matter. Scale bar = 50μm

3.2.2 Optogenetic stimulation of VGLUT2+ afferents in SCI mice generates bilateral muscle spasms

After characterizing the specificity of $Isl1^{+}$/$VGLUT2^{+}$-driven transgene expression in DRG neuron populations, we sought to determine whether optogenetic stimulation of the VGLUT2+ afferents in the hindpaws could generate a motor response and evoke spastic behaviours during the course of spinal cord injury. We used 15 mice (n=10 F, n=5 M, Age 2-4 months) that received a complete transection of the spinal cord at T9-T10. Next, EMG electrodes were chronically implanted in right and left gastrocnemius and tibialis anterior muscles of the hindlimbs so that we could measure the EMG signals in response to photostimulation of nociceptive afferents in the paws (Fig. 3.13A). One week post-surgery, we started EMG data collection twice weekly for four weeks. We photostimulated cutaneous VGLUT2+ afferents of the left and right hind paws of the mice using a 100 ms pulse of blue light from a 470 nm LED. We found the response rate to shorter intervals, such as 10 ms, was lower. We observed spasticity events as early as two weeks post-injury. Upon stimulation, we observed visually and electrophysiologically several events of spastic behaviours of hyperflexion such as toe extensor spams and hip adductor spasms and multiple cases of prolonged involuntary muscle contractions also known as clonus (Fig. 3.13B, C).

We measured the motor responses through the implanted EMG electrodes in the tibialis anterior and gastrocnemius muscles of the hindlimb during weeks 2-5 post-injury (Fig. 3.13 and 3.14). Each EMG recording involved nine stimulation episodes per paw and two control episodes, where the light pulse was directed away from the mouse. We observed that stimulation of hindpaws elicited bilateral EMG responses and amplitude of EMG response was not significantly different when stimulation was applied to the same or contralateral side (Fig. 3.13D-G; Mixed effects analysis: $p = 0.0964$).

At most time points after the stimulation, the EMG response to stimulation of either right or left paw was greater compared to an off-body stimulation. At week 2 post-injury (Fig. 3.13D, E), the response in left and right TA to left and right paw stimulation was greater than to off-body stimulation at the time of stimulation and up to 2s after (Mixed effects analysis: $p < 0.0001$); whereas at week 5 (Fig. 3.13F, G), the response to paw stimulation was greater from the time of stimulation till 5s or longer than in response to off-body stimulation (Mixed effects analysis: $p < 0.0001$).

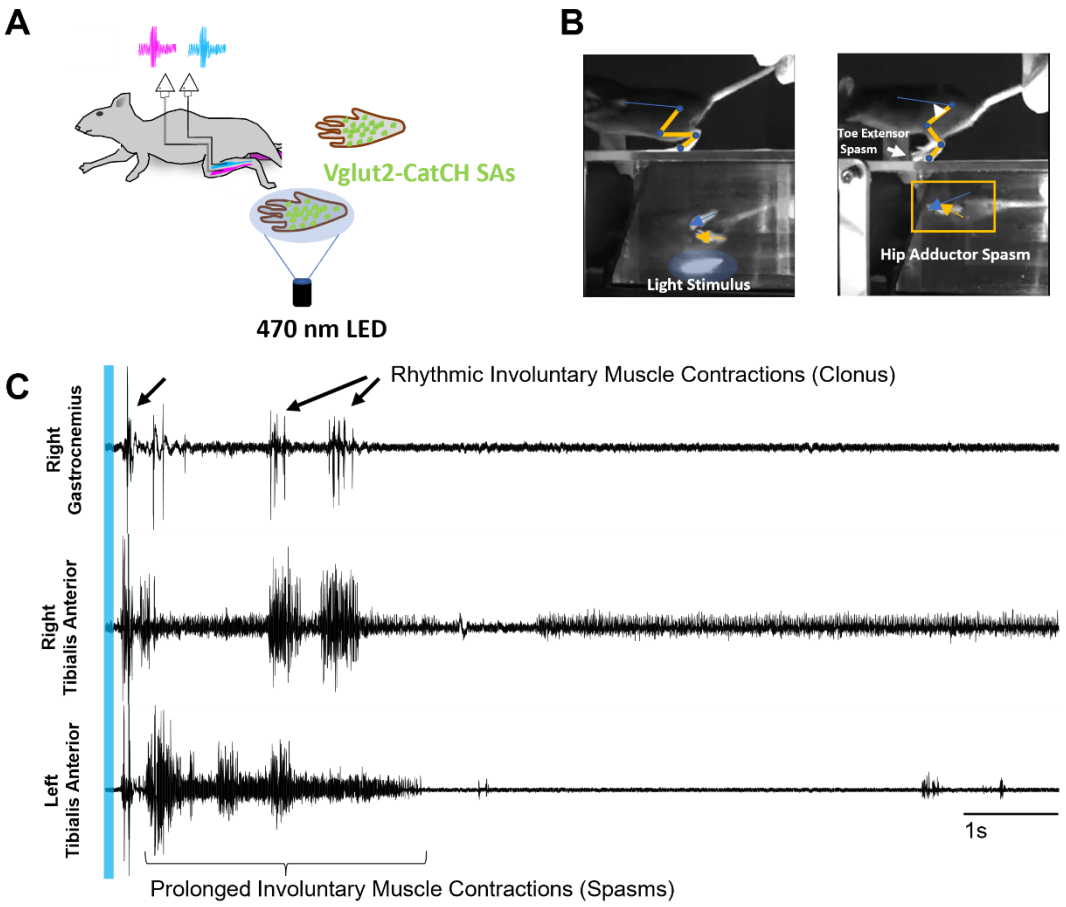
A
Vglut2-CatCH SAs
470 nm LED
B
Light Stimulus
Toe Extensor Spasm
Hip Adductor Spasm
C
Rhythmic Involuntary Muscle Contractions (Clonus)
Right Gastrocnemius
Right Tibialis Anterior
Left Tibialis Anterior
1s
Prolonged Involuntary Muscle Contractions (Spasms)

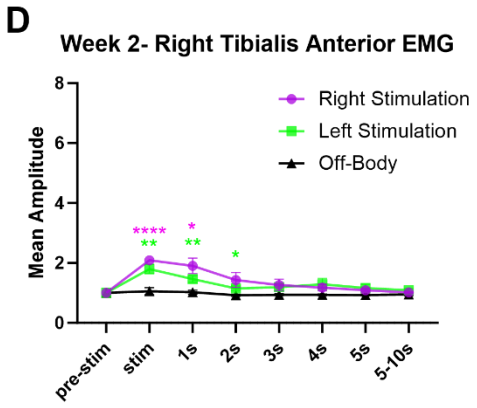
D
Week 2- Right Tibialis Anterior EMG
Mean Amplitude
Right Stimulation
Left Stimulation
Off-Body
pre-stim
stim
1s
2s
3s
4s
5s
5-10s

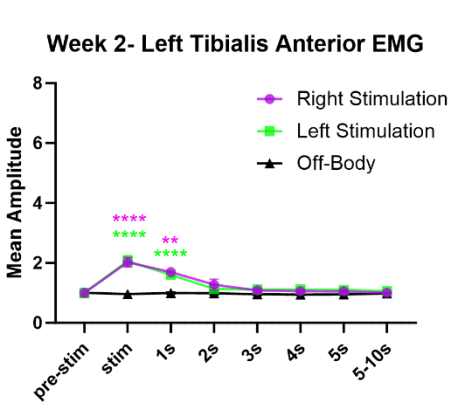
E
Week 2- Left Tibialis Anterior EMG
Mean Amplitude
Right Stimulation
Left Stimulation
Off-Body
pre-stim
stim
1s
2s
3s
4s
5s
5-10s

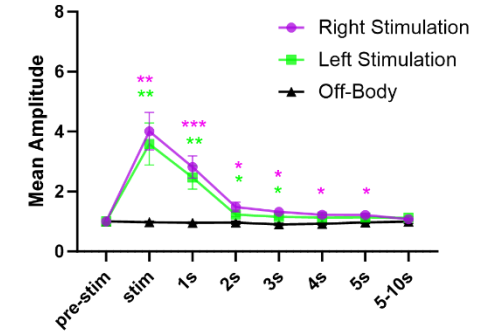
F
Week 5- Right Tibialis Anterior EMG
Mean Amplitude
Right Stimulation
Left Stimulation
Off-Body
pre-stim
stim
1s
2s
3s
4s
5s
5-10s

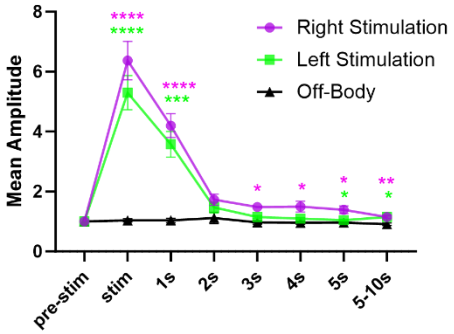
G
Week 5- Left Tibialis Anterior EMG
Mean Amplitude
Right Stimulation
Left Stimulation
Off-Body
pre-stim
stim
1s
2s
3s
4s
5s
5-10s

Figure 3.13 Time course of TA EMG responses to hindpaw stimulation of SCI Isl1-Vglut2^{CatCh} mice. (A) Schematic representation of EMG recordings in tibialis anterior and gastrocnemius of optogenetic stimulation of the hindpaw of SCI Isl1-Vglut2CatCh mice. **(B)** Bottom and side views of hip adductor and toe extensor spasms following 470 nm light stimulation of the left hindpaw **(C)** Representative EMG recordings at week 8 post-injury showing examples of muscle spasms and clonus elicited by blue-light illumination of the hind paw. **(D, F)** Amplitude of EMG response at 2 and 5 weeks after spinal cord injury recorded in right tibialis anterior and **(E, G)** in left tibialis anterior to light stimulation of the right or left hindpaw or illumination projected off the body. Mixed effects analysis model followed by Tukey's multiple comparison test: $^{*}p \leq 0.05$, $^{**}p \leq 0.01$, $^{***}p \leq 0.001$, $^{****}p \leq 0.0001$. Violet asterisks denote the difference between the right stimulation and off-body and green asterisks denote the difference between the left stimulation compared to off-body.

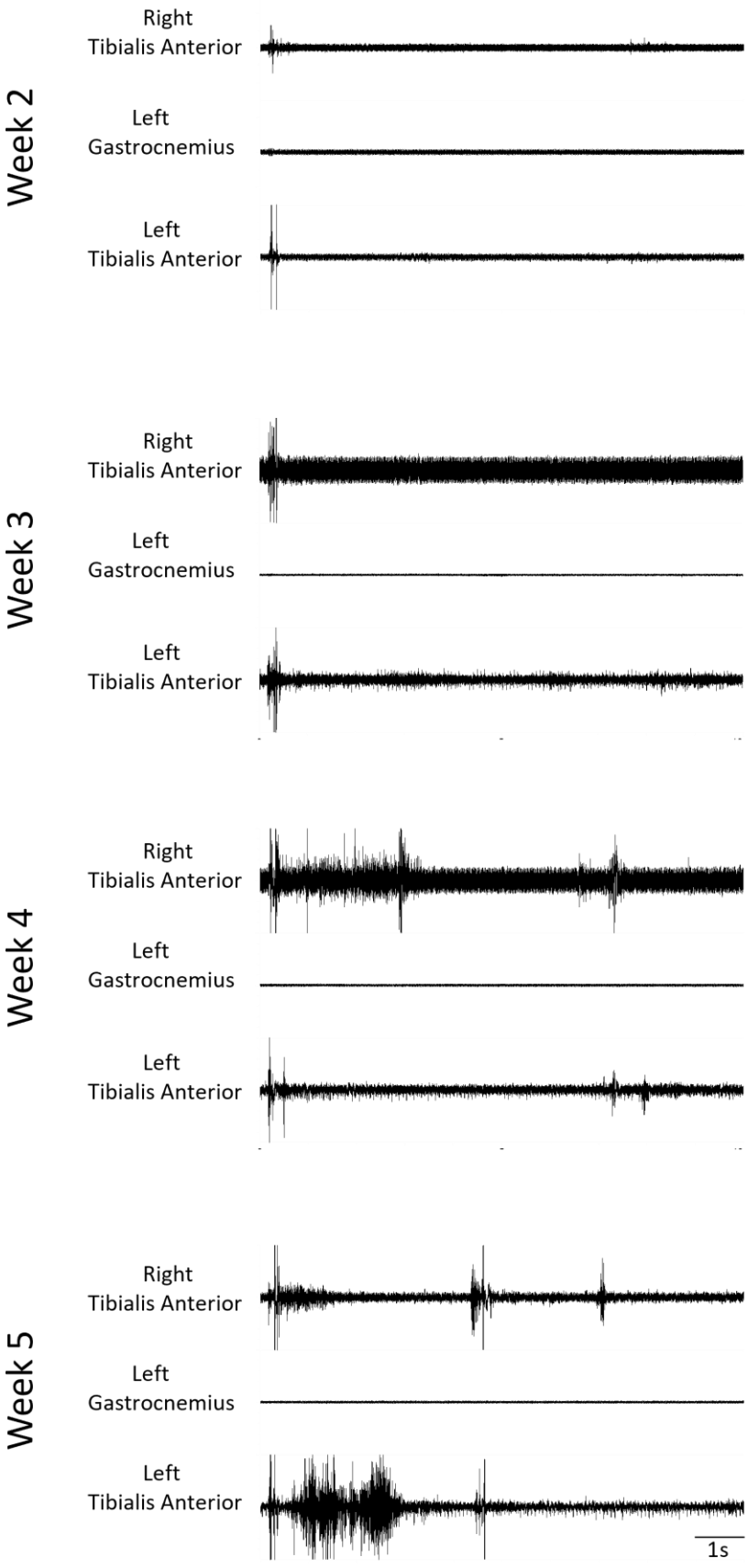
Week 2
Right
Tibialis Anterior
Left
Gastrocnemius
Left
Tibialis Anterior
Week 3
Right
Tibialis Anterior
Left
Gastrocnemius
Left
Tibialis Anterior
Week 4
Right
Tibialis Anterior
Left
Gastrocnemius
Left
Tibialis Anterior
Week 5
Right
Tibialis Anterior
Left
Gastrocnemius
Left
Tibialis Anterior
1s

Figure 3.14 EMG recordings from Right and Left Tibialis Anterior and Left Gastrocnemius muscles from a single SCI Isl1-Vglut2^{CatCh} mouse during weeks 2-5.

3.2.3 VGLUT2+ sensory afferent stimulation triggers hindlimb spasms in SCI mice

We measured EMG recordings from the left and right gastrocnemius and tibialis anterior muscles. Whether individually or when grouped together, the EMG recordings from these muscles revealed that the stimulation of Isl1+/VGLUT2+ afferents of right and left paws led to a progressive hindlimb hyperreflexia in both the left and right extensor and flexor muscles in the SCI mice from weeks 2-5 (Fig. 3.15). This was evident in the EMG recordings as the amplitude of the post-stimulus motor activity, and the first second after the initial reflex significantly increased over the weeks 2-5 post injury ($p < 0.0001$, Mixed effects model, grouping all the EMG recordings from different muscles together). This time-related increase in EMG response also showed a statistically significant interaction with the muscle group measured ($p = 0.0002$), with the larger effects being observed in the tibialis anterior muscles of both left and right hindlimbs.

These data suggest that stimulation of VGLUT2+ sensory afferents produce a strong response across both hindlimbs, closely approximating spasticity to a noxious or unexpected sensory stimulus.

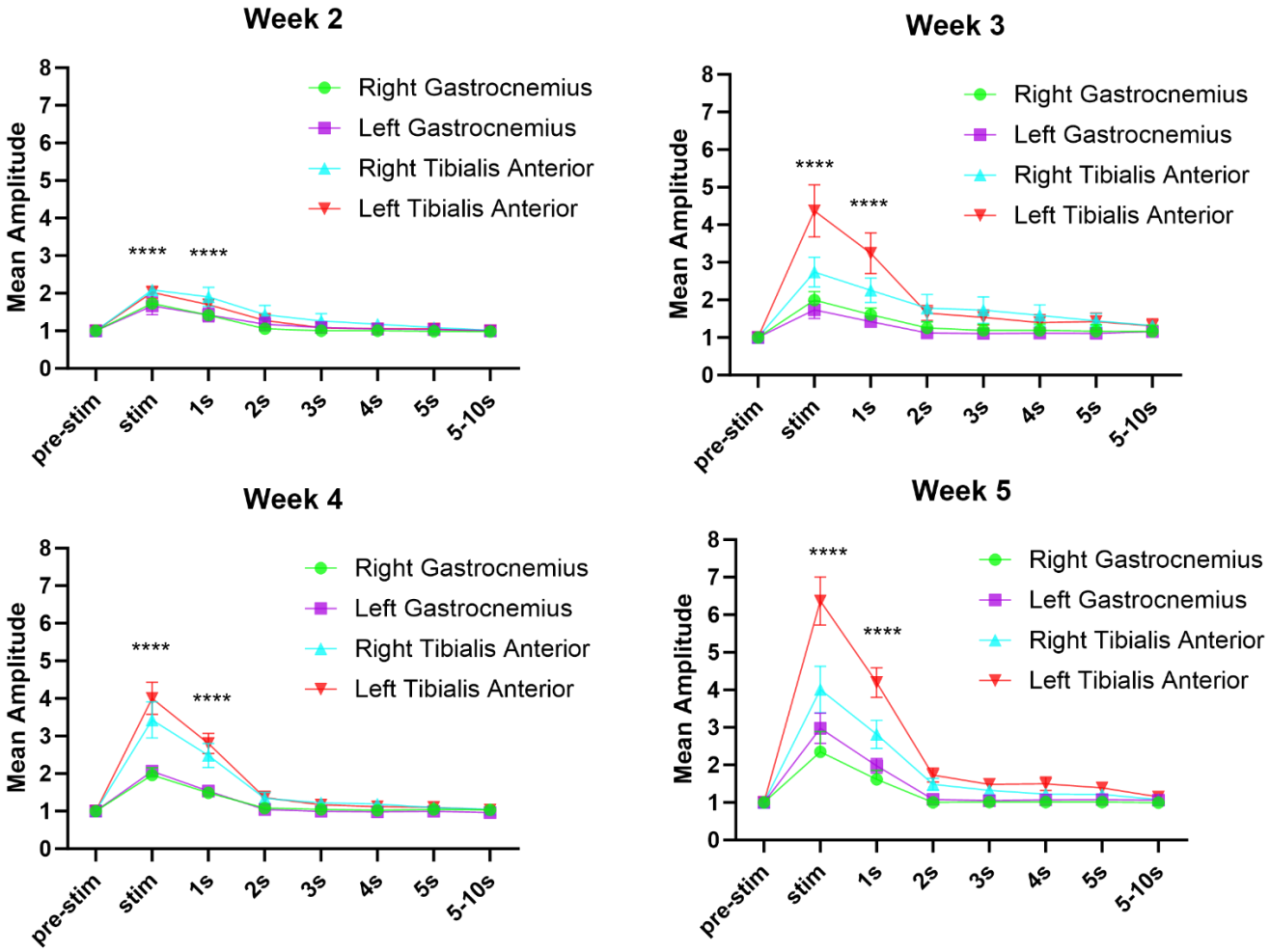

Figure 3.15 Time course of EMG responses in right and left gastrocnemius and tibialis anterior to hindpaw stimulation of SCI Isl1-Vglut2^{CatCh} mice. Amplitude of EMG response from 2-5 weeks after spinal cord injury. $^{****}p \leq 0.0001$ (Mixed effects model). Asterisks denote a difference between at least one pair of groups at a given time-point.

3.2.4 Sex affects onset and severity of hyperreflexia

During our experiments, we observed that some of the mice showed higher levels of spastic events and clonus episodes compared to the other mice every week. Since there are sex differences in motor circuits in the spinal cord, we sought to determine if it has an impact on the onset and severity of spastic events. Figure 3.16A-D shows sex-specific differences in spasticity triggered by hindpaw stimulation where the amplitude of EMG responses in the right tibialis anterior muscle of female and male mice were recorded between 2-5 weeks post-injury. Comparison of sex differences across the cohort suggested that female mice exhibited a greater extent of hyperreflexia after SCI (n = 10 F, n = 5 M). This was evident as the mean amplitude of EMG recordings from tibialis anterior muscles were greater in female mice (Mean range between 2.09 and 5.46) compared to male (Mean range 2.09 to 3.14) during stimulation every week from week 2-5. There was a statistically significant sex effect at week 4 (p = 0.022; Mixed effects model) and a significant time/sex interaction at week 4 (p = 0.0014) and at week 5 (p = 0.006; Mixed effects model); however, post-hoc comparisons did not reveal any differences at specific time points (Fig. 3.16A-D). Figure 3.16E illustrates the percentage of episodes featuring spasms in female and male mice during weeks 2-10. Sidak's multiple comparison test failed to reveal any difference between the male and female mice.

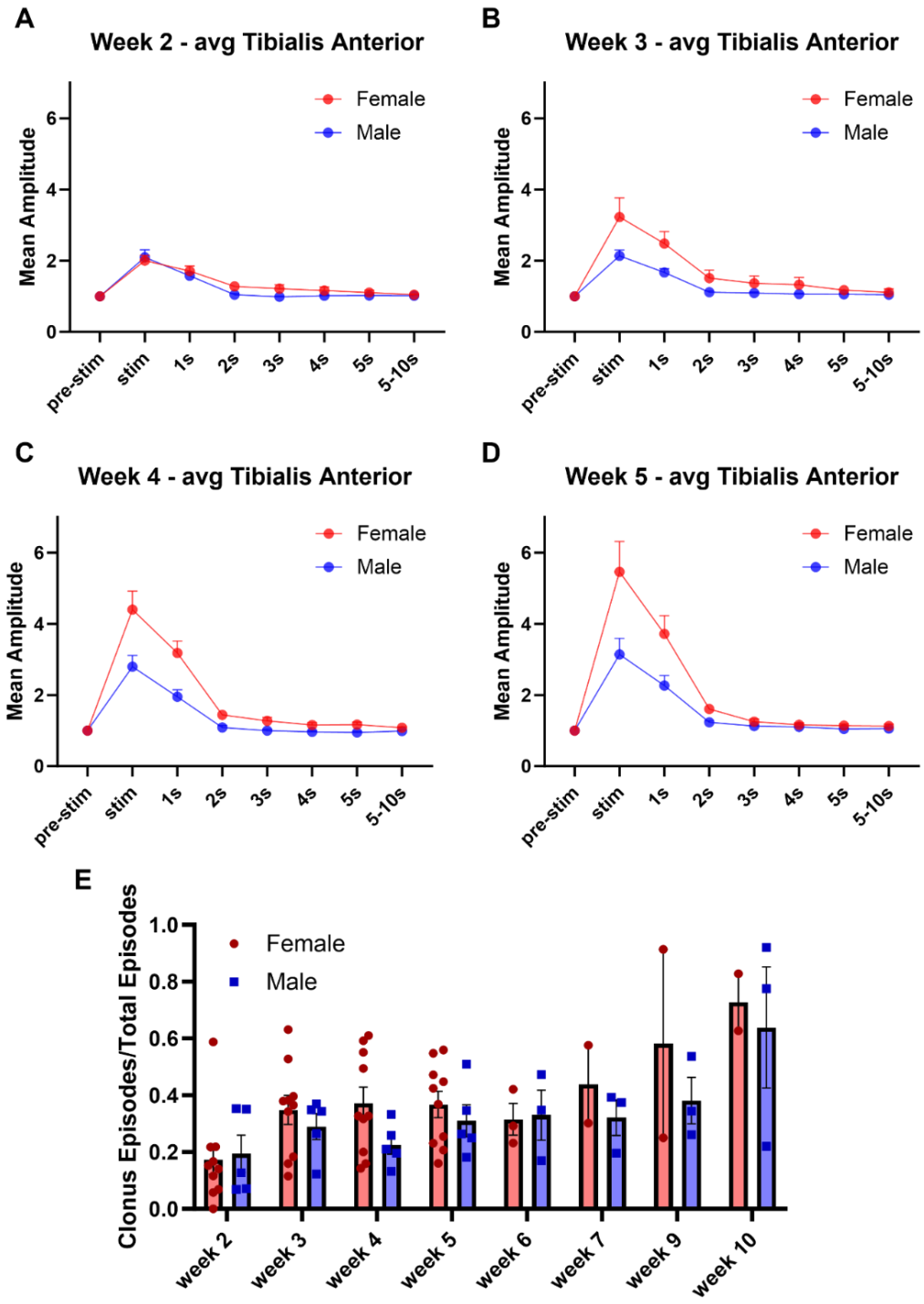

Figure 3.16 Sex-differences in spasticity evoked by hindpaw stimulation of SCI Isl1-Vglut2^{CatCh} mice. (A-D) Amplitude of EMG response from 2-5 weeks after spinal cord injury recorded in right tibialis anterior of female and male mice. (**E**) Percentage of episodes with spasms. Episodes are defined as post reflex, continuous activity lasting longer than 1 or 2 s.

3.2.5 Chronic stimulation

We sought to determine whether repetitive stimulation of VGLUT2+ sensory afferents with blue light would affect the onset or severity of hyperreflexia after SCI. We stimulated both hindlimbs of seven mice with blue light three times a day and used eight mice as control that didn't receive any stimulation. Specifically, each stimulation session consisted of 3-minute testing session, divided equally between the hindpaws and delivered in bursts of 30 s before switching to the other paw. Upon this repetitive stimulation from weeks 2 to 5, we did not observe any difference in the amplitudes or latencies of the EMG responses between the chronically stimulated and non-chronically stimulated mice (Fig. 3.17A-D). A mixed effects models was used to detect differences between the two groups across the time course of stimulation. Each week was analyzed individually. The main effect (stimulation treatment) was not significant (week 2, p = 0.4557; week 3, p = 0.1296; week 4, p = 0.7916; week 5, p = 0.8001). This was for the average TA value (across left and right). The stimulation effect was not significant either for the average GS muscles (week 2, p = 0.0781; week 3, p = 0.172; week 4, p = 0.18 and week 5, p = 0.9). Therefore, chronic stimulation of VGLUT2+ sensory afferents doesn't affect the onset or severity of spasticity after SCI.

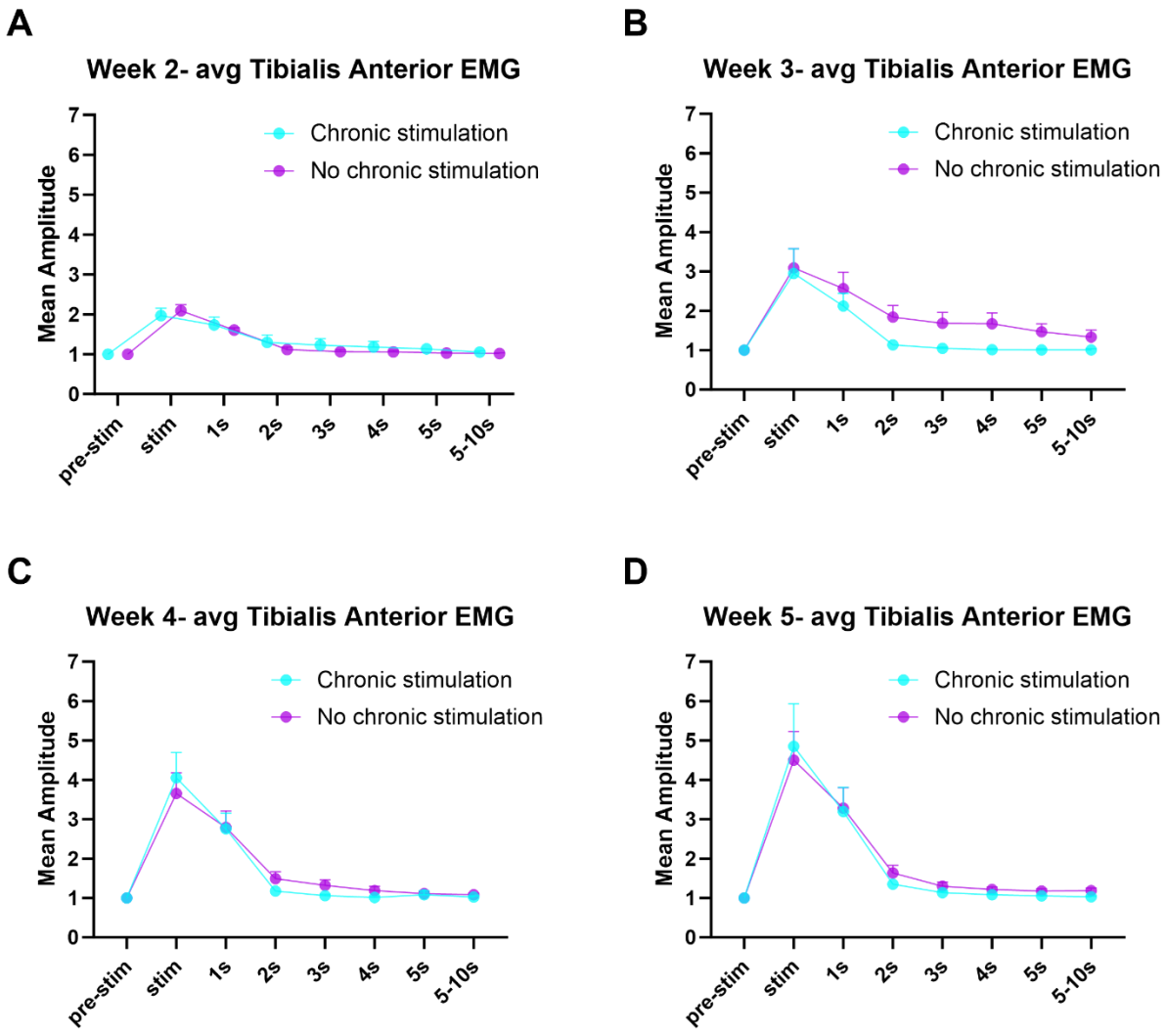

Figure 3.17. Time course of EMG responses in tibialis anterior to paw stimulation in SCI Isl1-Vglut2^{CatCh} mice with or without chronic hindpaw stimulation. A-D. Amplitude of tibialis anterior EMG response from 2-5 weeks after spinal cord injury were not significant between the chronically stimulated and non-stimulated groups (Mixed effects model).

CHAPTER 4: DISCUSSION

Injury to the spinal cord disrupts the descending fibres from the brain onto the spinal cord. However, spinal circuits caudal to the spinal cord lesions regain some capacity to generate locomotor activity. Locomotor activity after spinalization can be readily expressed on a treadmill in some mammals. Whether the recovery of locomotor function after SCI relies upon changes in the connectivity of spinal circuits is unknown. In the present study, we investigated changes in synaptic inputs to dI3 INs and MNs with a focus on sensorimotor integration.

4.1.1 Time course of changes in synaptic inputs to dI3 INs and MNS

We first investigated possible changes in sensory afferent inputs onto dI3 INs and MNs following SCI and in response to treadmill training. We quantified the number of VGLUT1$^+$ boutons on the soma and perisomatic dendrites of the dI3 INs and MNs. Our data reveal decreases (in untrained animals) or short-term increases (in trained animals) at several time points in the number of VGLUT1$^+$ boutons to dI3 INs. Normalizing the number of VGLUT1$^+$ inputs to dI3 INs by an estimate of soma area suggests a decrease in VGLUT1$^+$ bouton density in dI3 INs from untrained animals. MNs did not show any changes in the number of VGLUT1$^+$ inputs, but when normalized to an estimate of soma area, there was an increase at longer time points after injury. We also observed a slight decrease in the size of VGLUT1$^+$ boutons to dI3 INs and MNs.

Other studies investigating changes in VGLUT1$^+$ boutons in the spinal cord have reported either decreases or a lack of change in these inputs after spinal cord injury. Khalki et al. (2018) observed a lower density of VGLUT1$^+$ terminals on the surface of gastrocnemius (GS) and tibialis anterior (TA) MNs in untrained adult rats with a complete mid-thoracic transection compared to intact animals. No differences were observed in the density of VGLUT1$^+$ terminals between trained SCI and intact animals (Khalki et al., 2018). Following complete sacral transection in the adult rat, Kapitza et al. (2012) observed decreases in VGLUT1$^+$ bouton density in medial lamina VII at 12

wpi but not earlier and decreases at 4 wpi but not 1 or 12 wpi in lateral laminae VII. No changes were observed in lamina IX of S3-S4 segments (Kapitza et al., 2012). Thus, our observations in dI3 INs but not in MNs are consistent with previous reports of the intact or decreased density of VGLUT1$^+$ boutons after spinal cord injury. Khalki et al. (2018) observed an increase in the size of VGLUT1$^+$ boutons to motoneurons whereas we observed a minimal but significant decrease in the size of these inputs to both dI3 INs and MNs.

We then looked at changes in central excitatory inputs onto dI3 INs and MNs using VGLUT2 as a marker for intact propriospinal interneuron inputs assuming a lack of descending supraspinal inputs due to the spinal transection. We observed a significant increase in VGLUT2$^+$ inputs to dI3 INs at 2-3 wpi, which decreased in the time points after 4-6 wpi in trained animals. In the untrained animals, VGLUT2$^+$ inputs to dI3 INs decreased significantly at time points after 4-6 wpi. We also observed a significant decrease in VGLUT2$^+$ inputs to MNs in both untrained and trained animals at 6 dpi compared to sham levels. Subsequently, there were increases in both groups at 2-3 wpi followed by decreases after 4-6 wpi such that levels at 10-12 wpi were below sham levels. A similar reduction by 20% of VGLUT2$^+$ inputs in the spinal cord was observed 1 week after S2 transection in adult rats, and this reduction remained up to 12 weeks post-injury (Kapitza et al., 2012). The rise in VGLUT2+ inputs might result from sprouting of nociceptors and excitatory interneurons. However, since we did not utilize distinct markers to distinguish between these groups, it is not feasible to discern the extent of inputs derived from each possible source of VGLUT2+ inputs. An increase arising from nociceptor sprouting could lead to the development of spasticity following SCI.

In addition to changes in excitatory inputs after SCI, the loss of supraspinal descending inputs also alters inhibitory synaptic transmission. Transmission of sensory excitation to spinal

circuits can be regulated by GABAergic transmission onto the central terminals of sensory afferents (Rudomin, 1999; Betley et al., 2009; Hari et al., 2022). We looked at changes in the GABApre boutons onto VGLUT1$^+$ sensory afferents onto dI3 INs and MNs. Changes in GABApre boutons onto sensory afferents in dI3 INs and MNs in SCI mice were modest and occurred in a limited number of time points studied. There was a significant increase to dI3 INs in the untrained mice at 2-3 wpi compared to sham, which was followed by a decrease at 10-12 wpi. In the MNs, a significant increase in the level of GABApre boutons in both untrained and trained mice was observed at 6 dpi. However, this increase was lost afterwards, with the level of GABApre boutons on VGLUT1$^+$ inputs decreasing in the untrained mice at 2-3 wpi and in the trained mice at 4-6 wpi. Levels of GABApre boutons on VGLUT1$^+$ inputs were never observed to fall below sham levels for dI3 INs and MNs in untrained or trained animals. The initial rise in GABApre bouton levels might be part of an adaptive decrease in the transmission of sensory inputs to spinal inputs, which would be consistent with the absence of any increase in VGLUT1+ inputs to dI3 INs that we observed. Moreover, the subsequent decline in GABApre bouton levels in both dI3 INs and MNs in long term injury could potentially contribute to spasticity and reduction of rate dependent depression over time.

Why would the injured nervous system seek to decrease sensory function to spinal circuits after spinal cord injury? After the initial spinal shock after injury and the depression of neuronal circuits and muscle reflexes, spinal neurons gradually regain their excitability and reflexes reappear (Ko., 2018). There is evidence for an increase in the excitability of resting motoneurons after SCI (D'Amico et al., 2014) and the re-emergence of Na^+ and Ca^{2+} dependent PICs in MNs that cause constant depolarization (Bennett et al., 2004). Also, in a neonatal rat *in-vitro* spinal cord injury model, it was demonstrated that a chemically-induced lesion prompts a swift enhancement

in the functionality of sublesional dorsal horn networks, which predominantly display hyperexcitatory characteristics within minutes after SCI (Deumens et al., 2013). Several studies in human patients with SCI have shown that muscle spasms involve a heightened sensitivity to inputs from muscle afferents that are sensitive to force (Schmit et al., 20000; Conway and Knikou, 2008) where various innocuous or noxious cutaneous and proprioceptive stimuli applied to the lower limb can provoke an extended, coordinated response involving hip flexion and ankle dorsiflexion (Schmit et al.,2000). Furthermore, the observed pattern of reflex recovery after the spinal shock suggests the sequential restoration of cutaneous polysynaptic reflexes preceding monosynaptic reflexes such as deep tendon reflexes (Ko et al.,1999; Ditunno et al., 2004). The rise in excitability of motoneurons and dorsal horn neurons as well as excessive reflexes might be deleterious shortly after SCI and could setup eventual increases in neuropathic pain and spasticity (Finnerup et al., 2001; D'Amico et al., 2014).

Khalki et al. (2018) reported an increase in the density of presynaptic GABAergic terminals onto VGLUT1^{+} terminals to GS and TA MNs, in addition to increases in inhibitory GABAergic and glycinergic inputs onto cell bodies of GS and TA MNs of the trained and untrained SCI rats compared to intact. Interestingly, the size of the presynaptic inhibitory boutons was increased in untrained SCI rats but reduced in trained SCI rats, suggesting that the increased density of presynaptic inhibitory terminals was due to the sprouting of existing axons conveying presynaptic inhibition (Khalki et al., 2018). While we observed a decrease in the size of GABApre terminals on dI3 INs and MNs in both untrained and trained SCI mice, the decrease was greater in trained mice, perhaps due to more sprouting in the latter population. A different study reported a sustained decrease in GABAergic terminals contacting VGLUT1^{+} boutons in the sacral spinal cord after sacral transection (Kapitza et al., 2012).

The changes in the overall levels of GAD65 or GAD67 expression in the spinal cord after SCI have also been studied. Adult cats with complete thoracic transection exhibit increased GAD67 puncta in lamina IX (Tillakaratne et al., 2002). There were also increased levels of GAD67 expression in the ventral and dorsal horns of L5-L7 after thoracic transection, which decreased to control levels with step training (Tillakaratne et al., 2002). No increases in GAD65 levels were observed after thoracic transection in the adult cat (Tillakaratne et al., 2000). The balance of inhibitory to excitatory synaptic inputs to motoneurons shifts towards inhibition in neonatal rats with a midthoracic spinal cord transection at postnatal day 5. This balance seems to be restored to intact levels by locomotor training (Ichiyama et al., 2011). Reduced GAD65 and GAD67 immunoreactivity was observed in the L4-L5 dorsal horn of mice compared to sham at 6 wpi following a moderate contusion injury to T11 of GAD67:GFP mice (Meisner et al., 2010). Decreased levels of GAD65 and 67 expressions were also observed in the rat dorsal horn following contusion at T10 (Li et al., 2020).

We did not investigate GABA-mediated presynaptic inhibition of VGLUT2+ afferents in the spinal cord. Central terminals of Aδ-fibers can be gated by GABA-mediated presynaptic inhibition (Zimmerman et al., 2019). dI3 INs may receive direct inputs from these fibers based on electrophysiological recordings (Bui et al., 2013), but this sensory connection has not been confirmed anatomically. Presynaptic inhibition of VGLUT2+ terminals from spinal or supraspinal neurons to motor circuits has not been reported to the best of our knowledge.

4.1.2 Possible mechanisms underlying plasticity

Losses of VGLUT1^{+} and VGLUT2^{+} inputs shortly after SCI may reflect the severing of descending supraspinal and propriospinal inputs to circuits below the lesion. However, we did not observe any loss of VGLUT1^{+} inputs to dI3 INs and MNs shortly after SCI, and short-term losses

in VGLUT2^{+} inputs were only observed to MNs and not dI3 INs. This absence of immediate loss of VGLUT1^{+} and VGLUT2^{+} inputs could reflect a paucity of descending supraspinal or propriospinal inputs to dI3 INs or could indicate these connections are made to the dendritic regions that were not sampled in our image analysis.

Some studies have linked changes in neurotransmitter expression after SCI to neurotrophin signalling. For example, BDNF has been linked to several signal transduction cascades that promote neurogenesis, axonal sprouting, and neuronal survival (Arvanian and Mendell, 2001; Friedman et al., 1995; Keefe et al., 2017; Koda et al., 2002; Nakajima et al., 2010). BDNF levels may decrease shortly after spinal cord injury (Gómez-Pinilla et al., 2004; Gulino et al., 2004). However, rehabilitation programs, such as treadmill training or cycling, may reactivate silent spinal circuits, which could increase the level of BDNF in the spinal cord (Gómez-Pinilla et al., 2002; Ying et al., 2005; Côté et al., 2011; Boyce et al., 2012).

BDNF signalling can shape presynaptic inhibition of sensory inputs in the spinal cord. Activity-based exercise training seems to increase the synthesis of GAD65 and 67, and this mechanism may be related to exercise-induced BDNF synthesis and TrKB signalling activation in the spinal cord (Keeler et al., 2012; Huang et al., 2017; Leech and Hornby, 2017). Furthermore, the release of glutamate from sensory terminals seems to affect the differentiation and function of GABAergic terminals mediating presynaptic inhibition of sensory afferents via metabotropic glutamate receptor mGluR1 expressed on the GABAergic terminals (Mende et al., 2016). Since the expression of GAD65 is regulated by autocrine influence of BDNF on sensory terminals (Betley et al., 2009), the combined reduction of glutamate release from sensory neurons and BDNF that could result from loss of locomotor activity after spinal cord injury could theoretically drive

the loss of GAD65 expression in spinal circuits. However, we failed to observe large changes in GAD65 expressing boutons on VGLUT1$^+$ terminals to dI3 INs or MNs.

Recent findings have uncovered a novel mechanism underlying changes in neurotransmitter levels in the injured spinal cord. A subset of VGLUT2$^+$ interneurons, including dI3 INs, were found to switch neurotransmitter phenotype from excitatory glutamatergic to inhibitory GABAergic synapses contacting MNs after a complete T10 transection in adult mice (Bertels et al., 2022b). This neurotransmitter phenotype switching could also explain some of the reported loss of VGLUT2$^+$ boutons or rise in GAD65+/67+ boutons in the spinal cord observed after SCI (Tillakaratne et al., 2002; Kapitza et al., 2012; Khalki et al., 2018).

4.1.3 Training vs. Non training

We investigated for possible differences in synaptic inputs to dI3 INs and MNs from SCI animals with or without treadmill training. We observed more VGLUT1$^+$ boutons onto the surface of dI3 INs at 2-3 wpi in trained animals than untrained animals. However, no difference was observed in the level of VGLUT1$^+$ boutons on MNs between the trained and untrained animals, nor were there differences in VGLUT1$^+$ boutons to MNs from SCI or sham groups. Similar to VGLUT1$^+$ inputs, we found more VGLUT2$^+$ boutons onto dI3 INs of trained mice compared to untrained at 2-3 wpi and in MNs of trained mice at 2-3 wpi compared to untrained animals. On the other hand, we did not observe any effect of training on the level of presynaptic inhibition in dI3 INs. However, the trained mice had more presynaptic inhibition of VGLUT1$^+$ inputs to MNs at 2-3 wpi than untrained animals. We found only modest differences in synaptic inputs to dI3 INs and MNs between SCI animals with or without treadmill training.

Our results contrast with Khalki et al. (2018), who showed that MNs from SCI-trained mice had a higher density of VGLUT1$^+$ boutons compared to MNs from both intact and untrained SCI mice. Their study also reported that VGLUT1$^+$ terminals on MNs were larger in both untrained and trained mice compared to intact mice (Khalki et al., 2018), something that we have not quantified. Step training has been suggested to restore levels of the g2 subunit of $GABA_A$ receptors in motoneurons of rats three months after complete midthoracic transections at neonatal stages (Khristy et al., 2009). On the other hand, (Cantoria et al., 2011) failed to detect any significant difference in the densities of VGLUT1$^+$ and glycinergic GLYT2 inputs within the spinal cord of trained and untrained neonatal rats with complete transection (Cantoria et al., 2011).

4.1.4 Methodological considerations

Differences in how activity-based training influences the plasticity of spinal circuits after SCI may be related to variations in how SCI animals are trained. Our training regimen was comparatively lighter in frequency and duration than in several other studies, which may have led to the lack of significant improvements in stepping function in trained versus untrained animals. The lighter locomotor training regimen could have limited the release of any signalling molecule, such as neurotrophins, and any remodelling of spinal circuits. Furthermore, we did not consider the administration of supplementary interventions to improve locomotor recovery, such as the administration of pharmacological neuromodulation (Khalki et al., 2018) or electrical stimulation ; (Lavrov et al., 2008; Taccola et al., 2018; Gerasimenko et al., 2019; Kathe et al., 2022; Zhang et al., 2021). However, recovery of locomotor function could also be associated with the levels of home-cage activity between training sessions (Caudle et al., 2011; Torres-Espín et al., 2018). The lack of monitoring of this activity in our study and others makes it harder to truly associate training with recovery.

Several other factors may explain the discrepancies between our findings and those reported by other studies. These factors include the differences in animal model (species and age at which the injury occurs), injury type/severity, time after injury at which observations are made, the nature of any intervention (activity-based, neuromodulation, electrical), and the region of the spinal cord and the compartments of the neurons where the levels of $VGLUT1^+$, $VGLUT2^+$ and $GAD65/67^+$ inputs were quantified. For example, we investigated unidentified lumbar motoneurons located in L1-L5 in adult mice, while others have sampled from specific motor pools (Khalki et al., 2018) or motoneurons in sacral segments (Kapitza et al., 2012). Furthermore, we studied synaptic inputs made onto the soma of the motoneurons and the proximal 100um of the dendritic tree, while others sampled from further out into the dendritic tree. Thus, our conclusions of limited changes to sensory and central glutamatergic inputs and presynaptic inhibition to dI3 INs and MNs may apply only to the somatic and perisomatic regions of these neuron populations. Finally, the sex of the animals studied could also be a factor. For instance, in most experiments, only female rats (Kapitza et al., 2012; Khalki et al., 2018) or cats (Tillakaratne et al., 2002) were used, but we used both male and female mice. Whether there are sex differences in remodelling of spinal locomotor circuits remains to be investigated.

Overall, our results suggest modest changes in synaptic inputs related to sensorimotor integration to MNs and dI3 INs after spinal cord injury. Restoring motoneuron activity is evidently beneficial to the recovery of motor function after SCI. Silencing dI3 INs impairs locomotor recovery after SCI (Bui et al., 2016). Our data do not provide strong evidence that certain levels of synaptic inputs from any specific circuits must be prioritized in restoring movements after SCI. In fact, a negative correlation was found between central excitatory inputs and stepping function. It is unclear why the loss of excitation would improve stepping function after injury. We conclude

instead that the modest changes in synaptic inputs to MNs and dI3 INs suggest that those circuits are available to be recruited if this recruitment is eventually found to be beneficial to the recovery of locomotor function.

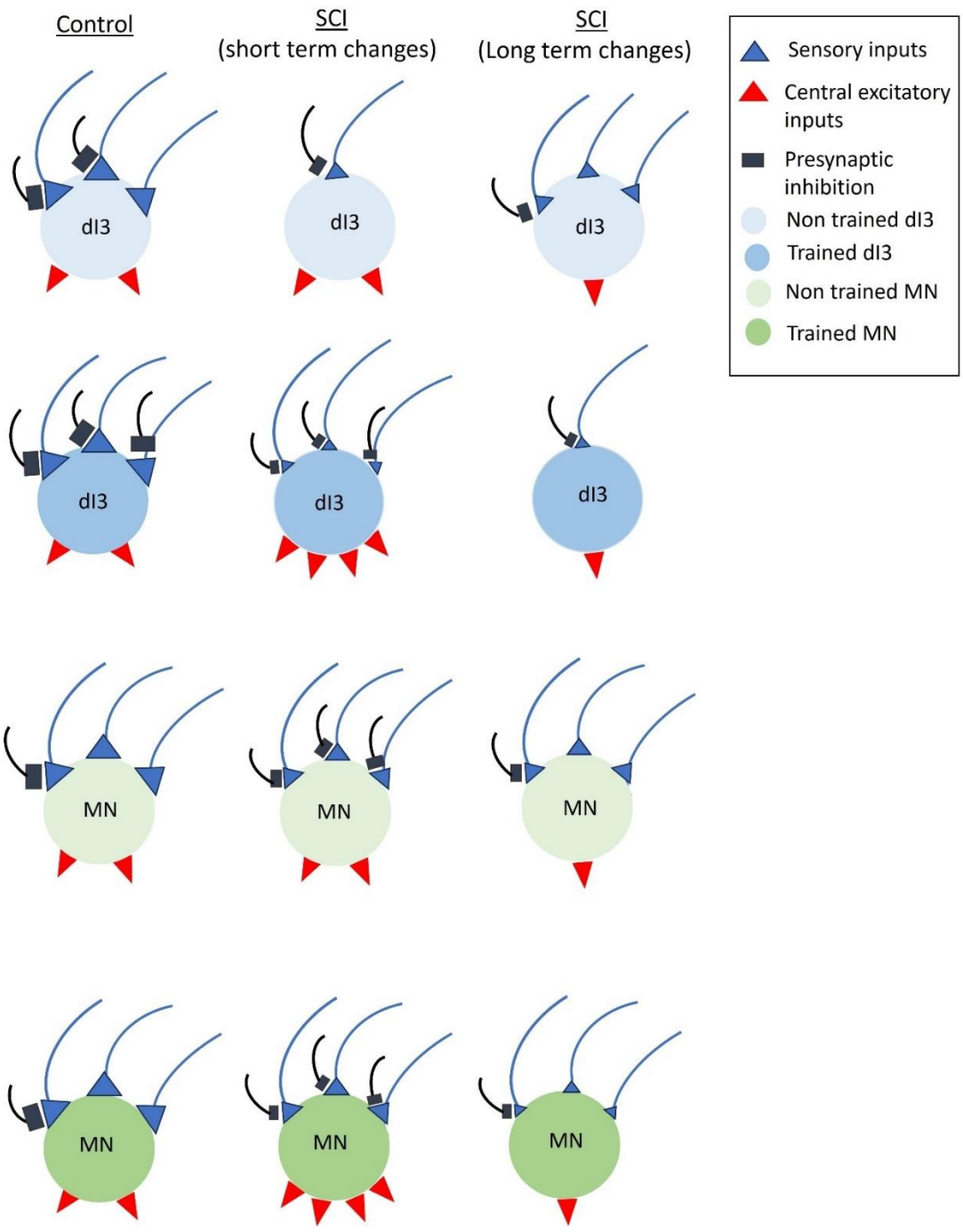

Figure 4.1 Summary of various short- and long-term changes in sensory inputs from the primary afferents, central excitatory inputs and presynaptic inhibition of sensory terminals observed in dI3 INs and MNs following SCI compared to control mice.

4.2 Characterization of CatCh mice

Our model of animal spasticity involves a transgenic strain of mice where the light sensitive channel, CatCh, is under the expression of Isl1 and VGLUT2. Hindlimb spasticity is elicited after a complete transection by blue light illumination of the hindlimbs, implicating the optogenetic activation of sensory neurons, supposedly expressing Isl1 and VGLUT2. Isl1 is expressed in most sensory neurons (Pfaff and Mendelsohn, 1996; Liem et al., 1997; Roy et al., 2012; Bui et al., 2013). VGLUT2 is a vesicular glutamate transporter. The prevalence of glutamate as a major excitatory neurotransmitter is very well documented in the literature (Fonnum, 1984; Watkins, 2000; Carlton, 2001; Willis and Coggeshall, 2004). Both electrophysiological and pharmacological experiments (Yoshimura and Jessell, 1990; Carlton, 2001; Willis and Coggeshall, 2004) and histochemical experiments (Wanaka et al., 1987; Battaglia and Rustioni, 1988; Kai-Kai and Howe, 1991; Valtschanoff et al., 1994; Keast and Stephensen, 2000) have demonstrated that glutamate serves as the major neurotransmitter in numerous sensory neurons located within the spinal cord and the DRGs.

VGLUT1 and VGLUT2, two of the three types of vesicular glutamate transporters, have been extensively studied in the spinal cord and DRG neurons of mice, rats, and guinea pigs. Brumovsky et al. (2007) have reported immunoreactivity of VGLUT1 to be around 11.9% +/- 1% and for VGLUT2, 65.4 % +/- 4.5% in the L4-5 DRGs of adult mice. Moreover, they observed the presence of VGLUT1 to be predominantly in medium to large-sized neurons whereas VGLUT2 was found predominantly in small to medium-sized neurons. Also, all CGRP immunoreactive and IB4 binding neurons were also VGLUT2 immunoreactive. Morris et al. (2005) also observed strong VGLUT1 immunoreactivity in larger DRG neurons but not detected in small neurons with CGRP. In contrast, VGLUT2 was strongly detected in small DRG neurons of both guinea pigs and mice

(Morris et al., 2005). Tong et al. (2001) has also demonstrated that many of the neurons of thoracic DRGs that innervate the gut displayed VGLUT2 immunoreactivity. Overall, the findings of these and other studies have suggested that VGLUT1 is predominantly present in large-sized, CGRP-negative DRG neurons, which are mechanoreceptors and proprioceptors (Tong et al., 2001; Li et al., 2003; Oliveira et al., 2003; Todd et al., 2003; Alvarez et al., 2004; Landry et al., 2004), whereas VGLUT2 is involved in nociception and divided into two groups: peptidergic nociceptors that are TRPV1 and CGRP positive; and the non-peptidergic nociceptors that bind to P2X3R and/or isolectin B4 (IB4) (Aoki et al., 2004; Shiers et al., 2020).

Liu et al. (2010) utilized homozygous conditional knockout mice to delete VGLUT2 in Nav1.8 expressing neurons in the DRG of adult mice. The animals exhibited diminished reactions to diverse heat, mechanical, inflammatory, and neuropathic pain stimuli, coupled with heightened instances of scratching associated with itchiness. Their findings underscore the pivotal role of VGLUT2 dependent synaptic glutamate release, primarily from Nav1.8-expressing nociceptors, as a crucial neuronal element essential for pain perception and the suppression of itch (Liu et al., 2010). This study also utilized double fluorescence labeling on the lumbar DRGs of mice at postnatal day 30 to provide quantitative evidence that VGLUT2, as opposed to VGLUT1, to provide further evidence that VGLUT2 was extensively present in sensory nociceptors identified by IB4, CGRP, and TRPV1. Remarkably, 100% of IB4- and CGRP-positive neurons, along with 94.2% of TRPV1-positive DRG neurons, were concurrently labeled by VGLUT2. In contrast, only 2.66%, 25.5%, and 0.45% of these neurons were labeled by VGLUT1, respectively, further reinforcing the involvement of VGLUT2 in nociceptive signaling. Lagerström et al. (2010) also identified that the regulation of both thermal pain sensation and itch transmission is dependent on VGLUT2-mediated glutamatergic transmission in TRPV1+ neurons. In their experiment, it was

shown that removing VGLUT2 from a subset of neurons, which partially overlapped with the vanilloid receptor (TRPV1) primary afferents, led to a significant rise in itch-related behavior while simultaneously decreasing sensitivity to thermal pain (Lagerström et al., 2010). Similarly, Scherrer et al. (2010) also knocked out VGLUT2 in mice by crossing $VGLUT2^{lox/lox}$ mice with mice that express Cre under the control of the peripherin gene promoter to excise the second exon of VGLUT2 gene. In behavioral tests, mice with conditional knockout of VGLUT2 exhibited reduced sensitivity to harmful heat, mechanical pressure, and chemical (capsaicin) stimuli. Surprisingly, their responses to cold stimulation and in the formalin test remained unchanged. Notably, while the conditional knockout mice did not display heightened sensitivity to heat caused by tissue injury, they developed mechanical hypersensitivity in a normal manner (Scherrer et al., 2010). Together, these studies suggest that VGLUT2 expression is primarily found in peptidergic and non peptidergic nociceptors involved with pain perception to heat and mechanical pressure, pruriception (itch) as well as inflammatory and neuropathic pain.

While VGLUT1 and VGLUT2 are often thought of as being expressed separately, these two transporters can be co-expressed in some DRG neurons. Brumovsky et al.,2007 observed a moderate co-expression of VGLUT1 and VGLUT2, primarily within medium and large-sized neurons, with fewer than half of all VGLUT1 neurons showing positivity for VGLUT2. The neurons displaying both markers are likely non-peptidergic, as indicated by the absence of peptidergic markers such as CGRP that is observed in VGLUT1 neurons (Brumovsky et al., 2007). Interestingly, Landry et al., 2004, using single labelling, observed that nearly all neurons expressed both VGLUT1 and VGLUT2 transcripts in rat DRG neurons. This finding was corroborated through a double in situ hybridization approach, revealing that all categories of sensory neurons—small, medium-sized, and large sensory neurons, exhibited both markers, despite their segregation

in the superficial laminae of the dorsal horn (Landry et al., 2004). The authors suggests that this disparity implies the existence of unique targeting mechanisms tailored for each transporter, and/or a separate regulation of their translation processes.

Wu et al., 2021 have further investigated proprioceptive sensory neurons and using single cell RNA sequencing have identified 3 main types of proprioceptive neurons which are further segregated into 8 distinct groups (Wu et al., 2021). While most proprioceptors express VGLUT1, they have identified two smaller populations of Ia afferents that co-express VGLUT1 and VGLUT2 (Wu et al., 2021).

We characterized the expression of the fluorescent reporter tdTomato in sensory neurons to understand which sensory neurons would be photoactivated in our SCI Isl1-Vglut2^{CatCh} mice. In part, we looked at the expression of VGLUT1 and VGLUT2 with tdTomato in the DRGs from L1-L5. Our data indicates that 1.0 ± 1.5% of the tdTomato+ cells express VGLUT1+/VGLUT2-, 77.1 ± 12.8% are VGLUT2+/VGLUT1- and 5.7 ± 4.0% co-express VGLUT1 and VGLUT2, which is in line with the conditional expression of the transgenes linked to VGLUT2 expression. We also observed the expression of tdTomato in 67.7% ± 16.5 of the TRPV1 cells and 38.7% ± 13.2 in the non peptidergic IB4 bound neurons. Surprisingly, expression in CGRP expressing cells was low.

Based on the expression of VGLUT2 in specific populations of sensory neurons and the expression of reporter proteins under the expression of Isl1-Cre and Vglut2-Flp, I conclude that the neurons that are photoactivated via CatCh expression are highly expressed in TRPV1 population and low expression in CGRP neurons and to a lesser extend in non peptidergic IB4 bound neurons. In general, TRPV1 is predominantly found in sensory neurons, where it functions as a detector for painful stimuli triggered by pungent chemicals and high temperatures (Shuba,

2021). The sensitization of primary afferent nociceptors through the activation of TRPV1 receptors can prompt the release of neuropeptides, such as CGRP and substance P, from the nociceptors. This release initiates neurogenic inflammation, potentially enhancing nociception (Li et al., 2008). IB4-positive nociceptors play a role in mechanical hyperalgesia triggered by inflammation and muscle damage (Alvarez et al., 2012). VGLUT1 expression in a small proportion of VGLUT2+ neurons suggests that some of the sensory neurons photostimulated via CatCh could be proprioceptors that are limb-innervating Ia afferents according to a recent transcriptomic study of proprioceptors (Wu et al., 2021).

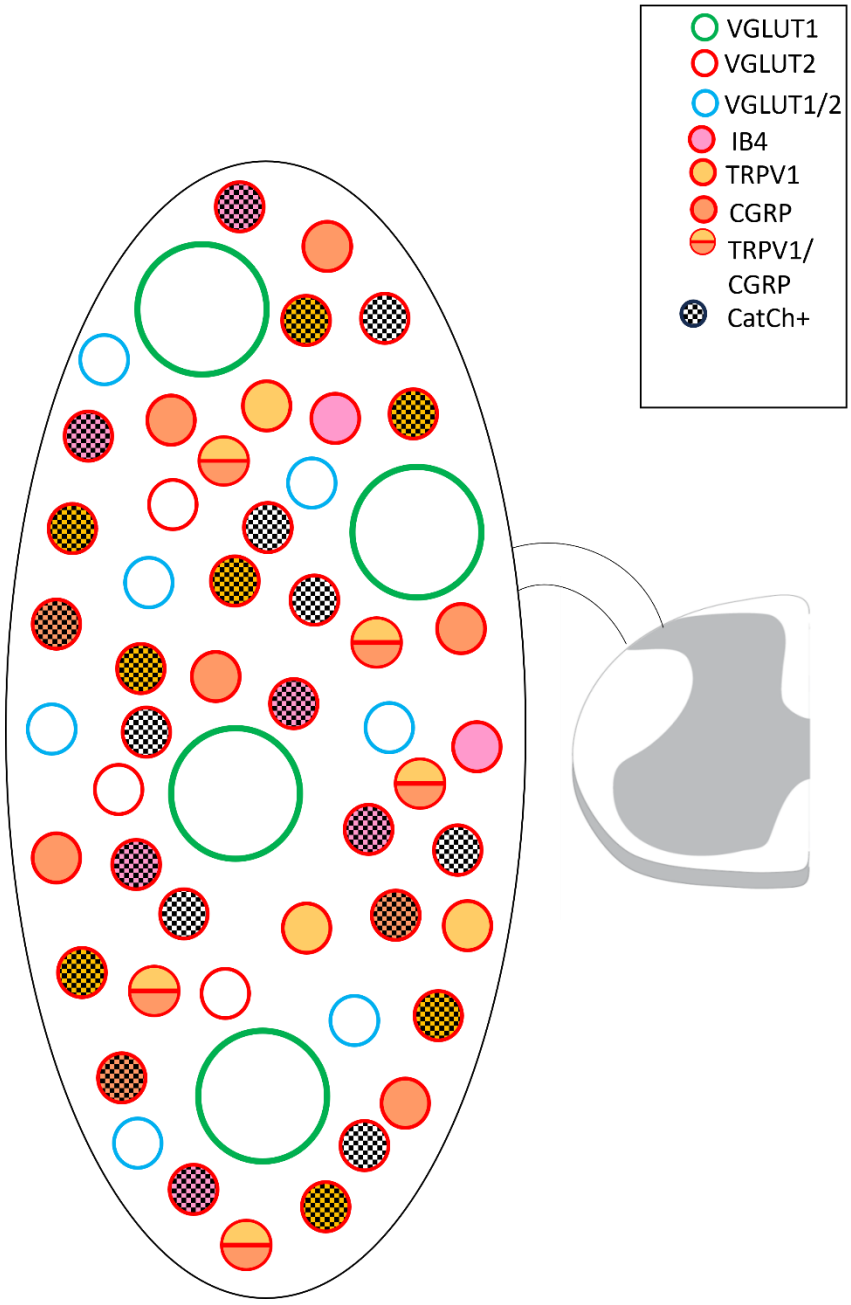

Figure 4.2 Different populations of neurons within the DRG that express the CatCh+ transgene in Isl1-Vglut2^{CatCh} mice

4.3 New model of spasticity

We have successfully generated a transgenic strain of mice that could serve as a viable model of spasticity through the stimulation of Isl1+/VGLUT2+ sensory afferents. We have shown that unilateral optogenetic stimulation of the hindpaws of Isl1-Vglut2^{CatCh} spinal cord-injured mice can reliably trigger episodes of hindlimb spasms in both hindlimbs as early as 2 weeks post-SCI. Muscle spasms or clonus were not observed in intact Isl1-Vglut2^{CatCh} mice. On the other hand, chronic stimulation of VGLUT2+ sensory afferents didn't appear to influence the onset or severity of spasticity after SCI. Finally, we observed that sex affects onset and severity of hyperreflexia in response to paw illumination. Female mice manifested hyperreflexia earlier with greater severity compared to male mice. Considering the lack of reliable animal models of spasticity besides the tail spasticity in a rat model (Bennett et al., 2001, 2004), this novel model of spasticity could be valuable in further understanding the mechanisms and treatments of spasticity.

4.3.1 Underlying mechanisms of spasticity in Isl1-Vglut2^{CatCh} mice

The value of the Isl1-Vglut2^{CatCh} mice model of limb spasticity after SCI depends on the mechanism by which spasticity arises in Isl1-Vglut2^{CatCh} mice after injury. Spasticity is a multidimensional sequela of SCI that may arise from maladaptive structural and functional neuroplasticity of spinal circuits and sensory afferents. However, the underlying causes of spasticity in spinal cord injury patients have yet to be fully determined.

Our immunostaining suggests that a relatively large portion of Isl1+/VGLUT2+ sensory neurons are nociceptors and there is evidence that nociceptors undergo changes after injury to the nervous system that could increase the activity of sensorimotor circuits causing spasticity. For instance, hyperreflexia could arise from the sprouting of nociceptive sensory afferents following SCI. Small and medium-sized sensory neurons dissociated from DRGs near or below the site of a

contusion injury at T10 in adult rats displayed increased neurite elongation compared to sensory neurons dissociated from DRGs of sham or intact animals (Bedi et al., 2012). This increased capacity for sprouting by putative nociceptors after SCI is consistent with reports of sprouting of CGRP-immunoreactive afferents within the dorsal horn of the spinal cord rats (Krenz and Weaver, 1998; Krenz et al., 1999; Weaver et al., 2001; Ondarza et al., 2003); and humans (Ackery et al., 2007) after SCI. A recent study observed that a T10 hemisection in rats led to cutaneously-evoked nociceptive hyperreflexia (Lee et al., 2019). Central projections of cutaneous nociceptive afferents were significantly increased in segments above and below the lesion, which increased synaptic terminals in the dorsal horn (Lee et al., 2019). Thus, sprouting of the central axons of nociceptive sensory neurons could lead to hyperreflexia and spasticity.

Concomitant with sprouting, SCI can alter the activity of nociceptors by causing chronic peripheral sensitization of nociceptors (Carlton et al., 2009) or facilitating the persistent generation of spontaneous action potentials. Putative DRG nociceptors dissociated after spinal contusion in rats showed increased events of spontaneous firing of action potentials (Bedi et al., 2010). Increased hyperactivity of DRG neurons after SCI could be in response to signals released due to an immune response to injury or inflammation (Miller et al., 2009).

The involvement of nociceptors in spasticity suggested by our study could be tested by expressing archaerhodopsin in Isl+/Vglut2+ afferents to deactivate nociceptors in order to determine whether inhibition of these afferents would reduce spontaneous spasticity. Note that other studies have found interesting effects of inhibiting nociceptors on recovery of locomotor function after injury. Hindlimb stretching after contusive T10 spinal cord injury has been observe to negatively affect locomotor function in rats after contusive T10 spinal cord injuries (Keller et al., 2019). These stretch-induced declines were absent in neonatal rats depleted of TRPV1+

sensory afferents through capsaicin treatment (Keller et al., 2019) suggesting that optogenetic inhibition of Isl1+/Vglut2+ afferents could have the dual benefit of reducing spasticity and muscle-stretch induced declines in locomotor recovery.

Hyperactivity of nociceptors and downstream motor circuitry after SCI could also occur in spinal neurons due to changes in their intrinsic properties. For example, changes in motoneuron excitability have been linked with spasticity. Motoneurons and ventral spinal interneurons possess persistent inward currents mediated by calcium currents from low threshold L-type calcium channels (Cav1.3 type) (Carlin et al., 2000) and persistent sodium currents (Lee and Heckman, 2001; Li and Bennett, 2003; Theiss et al., 2007) that can amplify and sustain their output (Bennett et al., 1998; Hounsgaard et al., 1988; Lee and Heckman, 1996). PICs are eliminated in motoneurons shortly after an acute spinal cord injury to the sacral cord (Bennett et al., 2001; Eken et al., 1989). However, in chronic phases of injury to the sacral cord, large PICs appear that lead to spasms in the tail muscles (Bennett et al., 2004, 2001; P. J. Harvey et al., 2006; P J Harvey et al., 2006).These PICs are facilitated by serotonin (Li et al., 2007) and may be enhanced by constitutive 5-HT2_C activity after SCI (Murray et al., 2010). Blocking the Ca^{2+} component of the PICs in the motoneurons of a mouse tail spasticity model has been shown to reduce tails spasms after SCI (Marcantoni et al., 2020).

Similarly, multimodal dorsal horn neurons display increased responses to ipsilateral or contralateral mechanical stimulation of the hindlimb at least 28 days after thoracic hemisections in adult rats (Hains et al., 2003a; Hains et al., 2003b). The hyperexcitability of these dorsal horn neurons has also been linked to dysregulation of serotonergic signalling. Thus, the interruption of descending serotonergic or other neurotransmitter inputs to the spinal cord could lead to hyperexcitability of spinal neurons below the level of injury (Baldissera et al., 1982; Jankowska,

1992), in addition to possible increased neurotransmitter release from sensory afferent or interneurons (Thor et al., 1994), receptor upregulation after chronic SCI (Mills and Hulsebosch, 2002) and increased sensitivity of metabotropic receptor facilitating PICs (Hains et al., 2002).

In any event, whether due to changes in intrinsic properties or morphological changes, enhanced activity of nociceptors or spinal neuron and the sensorimotor circuits these neurons form could lead to maladaptive changes following SCI such as central sensitization, autonomic or somatic hyperreflexia. The latter could include spasticity.

Spasticity in Isl1-Vglut2^{CatCh} mice could also arise from sprouting of Isl1^{+}/VGLUT2^{+} proprioceptors (Wu et al., 2021). While most proprioceptors are VGLUT1^{+}, two smaller populations of Ia afferents has been found to co-express VGLUT2 (Wu et al., 2021). VGLUT1^{+}/VGLUT2^{+} cells were only a small percentage of all tdTomato+ neurons of the DRG of Isl1-VGLUT2^{CatCh} mice.

However, we observed that unilateral stimulation of Isl1^{+}/VGLUT2^{+} sensory afferents generated muscle spasms that could affect either or both hindlimbs. Thus, unless the spinal cord injury caused sprouting of central branches of nociceptors across the midline, the bilateral nature of the spastic response to unilateral stimulation suggests the recruitment of sensorimotor circuits with some commissural component. One possible population of spinal neurons involved are the V3 spinal interneurons (Zhang et al., 2008). This population includes commissurally-projected neurons and has been implicated with muscle spasms in the tail after injury to the sacral cord (Lin et al., 2019).

Besides increased sprouting of sensory afferents or hyperexcitability of spinal excitatory neurons, increased activity of spinal sensorimotor circuits leading to spasticity could also arise

from disinhibition of spinal networks. Evidence suggests possible dysregulation of the inhibition of motoneurons by spinal Ib interneurons in hemiplegic patients (Delwaide and Oliver, 1988). Malfunction of the Renshaw Cell-mediated recurrent inhibition of motoneurons could also contribute to the development of extreme limb stiffness (Mazzocchio and Rossi, 1997).

The emergence of spasticity can also be attributed to the reduction in mechanisms that regulate the release of glutamate from sensory afferents. Research by Zimmerman and colleagues in 2019 indicates that the release of GABA onto the central terminals of Aβ, Aδ, and C-fibers can restrict the release of neurotransmitters onto spinal neurons. Furthermore, the activation of a trisynaptic circuit by C-fibers leads to NMDA release onto Aβ fibers, which, as demonstrated in the same study, can also limit sensory transmission to spinal circuits (Zimmerman et al., 2019).

A number of studies suggest that the Ia pathways are no longer inhibited by presynaptic inhibition after lesions to the spinal cord that sever the descending tracts that input to GABAergic neurons mediating presynaptic inhibition. This downregulation of presynaptic inhibition could contribute to the hyperexcitability of the stretch reflex seen in spastic patients (Faist et al., 1994). Several studies have also reported decreased gating of sensory transmission in spinal motor circuits after SCI though correlations between this decrease and spasticity have yet to be detected (Lalonde and Bui, 2021).

4.3.2 Onset or severity of spasticity is not affected by repetitive optogenetic stimulation

There were no differences in the amplitudes or latencies of the EMG responses to paw illumination between animals receiving chronic stimulation and those that did not. This suggests that there are no use-dependent changes in the mechanisms underlying spasticity in this animal model of limb spasticity with the caveat that animals without chronic stimulation were still

subjected to weekly testing. Whether this weekly paw illumination is sufficient to induce use-dependent changes that are equivalent to daily illumination remains to be ascertained. It is more likely that the lack of differences in the spasticity response of animals receiving chronic stimulation and those that did not arises from mechanisms of spasticity that are not affected in a use-dependent manner. This lack of use-dependent plasticity could serve as an additional benefit in the use of Isl1-VGlut2^{CatCh} mice for investigating the mechanisms and treatment of hindlimb spasticity.

4.3.3 Sex dependent differences

We have noticed sex differences in the spasticity of our spinalized mice where female mice showed higher mean amplitude in the EMG recordings from tibialis anterior muscles in response to paw illumination. Although there are numerous reports on different aspects of spasticity in the human patients from SCI to the best of our knowledge there are no studies that have reported sex differences in spasticity in patients. The sex differences in spasticity in spinalized Isl1-Vglut2^{CatCh} mice may speak to the specific mechanisms by which spasticity arises after injury in this animal model. Based on the neurons that express CatCh in the periphery, namely Isl1+/Vglut2+ sensory neurons, spasticity likely arises through nociceptive pathways. Several lines of evidence point to sex differences in pain pathways in the intact nervous system and after injury.

There is evidence that in general, females have higher prevalence of pain compared to males (Mogil, 2012). Sex hormones play a role in modulation of pain. For example, estrogen has been shown to increase proinflammatory cytokines and causing greater pain intensity in females

(Rosen et al., 2017). Sex-differences have been investigated in neuropathic pain after SCI in both human patients and in rodents (Burke et al., 2018).

In a survey from a group of male and female patients with SCI, female patients had a higher prevalence of nociceptive pain compared to males (Budh et al., 2003). In animal models of SCI, female rats have been shown to have lower threshold for pain and display mechanical hypersensitivity (Dominguez et al., 2012). Genome mapping in rats has revealed 3 loci associated with mechanical hypersensitivity where one of them is sex specific (Dominguez et al., 2012). For instance, a moderate T9 contusion was shown to cause mechanical and heat hypersensitivity in male and female mice with a greater magnification in female mice (Lee et al., 2023).

The mechanisms underlying sex differences in pain and spasticity after SCI remain to be elucidated but several possible mechanisms have shown to be implicated. Multiple studies have demonstrated elevated spontaneous activity in the DRGs following SCI (Bedi et al., 2010; Carlton et al., 2009) and a higher incidence of spontaneous activity in nociceptors was observed in females compared to males after a T10 contusion in rats (Bedi et al., 2010). Following a moderate T9 contusion in adult rats, it was reported that female rats have better tissue preservation of the white and gray matter (Datto et al., 2015). The preservation of spinal cord tissue could lead to more sparing of dorsal horn neurons as observed after a cervical hemicontusion in mice which developed mechanical allodynia after SCI (Dietz et al., 2022)

Since we observed a larger population of reporter protein expression in nociceptors compared to proprioceptive neurons within the DRG of Isl1-Vglut2^{tdTomato} mice, it is a distinct possibility that nociceptors are involved in the spasticity of spinalized Isl1-Vglut2^{CatCh} mice. The higher levels of neuropathic pain and hyperalgesia in females after SCI and greater amplitude of

EMG recordings in response to paw illumination in spinalized Isl1-Vglut2^{CatCh} mice may speak to shared mechanisms and led further support for the role of nociceptors in the spasticity of our animal model. Whether the hyperreflexia observed in female Isl1-Vglut2^{CatCh} mice could arise from sprouting of nociceptive sensory afferents or increased activation of nociceptive motor circuits after SCI remains to be determined.

4.3.4 Implications for treatment

While the mechanisms underlying spasticity is not fully understood, there are a number of treatments available to reduce the symptoms of spasticity. However, these treatments could also have their own side effects. For example, the most commonly used pharmaceutical treatment for spasticity is oral and intrathecal baclofen. Baclofen acts as GABA receptor agonist and may act to limit mono- and polysynaptic reflexes through potentiation of presynaptic or postsynaptic inhibition in the spinal cord (Abbruzzese, 2002; Awaad et al., 2012). However, the adverse side effects include sedation, fatigue, and muscle relaxation (Abbruzzese, 2002; Chou et al., 2004). Tizanidine is another drug that is often used with oral drugs such as baclofen. This drug is an agonist of imidazoline a2 receptors and decreases tone in the muscles putatively through increased presynaptic inhibition of motoneurons (Yelnik et al., 2009). It can cause dry mouth and drowsiness but doesn't cause muscle weakness like other antispastic drugs (Smith and Barton, 2000; Wagstaff and Bryson, 1997).

Our model of hindlimb spasticity in Isl1-Vglut2^{CatCh} mice could be useful in further testing of these drugs to better understand the site of action within the spinal cord that leads to reduced spasticity after SCI. Recently, the L-type calcium channel blocker, nimodipine, has been shown to

prevent the development of increased muscle tone and spontaneous spasms in mouse model of tail spasticity after a complete transection at S2 level (Marcantoni et al., 2020). Similarly, Isl1-Vglut2^{CatCh} mice could be useful for testing new drugs and approaches for prevention or treatment of hindlimb spasticity after SCI. The early manifestation of hindlimb spasticity in Isl1-Vglut2^{CatCh} mice could shorten the length of experiments aimed at testing new treatments.

4.4 Concluding thoughts

Spinal cord injury is a devastating condition that affects millions of people worldwide, resulting in profound physical and psychological consequences. However, recent advancements in the understanding of neuroplasticity—the brain and spinal cord's ability to reorganize and form new neural connections—have opened new avenues for the development of innovative treatments.

Recent groundbreaking discoveries in both preclinical and clinical studies related to SCI have defied the long-standing belief that significant functional recovery was unlikely after such injury. It has become evident that the injured spinal cord possesses the potential for various types of plasticity, including learning and memory (Wolpaw, 2010), challenging the previously held perspective that it’s not a plastic structure and can’t rewire itself.

The task of understanding the functional consequences of plasticity after injury is intricate due to the discovery of adaptive alterations in both spared and injured neural circuits throughout the entire CNS (Bareyre et al., 2004; Vavrek et al., 2006; Chen et al., 2018; Garraway and Huie, 2016; Vavrek et al., 2006). These changes occur at several physiological and molecular levels. The mechanisms involved in this plasticity are wide ranging and encompass the sprouting of sensory afferents (Krenz and Weaver, 1998; Ondarza et al., 2003), formation of new intraspinal connections (Bareyre et al., 2004; Courtine et al., 2008) , synaptic remodeling, and alterations in

excitability of neurons (Bennett et al., 2004; D'Amico et al., 2014). Since these adaptations occur concurrently, deciphering which changes are functionally significant and essential for recovery and which ones that are not, or even harmful, proves to be a challenging task. Additionally, a significant challenge in understanding plasticity lies in the tendency of most studies to focus exclusively on either the motor or sensory systems, overlooking the potential simultaneous contributions of adaptations in both systems to the recovery process.

In addition to the favorable impacts of plasticity on recovery, it is widely acknowledged that adaptive changes within the neuronal circuits, afferent sprouting and synaptogenesis can also have detrimental effects. As neurons attempt to either compensate for lost connections, the formation of new connections can lead to hyperexcitability of neurons (Gwak and Hulsebosch, 2011; Plantier et al., 2019). Moreover, alterations in pain pathways play a role in the development of post injury neuropathic pain and allodynia (Gwak and Hulsebosch, 2011; Bhagwani et al., 2022; Brown et al., 2022; Gwak and Hulsebosch, 2011), which is not entirely surprising given that mechanisms considered beneficial in the recovery of lost motor function, such as axonal sprouting, are undesirable in the context of pain pathways. Furthermore, there are other adverse consequences of plasticity following SCI, including autonomic dysreflexia and spasticity (Mazzocchio and Rossi, 1997; Hiersemenzel et al., 2000; Adams and Hicks, 2005; Bhagwani et al., 2022)

Several pharmacological methods are available to encourage plasticity in both injured and spared circuitries of the spinal cord. Some of these approaches aim to boost the existing natural plasticity, while others aim to overcome the inhibitory environment of the spinal cord. For example, chondroitinase ABC (Bradbury et al., 2002) has been used to promote axonal regeneration or application of neurotrophic factors such as BDNF (Vavrek et al., 2006; Ziemlińska et al., 2014) and NT3 (Zhou et al., 2003). The use of neurite growth promoting anti-NogoA

antibody and stem cell-based therapies, have advanced to the stage of clinical trials and has demonstrated specific functional improvements without any apparent adverse reactions. Curtis et al., 2018 have used neural stem cell transplantation (human NSI-566 cell line) for the very first time in chronic spinal trauma patients (Curtis et al., 2018). Kucher et al., 2018 observed an increase in motor scores in hemiplegic and tetraplegic patients upon intrathecal application of NogoA antibody (Kucher et al., 2018).

Besides pharmacological or cellular approaches, one of the most established approaches to promote plasticity and locomotor recovery is treadmill training, which has been effectively applied from animal experiments to clinical settings. Pioneering studies demonstrated that cats with complete spinal transection could relearn stepping, showcasing a remarkable display of plasticity and recovery driven by activity-dependent mechanisms (Lovely et al., 1986; Barbeau and Rossignol, 1987; De Leon et al., 1998). Notably, this observed plasticity occurred in the spinal cord independently of descending input.

For neurorehabilitation to be effective, there needs to be a finely tuned interplay between peripheral input and spinal motor circuits. It is essential to have sufficient and suitable afferent input that can modulate spinal circuitry, including the central pattern generator. The CPG can generate rhythmic locomotor activities, incorporating proprioceptive and sensory feedback, thereby optimizing adaptive spinal training (Kiehn et al., 2008).

Both human and animal studies have provided evidence of a direct increase in limb muscle activity and weight-bearing load with repeated training. This suggests that adaptive spinal plasticity depends on afferent input related to loading during locomotion (Domingo et al., 2007; Ferris et al., 2004; Behrman et al., 2017). Bouyer and Rossignol's research highlighted the essential role of afferent input in treadmill training. Their study demonstrated that in spinalized cats, at least

one intact cutaneous afferent nerve is necessary to achieve proper plantar foot placement and weight-bearing during locomotion (Bouyer and Rossignol, 2003). Takeoka et al., 2019 has demonstrated that proprioceptive feedback below the level of injury is essential for recovery of locomotion and establishment of detour circuits (Takeoka and Arber, 2019).

Neuromodulatory interventions such as Epidural Electrical Stimulation (EES) and Brain-Machine Interface (BMI) have also exhibited significant efficacy in clinical trials, making them potentially the most promising approaches for functional restoration after SCI (Gerasimenko et al., 2006; Formento et al., 2018; Gill et al., 2018; Wagner et al., 2018; Darrow et al., 2019; Lorach et al., 2023). EES applied to the spinal cord where the electrodes targeted the dorsal roots has successfully restored voluntary control of the trunk and legs in 3 patients with complete paralysis. EES recruits large diameter afferent fibers as they enter the spinal cord and activates the motor neurons (Formento et al., 2018; Gerasimenko et al., 2006). This type of neurorehabilitation has enabled individuals with severe SCI to engage in activities such as standing, walking, cycling, and swimming in real-world settings (Rowald et al., 2022).

In a recent study, a digital bridge between the brain and the spinal cord was established, allowing an individual with chronic tetraplegia to stand and walk naturally in community settings. This innovative brain–spine interface (BSI) comprises fully implanted recording and stimulation systems, establishing a direct connection between cortical signals and the precise modulation of epidural electrical stimulation. This targeted stimulation focuses on spinal cord regions crucial for the generation of walking movements and enabled continuous and robust control of walking (Lorach et al., 2023).

In this thesis, I have examined remodelling of synaptic inputs to dI3 INs and MNs using a transgenic mouse model. I have identified alterations in synaptic connectivity onto dI3 INs and

motoneurons below the injury site, both before and after the injury. The analysis encompassed central and peripheral glutamatergic inputs, as well as presynaptic inhibition of sensory inputs to dI3 INs and MNs, within experimental groups with or without locomotor training.

We have previously shown that dI3 INs play a role in recovery of locomotion after a complete transection of the spinal cord and silencing these neurons eliminates recovery of rhythmic limb movement (Bui et al., 2016). We have shown that dI3 INs receive a mixture of proprioceptive and mechanoreceptive sensory feedback and provide an excitatory drive to both motoneurons and spinal locomotor networks. This unique connectivity renders dI3 INs an ideal candidate population of spinal neurons for inducing beneficial compensatory changes in a spinal cord deprived of motor commands from the brain due to SCI. My data demonstrates a transient decrease in sensory inputs from sensory afferents onto dI3 INs even in later stages post-injury. Additionally, I observed an increase in the level of presynaptic inhibition of sensory afferents onto dI3 INs shortly after the injury. The brief post-injury window is crucial for enhancing the flow of sensory inputs. Given the mounting evidence emphasizing the importance of cutaneous and proprioceptive inputs in activating dormant spinal circuits, it is imperative that future therapies should focus on restoring sensory inputs to dI3 INs and decreasing presynaptic inhibition of sensory afferents. This approach holds potential for improving locomotor function after spinal cord injury. Additionally, I observed a transient increase in the level of central glutamatergic inputs after injury which is potentially very beneficial. This level of increase should be maintained through rehabilitative or pharmacological therapies due to the potential role of dI3 INs in driving activity of the CPG networks.

Furthermore, we have created an optogenetic mouse model that consistently induces spasticity in mice with SCI. This model shows promise for investigating the mechanisms

underlying limb spasticity in SCI, shedding light on the maladaptive changes occurring within the spinal cord. Overall, my thesis reveals changes in plasticity in spinal circuits that could be beneficial or detrimental to the recovery of locomotor function and suggests an invaluable model for further uncovering maladaptive plasticity.

Bibliography

Abbruzzese, G., 2002. The medical management of spasticity. Eur J Neurol 9 Suppl 1, 30–34.

Ackery, A.D., Norenberg, M.D., Krassioukov, A., 2007. Calcitonin gene-related peptide immunoreactivity in chronic human spinal cord injury. Spinal Cord 45, 678–686.

Adams, M.M., Hicks, A.L., 2005. Spasticity after spinal cord injury. Spinal Cord 43, 577–586.

Adriaansen, J.J.E., Ruijs, L.E.M., Van Koppenhagen, C.F., Van Asbeck, F.W.A., Snoek, G.J., Van Kuppevelt, D., Visser-Meily, J.M.A., Post, M.W.M., 2016. Secondary health conditions and quality of life in persons living with spinal cord injury for at least ten years. J Rehabil Med 48, 853–860.

Aigner, L., Arber, S., Kapfhammer, J.P., Laux, T., Schneider, C., Botteri, F., Brenner, H.R., Caroni, P., 1995. Overexpression of the neural growth-associated protein GAP-43 induces nerve sprouting in the adult nervous system of transgenic mice. Cell 83, 269–278.

Akay, T., Acharya, H.J., Fouad, K., Pearson, K.G., 2006. Behavioral and electromyographic characterization of mice lacking EphA4 receptors. J Neurophysiol 96, 642–651.

Akay, T., Fouad, K., Pearson, K.G., 2008. New technique for drug application to the spinal cord of walking mice. J Neurosci Methods 171, 39–47.

Alvarez, F.J., Taylor-Blake, B., Fyffe, R.E.W., De Rlas, A.L., Light, A.R., 1996. Distribution of Immunoreactivity for the p2 and p 3 Subunits of the GABAA Receptor in the Mammalian Spinal Cord. J Comp Neurol 365, 392–412.

Alvarez, F.J., Villalba, R.M., Zerda, R., Schneider, S.P., 2004. Vesicular Glutamate Transporters in the Spinal Cord, with Special Reference to Sensory Primary Afferent Synapses. Journal of Comparative Neurology 472, 257–280.

Alvarez, P., Gear, R.W., Green, P.G., Levine, J.D., 2012. IB4-saporin attenuates acute and eliminates chronic muscle pain in the rat. Exp Neurol 233, 859–865.

Angeli, C.A., Edgerton, V.R., Gerasimenko, Y.P., Harkema, S.J., 2014. Altering spinal cord excitability enables voluntary movements after chronic complete paralysis in humans. Brain 137, 1394–1409.

Aoki, Y., Takahashi, Y., Ohtori, S., Moriya, H., Takahashi, K., 2004. Distribution and immunocytochemical characterization of dorsal root ganglion neurons innervating the lumbar intervertebral disc in rats: A review. Life Sci 74, 2627–2642.

Arvanian, V.L., Mendell, L.M., 2001. Acute modulation of synaptic transmission to motoneurons by BDNF in the neonatal rat spinal cord. Eur J Neurosci 14, 1800–1808.

Asboth, L., Friedli, L., Beauparlant, J., Martinez-Gonzalez, C., Anil, S., Rey, E., Baud, L., Pidpruzhnykova, G., Anderson, M.A., Shkorbatova, P., Batti, L., Pagès, S., Kreider, J., Schneider, B.L., Barraud, Q., Courtine, G., 2018. Cortico–reticulo–spinal circuit reorganization enables functional recovery after severe spinal cord contusion. Nat Neurosci 21, 576–588.

Avraham, O., Hadas, Y., Vald, L., Hong, S., Song, M.R., Klar, A., 2010. Motor and Dorsal Root Ganglion Axons Serve as Choice Points for the Ipsilateral Turning of dI3 Axons. Journal of Neuroscience 30, 15546–15557.

Awaad, Y., Rizk, T., Siddiqui, I., Roosen, N., Mcintosh, K., Waines, G.M., 2012. Complications of Intrathecal Baclofen Pump: Prevention and Cure. International Scholarly Research Network ISRN Neurology 2012.

Baldissera, F., Campadelli, P., Piccinelli, L., 1982. Impulse coding of ramp currents intracellularly injected into pyramidal tract neurones. Exp Brain Res 48, 455–458.

Ballermann, M., Fouad, K., 2006. Spontaneous locomotor recovery in spinal cord injured rats is accompanied by anatomical plasticity of reticulospinal fibers. Eur J Neurosci 23, 1988–1996.

Ballion, B., Morin, D., Viala, D., 2001. Forelimb locomotor generators and quadrupedal locomotion in the neonatal rat. Eur J Neurosci 14, 1727–1738.

Barbeau, H., Rossignol, S., 1987. Recovery of locomotion after chronic spinalization in the adult cat. Brain Res 412, 84–95.

Bareyre, F.M., Kerschensteiner, M., Raineteau, O., Mettenleiter, T.C., Weinmann, O., Schwab, M.E., 2004. The injured spinal cord spontaneously forms a new intraspinal circuit in adult rats. Nature Neuroscience 2004 7:3 7, 269–277.

Battaglia, G., Rustioni, A., 1988. Coexistence of glutamate and substance P in dorsal root ganglion neurons of the rat and monkey. J Comp Neurol 277, 302–312.

Beaumont, E., Houlé, J.D., Peterson, C.A., Gardiner, P.F., 2004. Passive exercise and fetal spinal cord transplant both help to restore motoneuronal properties after spinal cord transection in rats. Muscle Nerve 29, 234–242.

Bedi, S.S., Lago, M.T., Masha, L.I., Crook, R.J., Grill, R.J., Walters, E.T., 2012. Spinal Cord Injury Triggers an Intrinsic Growth-Promoting State in Nociceptors. J Neurotrauma 29, 925.

Bedi, S.S., Yang, Q., Crook, R.J., Du, J., Wu, Z., Fishman, H.M., Grill, R.J., Carlton, S.M., Walters, E.T., 2010. Chronic Spontaneous Activity Generated in the Somata of Primary Nociceptors Is Associated with Pain-Related Behavior after Spinal Cord Injury. The Journal of Neuroscience 30, 14870.

Behrman, A.L., Ardolino, E.M., Harkema, S.J., 2017. Activity-Based Therapy: From Basic Science to Clinical Application for Recovery After Spinal Cord Injury. J Neurol Phys Ther 41 Suppl 3, S39–S45.

Bennett, D.J., Hultborn, H., Fedirchuk, B., Gorassini, M., 1998. Synaptic activation of plateaus in hindlimb motoneurons of decerebrate cats. J Neurophysiol 80, 2023–2037.

Bennett, D.J., Li, Y., Siu, M., 2001. Plateau potentials in sacrocaudal motoneurons of chronic spinal rats, recorded in vitro. J Neurophysiol 86.

Bennett, D.J., Sanelli, L., Cooke, C.L., Harvey, P.J., Gorassini, M.A., 2004. Spastic long-lasting reflexes in the awake rat after sacral spinal cord injury. J Neurophysiol 91, 2247–2258.

Bennett, J., Das, J.M., Emmady, P.D., 2022. Spinal Cord Injuries. StatPearls.

Bertels, H., Vicente-Ortiz, G., El Kanbi, K., Takeoka, A., 2022. Neurotransmitter phenotype switching by spinal excitatory interneurons regulates locomotor recovery after spinal cord injury. Nature Neuroscience 2022 25:5 25, 617–629.

Betley, J.N., Wright, C.V.E., Kawaguchi, Y., Erdélyi, F., Szabó, G., Jessell, T.M., Kaltschmidt, J.A., 2009. Stringent specificity in the construction of a GABAergic presynaptic inhibitory circuit. Cell 139, 161–174.

Bhagwani, A., Chopra, M., Kumar, H., 2022. Spinal Cord Injury Provoked Neuropathic Pain and Spasticity, and Their GABAergic Connection. Neurospine 19, 646–668.

Bouyer, L.J.G., Rossignol, S., 2003. Contribution of cutaneous inputs from the hindpaw to the control of locomotion. II. Spinal cats. J Neurophysiol 90, 3640–3653.

Boyce, V.S., Park, J., Gage, F.H., Mendell, L.M., 2012. Differential effects of brain-derived neurotrophic factor and neurotrophin-3 on hindlimb function in paraplegic rats. European Journal of Neuroscience 35, 221–232.

Bradbury, E.J., Moon, L.D.F., Popat, R.J., King, V.R., Bennett, G.S., Patel, P.N., Fawcett, J.W., McMahon, S.B., 2002. Chondroitinase ABC promotes functional recovery after spinal cord injury. Nature 416, 636–640.

Brown, A., Weaver, L.C., 2012. The dark side of neuroplasticity. Exp Neurol 235, 133–141.

Brown, E. V., Malik, A.F., Moese, E.R., McElroy, A.F., Lepore, A.C., 2022. Differential Activation of Pain Circuitry Neuron Populations in a Mouse Model of Spinal Cord Injury-Induced Neuropathic Pain. J Neurosci 42, 3271–3289.

Brownstone, R.M., Bui, T. v., 2010. Spinal interneurons providing input to the final common path during locomotion. Prog Brain Res 187, 81–95.

Brumovsky, P., Watanabe, M., Hökfelt, T., 2007. Expression of the vesicular glutamate transporters-1 and -2 in adult mouse dorsal root ganglia and spinal cord and their regulation by nerve injury. Neuroscience 147, 469–490.

Brus-Ramer, M., Carmel, J.B., Chakrabarty, S., Martin, J.H., 2007. Electrical stimulation of spared corticospinal axons augments connections with ipsilateral spinal motor circuits after injury. J Neurosci 27, 13793–13801.

Brustein, E., Rossignol, S., 1998. Recovery of locomotion after ventral and ventrolateral spinal lesions in the cat. I. Deficits and adaptive mechanisms. J Neurophysiol 80, 1245–1267.

Budh, C.N., Lund, I., Hultling, C., Levi, R., Werhagen, L., Ertzgaard, P., Lundeberg, T., 2003. Gender related differences in pain in spinal cord injured individuals. Spinal Cord 2003 41:2 41, 122–128.

Bui, T. V., Akay, T., Loubani, O., Hnasko, T.S., Jessell, T.M., Brownstone, R.M., 2013. Circuits for grasping: spinal dI3 interneurons mediate cutaneous control of motor behavior. Neuron 78, 191–204.

Bui, T. V., Stifani, N., Akay, T., Brownstone, R.M., 2016. Spinal microcircuits comprising dI3 interneurons are necessary for motor functional recovery following spinal cord transection. Elife 5.

Cafferty, W.B.J., Duffy, P., Huebner, E., Strittmatter, S.M., 2010. MAG and OMgp Synergize with Nogo-A to Restrict Axonal Growth and Neurological Recovery after Spinal Cord Trauma. Journal of Neuroscience 30, 6825–6837.

Cantoria, M.J., See, P.A., Singh, H., De Leon, R.D., 2011. Development/Plasticity/Repair Adaptations in Glutamate and Glycine Content within the Lumbar Spinal Cord Are Associated with the Generation of Novel Gait Patterns in Rats following Neonatal Spinal Cord Transection.

Cao, Q., Zhang, Y.P., Iannotti, C., DeVries, W.H., Xu, X.M., Shields, C.B., Whittemore, S.R., 2005. Functional and electrophysiological changes after graded traumatic spinal cord injury in adult rat. Exp Neurol 191 Suppl 1.

Carlin, K.P., Jones, K.E., Jiang, Z., Jordan, L.M., Brownstone, R.M., 2000. Dendritic L-type calcium currents in mouse spinal motoneurons: Implications for bistability. European Journal of Neuroscience 12, 1635–1646.

Carlton, S.M., 2001. Peripheral excitatory amino acids. Curr Opin Pharmacol 1, 52–56.

Carlton, S.M., Du, J., Tan, H.Y., Nesic, O., Hargett, G.L., Bopp, A.C., Yamani, A., Lin, Q., Willis, W.D., Hulsebosch, C.E., 2009. Peripheral and central sensitization in remote spinal cord regions contribute to central neuropathic pain after spinal cord injury. Pain 147, 265.

Carmel, J.B., Berrol, L.J., Brus-Ramer, M., Martin, J.H., 2010. Chronic electrical stimulation of the intact corticospinal system after unilateral injury restores skilled locomotor control and promotes spinal axon outgrowth. J Neurosci 30, 10918–10926.

Carmel, J.B., Martin, J.H., 2014. Motor cortex electrical stimulation augments sprouting of the corticospinal tract and promotes recovery of motor function. Front Integr Neurosci 8.

Caudle, K.L., Brown, E.H., Shum-Siu, A., Burke, D.A., Magnuson, T.S.G., Voor, M.J., Magnuson, D.S.K., 2011. Hindlimb Immobilization in a Wheelchair Alters Functional Recovery Following Contusive Spinal Cord Injury in the Adult Rat. Neurorehabil Neural Repair 25, 729.

Chang, E., Ghosh, N., Yanni, D., Lee, S., Alexandru, D., Mozaffar, T., 2013. A Review of Spasticity Treatments: Pharmacological and Interventional Approaches.

Chen, B., Li, Y., Yu, B., Zhang, Z., Brommer, B., Williams, P.R., Liu, Y., Hegarty, S.V., Zhou, S., Zhu, J., Guo, H., Lu, Y., Zhang, Y., Gu, X., He, Z., 2018. Reactivation of Dormant Relay Pathways in Injured Spinal Cord by KCC2 Manipulations. Cell 174, 521-535.e13.

Chou, R., Peterson, K., Helfand, M., 2004. Comparative efficacy and safety of skeletal muscle relaxants for spasticity and musculoskeletal conditions: A systematic review. J Pain Symptom Manage 28, 140–175.

Christensen, M.D., Hulsebosch, C.E., 1997. Chronic Central Pain after Spinal Cord Injury, JOURNAL OF NEUROTRAUMA. Mary Ann Liebert, Inc.

Chu, T., Zhou, H., Li, F., Wang, T., Lu, L., Feng, S., 2014. Astrocyte transplantation for spinal cord injury: current status and perspective. Brain Res Bull 107, 18–30.

Conta, A.C., Stelzner, D.J., 2004. Differential vulnerability of propriospinal tract neurons to spinal cord contusion injury. J Comp Neurol 479, 347–359.

Cope, T.C., Bodine, S.C., Fournier, M., Edgerton, V.R., 1986. Soleus motor units in chronic spinal transected cats: physiological and morphological alterations. J Neurophysiol 55, 1202–1220.

Côté, M.P., Azzam, G.A., Lemay, M.A., Zhukareva, V., Houlé, J.D., 2011. Activity-dependent increase in neurotrophic factors is associated with an enhanced modulation of spinal reflexes after spinal cord injury. J Neurotrauma 28, 299–309.

Courtine, G., Gerasimenko, Y., Van Den Brand, R., Yew, A., Musienko, P., Zhong, H., Song, B., Ao, Y., Ichiyama, R.M., Lavrov, I., Roy, R.R., Sofroniew, M. V., Edgerton, V.R., 2009. Transformation of nonfunctional spinal circuits into functional states after the loss of brain input. Nat Neurosci 12, 1333–1342.

Courtine, G., Song, B., Roy, R.R., Zhong, H., Herrmann, J.E., Ao, Y., Qi, J., Edgerton, V.R., Sofroniew, M. V, 2008. Recovery of supraspinal control of stepping via indirect propriospinal relay connections after spinal cord injury. Nat Med 14, 69–74.

Cowley, K.C., Lane, M.A., Meehan, C.F., Rank, M.M., Stecina, K., 2021. Editorial: Propriospinal Neurons: Essential Elements in Locomotion, Autonomic Function and Plasticity After Spinal Cord Injury and Disease. Front Cell Neurosci 15, 695424.

Cowley, K.C., Zaporozhets, E., Schmidt, B.J., 2008. Propriospinal neurons are sufficient for bulbospinal transmission of the locomotor command signal in the neonatal rat spinal cord. J Physiol 586, 1623–35.

Craven, B.C., Morris, A.R., 2010. Modified Ashworth scale reliability for measurement of lower extremity spasticity among patients with SCI. Spinal Cord 48, 207–213.

Cui, Y.-Y., Xu, H., Wu, H.-H., Qi, J., Shi, J., Li, Y.-Q., Y-y, C., H-h, W., 2014. Spatio-Temporal Expression and Functional Involvement of Transient Receptor Potential Vanilloid 1 in Diabetic Mechanical Allodynia in Rats. PLoS One 9, 102052.

Curtis, E., Martin, J.R., Gabel, B., Sidhu, N., Rzesiewicz, T.K., Mandeville, R., Van Gorp, S., Leerink, M., Tadokoro, T., Marsala, S., Jamieson, C., Marsala, M., Ciacci, J.D., 2018. A First-in-Human, Phase I Study of Neural Stem Cell Transplantation for Chronic Spinal Cord Injury. Cell Stem Cell 22, 941-950.e6.

D'Amico, J.M., Condliffe, E.G., Martins, K.J.B., Bennett, D.J., Gorassini, M.A., 2014. Recovery of neuronal and network excitability after spinal cord injury and implications for spasticity. Front Integr Neurosci.

Darrow, D., Balser, D., Netoff, T.I., Krassioukov, A., Phillips, A., Parr, A., Samadani, U., 2019. Epidural Spinal Cord Stimulation Facilitates Immediate Restoration of Dormant Motor and Autonomic Supraspinal Pathways after Chronic Neurologically Complete Spinal Cord Injury. J Neurotrauma 36, 2325–2336.

Datto, J.P., Bastidas, J.C., Miller, N.L., Shah, A.K., Arheart, K.L., Marcillo, A.E., Dietrich, W.D., Pearse, D.D., 2015. Female Rats Demonstrate Improved Locomotor Recovery and Greater Preservation of White and Gray Matter after Traumatic Spinal Cord Injury Compared to Males. J Neurotrauma 32, 1146–1157.

De Leon, R.D., Hodgson, J.A., Roy, R.R., Edgerton, V.R., 1998. Locomotor capacity attributable to step training versus spontaneous recovery after spinalization in adult cats. J Neurophysiol 79, 1329–1340.

Dell'Anno, M.T., Strittmatter, S.M., 2017. Rewiring the spinal cord: Direct and indirect strategies. Neurosci Lett 652, 25–34.

Delwaide, P.J., Oliver, E., 1988. Short-latency autogenic inhibition (IB inhibition) in human spasticity. J Neurol Neurosurg Psychiatry 51.

Deumens, R., Mazzone, G. L., & Taccola, G. (2013). Early spread of hyperexcitability to caudal dorsal horn networks after a chemically-induced lesion of the rat spinal cord in vitro. *Neuroscience*, *229*, 155–163.

Dietz, V., Knox, K., Moore, S., Roberts, N., Corona, K.K., Dulin, J.N., 2022. Dorsal horn neuronal sparing predicts the development of at-level mechanical allodynia following cervical spinal cord injury in mice. Exp Neurol 352, 114048.

Ditunno, J. F., Little, J. W., Tessler, A., & Burns, A. S. (2004). Spinal shock revisited: a four-phase model. *Spinal Cord*, *42*(7), 383–395.

Domingo, A., Sawicki, G.S., Ferris, D.P., 2007. Kinematics and muscle activity of individuals with incomplete spinal cord injury during treadmill stepping with and without manual assistance. J Neuroeng Rehabil 4.

Dominguez, C.A., Ström, M., Gao, T., Zhang, L., Olsson, T., Wiesenfeld-Hallin, Z., Xu, X.J., Piehl, F., 2012. Genetic and sex influence on neuropathic pain-like behaviour after spinal cord injury in the rat. European Journal of Pain (United Kingdom) 16, 1368–1377.

Edgerton, V.R., Tillakaratne, N.J.K., Bigbee, A.J., De Leon, R.D., Roy, R.R., 2004. Plasticity of the spinal neural circuitry after injury. Annu Rev Neurosci 27, 145–167.

Eken, T., Hultborn, H., Kiehn, O., 1989. Possible functions of transmitter-controlled plateau potentials in α motoneurones. Prog Brain Res 80, 257–267.

Erlander, M.G., Tobin, A.J., 1991. The structural and functional heterogeneity of glutamic acid decarboxylase: a review. Neurochem Res 16, 215–226.

Esclapez, M., Tillakaratne, N.J.K., Kaufman, D.L., Tobin, A.J., Houser, C.R., 1994. Comparative localization of two forms of glutamic acid decarboxylase and their mRNAs in rat brain supports the concept of functional differences between the forms. J Neurosci 14, 1834–1855.

Faist, M., Mazevet, D., Dietz, V., Pierrot-deseilligny, E., 1994. A quantitative assessment of presynaptic inhibition of la afferents in spastics: Differences in hemiplegics and paraplegics. Brain 117, 1449–1455.

Ferris, D.P., Gordon, K.E., Beres-Jones, J.A., Harkema, S.J., 2004. Muscle activation during unilateral stepping occurs in the nonstepping limb of humans with clinically complete spinal cord injury. Spinal Cord 42, 14–23.

Field-Fote, E.C., Roach, K.E., 2011. Influence of a Locomotor Training Approach on Walking Speed and Distance in People With Chronic Spinal Cord Injury: A Randomized Clinical Trial. Phys Ther 91, 48.

Filli, L., Engmann, A.K., Zörner, B., Weinmann, O., Moraitis, T., Gullo, M., Kasper, H., Schneider, R., Schwab, M.E., 2014. Bridging the gap: a reticulo-propriospinal detour bypassing an incomplete spinal cord injury. J Neurosci 34, 13399–13410.

Fink, K.L., Cafferty, W.B.J., 2016. Reorganization of Intact Descending Motor Circuits to Replace Lost Connections After Injury. Neurotherapeutics 13, 370–381.

Finnerup, N. B., Johannesen, I. L., Sindrup, S. H., Bach, F. W., & Jensen, T. S. (2001). Pain and dysesthesia in patients with spinal cord injury: A postal survey. *Spinal Cord 2001 39:5*, *39*(5), 256–262.

Fonnum, F., 1984. Glutamate: a neurotransmitter in mammalian brain. J Neurochem 42, 1–11.

Formento, E., Minassian, K., Wagner, F., Mignardot, J.B., Le Goff-Mignardot, C.G., Rowald, A., Bloch, J., Micera, S., Capogrosso, M., Courtine, G., 2018. Electrical spinal cord stimulation must preserve proprioception to enable locomotion in humans with spinal cord injury. Nat Neurosci 21, 1728–1741.

Friedman, B., Kleinfeld, D., Ip, N.Y., Verge, V.M.K., Moulton, R., Boland, P., Zlotchenko, E., Lindsay, R.M., Liu, L., 1995. BDNF and NT-4/5 exert neurotrophic influences on injured adult spinal motor neurons. The Journal of Neuroscience 15, 1044.

Frigon, A., Rossignol, S., 2008. Adaptive changes of the locomotor pattern and cutaneous reflexes during locomotion studied in the same cats before and after spinalization. J Physiol 586, 2927–2945.

Garraway, S.M., Huie, J.R., 2016. Spinal Plasticity and Behavior: BDNF-Induced Neuromodulation in Uninjured and Injured Spinal Cord. Neural Plast 2016.

Gerasimenko, Y., Preston, C., Zhong, H., Roy, R.R., Edgerton, V.R., Shah, P.K., 2019. Rostral lumbar segments are the key controllers of hindlimb locomotor rhythmicity in the adult spinal rat. J Neurophysiol 122, 585–600.

Gerasimenko, Y.P., Ichiyama, R.M., Lavrov, I.A., Courtine, G., Cai, L., Zhong, H., Roy, R.R., Edgerton, V.R., 2007. Epidural spinal cord stimulation plus quipazine administration enable stepping in complete spinal adult rats. J Neurophysiol 98, 2525–2536.

Gerasimenko, Y.P., Lavrov, I.A., Courtine, G., Ichiyama, R.M., Dy, C.J., Zhong, H., Roy, R.R., Edgerton, V.R., 2006. Spinal cord reflexes induced by epidural spinal cord stimulation in normal awake rats. J Neurosci Methods 157, 253–263.

Gerasimenko, Y.P., Makarovskii, A.N., Nikitin, O.A., 2002. Control of locomotor activity in humans and animals in the absence of supraspinal influences. Neurosci Behav Physiol 32, 417–423.

Ghosh, A., Sydekum, E., Haiss, F., Peduzzi, S., Zörner, B., Schneider, R., Baltes, C., Rudin, M., Weber, B., Schwab, M.E., 2009. Functional and Anatomical Reorganization of the Sensory-Motor Cortex after Incomplete Spinal Cord Injury in Adult Rats. The Journal of Neuroscience 29, 12210.

Ghosh, S., Hui, S.P., 2016. Regeneration of Zebrafish CNS: Adult Neurogenesis. Neural Plast 2016.

Gill, M.L., Grahn, P.J., Calvert, J.S., Linde, M.B., Lavrov, I.A., Strommen, J.A., Beck, L.A., Sayenko, D.G., Van Straaten, M.G., Drubach, D.I., Veith, D.D., Thoreson, A.R., Lopez, C., Gerasimenko, Y.P., Edgerton, V.R., Lee, K.H., Zhao, K.D., 2018. Neuromodulation of lumbosacral spinal networks enables independent stepping after complete paraplegia. Nat Med 24, 1677–1682.

Gómez-Pinilla, F., Ying, Z., Roy, R.R., Hodgson, J., Reggie Edgerton, V., Fernando, G.-P., Hodg, J., 2004. Afferent Input Modulates Neurotrophins and Synaptic Plasticity in the Spinal Cord. J Neurophysiol 92, 3423–3432.

Gómez-Pinilla, F., Ying, Z., Roy, R.R., Molteni, R., Reggie Edgerton, V., 2002. Voluntary exercise induces a BDNF-mediated mechanism that promotes neuroplasticity. J Neurophysiol 88, 2187–2195.

Gorassini, M.A., Knash, M.E., Harvey, P.J., Bennett, D.J., Yang, J.F., 2004. Role of motoneurons in the generation of muscle spasms after spinal cord injury. Brain 127, 2247–2258.

Gulino, R., Lombardo, S.A., Casabona, A., Leanza, G., Perciavalle, V., 2004. Levels of brain-derived neurotrophic factor and neurotrophin-4 in lumbar motoneurons after low-thoracic spinal cord hemisection. Brain Res 1013, 174–181.

Gwak, Y.S., Hulsebosch, C.E., 2011. Neuronal hyperexcitability: A substrate for central neuropathic pain after spinal cord injury. Curr Pain Headache Rep 15, 215–222.

Hains, B.C., Everhart, A.W., Fullwood, S.D., Hulsebosch, C.E., 2002. Changes in serotonin, serotonin transporter expression and serotonin denervation supersensitivity: Involvement in chronic central pain after spinal hemisection in the rat. Exp Neurol 175, 347–362.

Hains, B. C., Johnson, K.M., Eaton, M.J., Willis, W.D., Hulsebosch, C.E., 2003. Serotonergic neural precursor cell grafts attenuate bilateral hyperexcitability of dorsal horn neurons after spinal hemisection in rat. Neuroscience 116, 1097–1110.

Hains, Bryan C., Willis, W.D., Hulsebosch, C.E., 2003. Temporal plasticity of dorsal horn somatosensory neurons after acute and chronic spinal cord hemisection in rat. Brain Res 970, 238–241.

Hari, K., Lucas-Osma, A.M., Metz, K., Lin, S., Pardell, N., Roszko, D., Black, S., Minarik, A., Singla, R., Stephens, M.J., Fouad, K., Jones, K.E., Gorassini, M.A., Fenrich, K.K., Li, Y., Bennett, D.J., 2021. Nodal GABA facilitates axon spike transmission in the spinal cord. bioRxiv 2021.01.20.427494.

Hari, K., Lucas-Osma, A.M., Metz, K., Lin, S., Pardell, N., Roszko, D.A., Black, S., Minarik, A., Singla, R., Stephens, M.J., Pearce, R.A., Fouad, K., Jones, K.E., Gorassini, M.A., Fenrich, K.K., Li, Y., Bennett, D.J., 2022. GABA facilitates spike propagation through branch points of sensory axons in the spinal cord. Nat Neurosci 25, 1288–1299.

Harkema, S., Gerasimenko, Y., Hodes, J., Burdick, J., Angeli, C., Chen, Y., Ferreira, C., Willhite, A., Rejc, E., Grossman, R.G., Edgerton, V.R., 2011. Effect of epidural stimulation of the lumbosacral spinal cord on voluntary movement, standing, and assisted stepping after motor complete paraplegia: a case study. Lancet 377, 1938–1947.

Harkema, S.J., Schmidt-Read, M., Lorenz, D.J., Edgerton, V.R., Behrman, A.L., 2012. Balance and ambulation improvements in individuals with chronic incomplete spinal cord injury using locomotor trainingbased rehabilitation. Arch Phys Med Rehabil 93, 1508–1517.

Harvey, P J, Li, X., Li, Y., Bennett, D J, Bennett, David J, 2006. 5HT 2 receptor activation facilitates a persistent sodium current and repetitive firing in spinal motoneurons of rats with and without chronic spinal cord injury Running Title: 5-HT 2 receptor activation facilitates a persistent sodium current. Articles in PresS. J Neurophysiol.

Harvey, P. J., Li, Y., Li, X., Bennett, D.J., 2006. Persistent sodium currents and repetitive firing in motoneurons of the sacrocaudal spinal cord of adult rats. J Neurophysiol 96, 1141–1157.

Heetla, H.W., Staal, M.J., Proost, J.H., Van Laar, T., 2014. Clinical relevance of pharmacological and physiological data in intrathecal baclofen therapy. Arch Phys Med Rehabil 95, 2199–2206.

Helms, A.W., Johnson, J.E., 2003. Specification of dorsal spinal cord interneurons. Curr Opin Neurobiol 13, 42–49.

Hiersemenzel, L.P., Curt, A., Dietz, V., 2000. From spinal shock to spasticity: neuronal adaptations to a spinal cord injury. Neurology 54, 1574–1582.

Hochman, S., McCrea, D.A., 1994. Effects of chronic spinalization on ankle extensor motoneurons. II. Motoneuron electrical properties. J Neurophysiol 71, 1468–1479.

Hochman, S., Shreckengost, J., Kimura, H., Quevedo, J., 2010. Presynaptic inhibition of primary afferents by depolarization: observations supporting nontraditional mechanisms. Ann N Y Acad Sci 1198, 140–152.

HÖKFELT, T., ARVIDSSON, U., CECCATELLI, S., CORTÉS, R., CULLHEIM, S., DAGERLIND, Å., JOHNSON, H., ORAZZO, C., PIEHL, F., PIERIBONE, V., SCHALLING, M., TERENIUS, L., ULFHAKE, B., VERGE, V.M., VILLAR, M., WIESENFELD-HALLIN, Z., XU, X. -J, XU, Z., 1992. Calcitonin Gene-Related Peptide in the Brain, Spinal Cord, and Some Peripheral Systems. Ann N Y Acad Sci 657, 119–134.

Holtz, K.A., Lipson, R., Noonan, V.K., Kwon, B.K., Mills, P.B., 2017. Prevalence and Effect of Problematic Spasticity After Traumatic Spinal Cord Injury. Arch Phys Med Rehabil 98, 1132–1138.

Hounsgaard, J., Hultborn, H., Jespersen, B., Kiehn, O., 1988. Bistability of alpha-motoneurones in the decerebrate cat and in the acute spinal cat after intravenous 5-hydroxytryptophan. J Physiol 405, 345–367.

Huang, Y.J., Lee, K.H., Grau, J.W., 2017. Complete spinal cord injury (SCI) transforms how brain derived neurotrophic factor (BDNF) affects nociceptive sensitization. Exp Neurol 288, 38–50.

Ichiyama, R.M., Broman, J., Roy, R.R., Zhong, H., Edgerton, V.R., Havton, L.A., 2011. Locomotor Training Maintains Normal Inhibitory Influence on Both Alpha- and Gamma-Motoneurons after Neonatal Spinal Cord Transection. Journal of Neuroscience 31, 26–33.

Ichiyama, R.M., Gerasimenko, Y.P., Zhong, H., Roy, R.R., Edgerton, V.R., 2005. Hindlimb stepping movements in complete spinal rats induced by epidural spinal cord stimulation. Neurosci Lett 383, 339–344.

Jalan, D., Saini, N., Zaidi, M., Pallottie, A., Elkabes, S., Heary, R.F., 2017. Effects of early surgical decompression on functional and histological outcomes after severe experimental thoracic spinal cord injury. J Neurosurg Spine 26, 62–75.

Jankowska, E., 1992. Interneuronal relay in spinal pathways from proprioceptors. Prog Neurobiol 38, 335–378.

Jankowska, E., Lundberg, A., Roberts, W.J., Stuart, D., 1974. A long propriospinal system with direct effect on motoneurones and on interneurones in the cat lumbosacral cord. Exp Brain Res 21, 169–194.

Jankowska, E., Lundberg, A., Stuart, D., 1983. Propriospinal control of interneurons in spinal reflex pathways from tendon organs in the cat. Brain Res 261, 317–320.

Jazayeri, S.B., Firouzi, M., Zadegan, S.A., Saeedi, N., Pirouz, E., Nategh, M., Jahanzad, I., Ashtiani, A.M., Rahimi-Movaghar, V., 2013. The Effect of Timing of Decompression on Neurologic Recovery and Histopathologic Findings After Spinal Cord Compression in a Rat Model. Acta Med Iran 51, 431–437.

Jensen, V.N., Alilain, W.J., Crone, S.A., 2019. Role of Propriospinal Neurons in Control of Respiratory Muscles and Recovery of Breathing Following Injury. Front Syst Neurosci 13.

Jordan, L.M., Schmidt, B.J., 2002. Propriospinal neurons involved in the control of locomotion: potential targets for repair strategies? Prog Brain Res 137, 125–139.

Kabayiza, K.U., Masgutova, G., Harris, A., Rucchin, V., Jacob, B., Clotman, F., Taymans, J.-M., Forsyth Copenhaver, P., 2017. The Onecut Transcription Factors Regulate Differentiation and Distribution of Dorsal Interneurons during Spinal Cord Development.

Kai-Kai, M.A., Howe, R., 1991. Glutamate-immunoreactivity in the trigeminal and dorsal root ganglia, and intraspinal neurons and fibres in the dorsal horn of the rat. Histochem J 23, 171–179.

Kapitza, S., Zörner, B., Weinmann, O., Bolliger, M., Filli, L., Dietz, V., Schwab, M.E., 2012. Tail spasms in rat spinal cord injury: Changes in interneuronal connectivity. Exp Neurol 236, 179–189.

Karamehmetoğlu, Ş.S., Nas, K., Karacan, I., Sarac, A.J., Koyuncu, H., Ataoğlu, S., Erdoğan, F., 1997. Traumatic spinal cord injuries in southeast Turkey: an epidemiological study. Spinal Cord 35, 531–533.

Kathe, C., Skinnider, M.A., Hutson, T.H., Regazzi, N., Gautier, M., Demesmaeker, R., Komi, S., Ceto, S., James, N.D., Cho, N., Baud, L., Galan, K., Matson, K.J.E., Rowald, A., Kim, K., Wang, R., Minassian, K., Prior, J.O., Asboth, L., Barraud, Q., Lacour, S.P., Levine, A.J., Wagner, F., Bloch, J., Squair, J.W., Courtine, G., 2022. The neurons that restore walking after paralysis. Nature 2022 611:7936 611, 540–547.

Katz, R., Pierrot-deseilligny, E., 1982. Recurrent inhibition of α - Motoneurons in patients with upper motor neuron lesions. Brain 105, 103–124.

Keast, J.R., Stephensen, T.M., 2000. Glutamate and Aspartate Immunoreactivity in Dorsal Root Ganglion Cells Supplying Visceral and Somatic Targets and Evidence for Peripheral Axonal Transport. J. Comp. Neurol 424, 577–587.

Keefe, K.M., Sheikh, I.S., Smith, G.M., 2017. Targeting Neurotrophins to Specific Populations of Neurons: NGF, BDNF, and NT-3 and Their Relevance for Treatment of Spinal Cord Injury. Int J Mol Sci 18.

Keeler, B.E., Liu, G., Siegfried, R.N., Zhukareva, V., Murray, M., Houlé, J.D., 2012. Acute and Prolonged Hindlimb Exercise Elicits Different Gene Expression in Motoneurons than Sensory Neurons after Spinal Cord Injury. Brain Res 1438, 8.

Keller, A. V., Hainline, C., Rees, K., Krupp, S., Prince, D., Wood, B. D., Shum-Siu, A., Burke, D. A., Petruska, J. C., & Magnuson, D. S. K. (2019). Nociceptor-dependent locomotor dysfunction after clinically-modeled hindlimb muscle stretching in adult rats with spinal cord injury. *Experimental Neurology*, *318*, 267–276. https://doi.org/10.1016/J.EXPNEUROL.2019.03.006

Kernell, D., Kernell, D., 2006. 1 Why bother about motoneurones ? □ 1 . 1 . General layout and functions of the vertebrate neuromuscular system 2–5.

Khalki, L., Sadlaoud, K., Lerond, J., Coq, J.O., Brezun, J.M., Vinay, L., Coulon, P., Bras, H., 2018. Changes in innervation of lumbar motoneurons and organization of premotor network following training of transected adult rats. Exp Neurol 299, 1–14.

Khristy, W., Ali, N.J., Bravo, A.B., de Leon, R., Roy, R.R., Zhong, H., London, N.J.L., Edgerton, V.R., Tillakaratne, N.J.K., 2009. Changes in GABAA receptor subunit gamma 2 in extensor and flexor motoneurons and astrocytes after spinal cord transection and motor training. Brain Res 1273, 9–17.

Kiehn, O., Quinlan, K.A., Restrepo, C.E., Lundfald, L., Borgius, L., Talpalar, A.E., Endo, T., 2008. Excitatory components of the mammalian locomotor CPG. Brain Res Rev 57, 56–63.

Kim, J.E., Liu, B.P., Park, J.H., Strittmatter, S.M., 2004. Nogo-66 receptor prevents raphespinal and rubrospinal axon regeneration and limits functional recovery from spinal cord injury. Neuron 44, 439–451.

Ko, H. Y., Ditunno, J. F., Graziani, V., & Little, J. W. (1999). The pattern of reflex recovery during spinal shock. *Spinal Cord*, *37*(6), 402–409.

Ko, H. Y. (2018). Revisit Spinal Shock: Pattern of Reflex Evolution during Spinal Shock. *Korean Journal of Neurotrauma*, *14*(2), 47.

Koda, M., Murakami, M., Ino, H., Yoshinaga, K., Ikeda, O., Hashimoto, M., Yamazaki, M., Nakayama, C., Moriya, H., 2002. Brain-derived neurotrophic factor suppresses delayed apoptosis of oligodendrocytes after spinal cord injury in rats. J Neurotrauma 19, 777–785.

Krenz, N.R., Meakin, S.O., Krassioukov, A. V., Weaver, L.C., 1999. Neutralizing Intraspinal Nerve Growth Factor Blocks Autonomic Dysreflexia Caused By Spinal Cord Injury. The Journal of Neuroscience 19, 7405.

Krenz, N.R., Weaver, L.C., 1998. SPROUTING OF PRIMARY AFFERENT FIBERS AFTER SPINAL CORD TRANSECTION IN THE RAT.

Kucher, K., Johns, D., Maier, D., Abel, R., Badke, A., Baron, H., Thietje, R., Casha, S., Meindl, R., Gomez-Mancilla, B., Pfister, C., Rupp, R., Weidner, N., Mir, A., Schwab, M.E., Curt, A., 2018. First-in-man intrathecal application of neurite growth-promoting anti-nogo- a antibodies in acute spinal cord injury. Neurorehabil Neural Repair 32, 578–589.

Kumru, H., Murillo, N., Vidal Samso, J., Valls-Sole, J., Edwards, D., Pelayo, R., Valero-Cabre, A., Tormos, J.M., Pascual-Leone, A., 2010. Reduction of spasticity with repetitive transcranial magnetic stimulation in patients with spinal cord injury. Neurorehabil Neural Repair 24, 435–441.

Kuriyama, K., Hirouchi, M., Kimura, H., 2000. Neurochemical and Molecular Pharmacological Aspects of the GABAB Receptor. Neurochem Res 25, 1233–1239.

Lagerström, M.C., Rogoz, K., Abrahamsen, B., Persson, E., Reinius, B., Nordenankar, K., Ölund, C., Smith, C., Mendez, J.A., Chen, Z.F., Wood, J.N., Wallén-Mackenzie, Å., Kullander, K., 2010. VGLUT2-Dependent Sensory Neurons in the TRPV1 Population Regulate Pain and Itch. Neuron 68, 529–542.

Laliberte, A.M., Goltash, S., Lalonde, N.R., Bui, T.V., 2019. Propriospinal Neurons: Essential Elements of Locomotor Control in the Intact and Possibly the Injured Spinal Cord. Front Cell Neurosci 13, 512.

Lalonde, N.R., Bui, T. V., 2021. Do spinal circuits still require gating of sensory information by presynaptic inhibition after spinal cord injury? Curr Opin Physiol 19, 113–118.

Lance, J.W., 1990. What is spasticity? The Lancet.

Landry, M., Bouali-Benazzouz, R., El Mestikawy, S., Ravassard, P., Dé, F., Nagy, R., 2004. Expression of Vesicular Glutamate Transporters in Rat Lumbar Spinal Cord, with a Note on Dorsal Root Ganglia. J. Comp. Neurol 468, 380–394.

Lavrov, I., Courtine, G., Dy, C.J., van den Brand, R., Fong, A.J., Gerasimenko, Y., Zhong, H., Roy, R.R., Edgerton, V.R., 2008. Facilitation of stepping with epidural stimulation in spinal rats: Role of sensory input. Journal of Neuroscience 28, 7774–7780.

Lavrov, I., Gerasimenko, Y.P., Ichiyama, R.M., Courtine, G., Zhong, H., Roy, R.R., Reggie Edgerton, V., Reggie, V., 2006. Plasticity of Spinal Cord Reflexes After a Complete Transection in Adult Rats: Relationship to Stepping Ability. J Neuro-physiol 96, 1699–1710.

Lee, H.J., Malone, P.S., Chung, J., White, J.M., Wilson, N., Tidwell, J., Tansey, K.E., 2019. Central Plasticity of Cutaneous Afferents Is Associated with Nociceptive Hyperreflexia after Spinal Cord Injury in Rats. Neural Plast 2019.

Lee, R.H., Heckman, C.J., 1996. Influence of voltage-sensitive dendritic conductances on bistable firing and effective synaptic current in cat spinal motoneurons in vivo. J Neurophysiol 76, 2107–2110.

Lee, R.H., Heckman, C.J., 2001. Essential role of a fast persistent inward current in action potential initiation and control of rhythmic firing. J Neurophysiol 85, 472–475.

Lee, S.E., Greenough, E.K., Oancea, P., Scheinfeld, A.R., Douglas, A.M., Gaudet, A.D., 2023. Sex Differences in Pain: Spinal Cord Injury in Female and Male Mice Elicits Behaviors Related to Neuropathic Pain. J Neurotrauma 40, 833–844.

Leech, K.A., Hornby, T.G., 2017. High-Intensity Locomotor Exercise Increases Brain-Derived Neurotrophic Factor in Individuals with Incomplete Spinal Cord Injury. J Neurotrauma 34, 1240.

Leo, A., Naro, A., Molonia, F., Tomasello, P., Saccà, I., Bramanti, A., Russo, M., Bramanti, P., Quartarone, A., Calabrò, R.S., 2017. Spasticity Management: The Current State of Transcranial Neuromodulation. PM and R.

Leonardo Garcia-Ramirez, D., Ha, N. T., Bibu, S., Stachowski, N. J., & Dougherty, K. J. (2021). *Spinal Cord Injury Alters Spinal Shox2 Interneurons by Enhancing Excitatory Synaptic Input and Serotonergic Modulation While Maintaining Intrinsic Properties in Mouse*. https://doi.org/10.1523/JNEUROSCI.1576-20.2021

Li, D., Ren, Y., Xu, X., Zou, X., Fang, L., Lin, Q., 2008. Sensitization of Primary Afferent Nociceptors Induced by Intradermal Capsaicin Involves the Peripheral Release of Calcitonin Gene-Related Peptide Driven by Dorsal Root Reflexes.

Li, J.L., Xiong, K.H., Dong, Y.L., Fujiyama, F., Kaneko, T., Mizuno, N., 2003. Vesicular glutamate transporters, VGluT1 and VGluT2, in the trigeminal ganglion neurons of the rat, with special reference to coexpression. J Comp Neurol 463, 212–220.

Li, X., Murray, K., Harvey, P.J., Ballou, E.W., Bennett, D.J., 2007. Serotonin facilitates a persistent calcium current in motoneurons of rats with and without chronic spinal cord injury. J Neurophysiol 97.

Li, X., Wang, Q., Ding, J., Wang, S., Dong, C., Wu, Q., 2020. Exercise training modulates glutamic acid decarboxylase-65/67 expression through TrkB signaling to ameliorate neuropathic pain in rats with spinal cord injury. Mol Pain 16.

Li, Y., Bennett, D.J., 2003. Persistent Sodium and Calcium Currents Cause Plateau Potentials in Motoneurons of Chronic Spinal Rats.

Liem, K.F., Tremml, G., Jessell, T.M., 1997. A role for the roof plate and its resident TGFbeta-related proteins in neuronal patterning in the dorsal spinal cord. Cell 91, 127–138.

Lin, S., Li, Y., Lucas-Osma, A.M., Hari, K., Stephens, M.J., Singla, R., Heckman, C.J., Zhang, Y., Fouad, K., Fenrich, K.K., Bennett, D.J., 2019. Locomotor-related V3 interneurons initiate and coordinate muscles spasms after spinal cord injury. J Neurophysiol 121, 1352–1367.

Liu, K., Lu, Y., Lee, J.K., Samara, R., Willenberg, R., Sears-Kraxberger, I., Tedeschi, A., Park, K.K., Jin, D., Cai, B., Xu, B., Connolly, L., Steward, O., Zheng, B., He, Z., 2010. PTEN deletion enhances the regenerative ability of adult corticospinal neurons. Nature Neuroscience 2010 13:9 13, 1075–1081.

Liu, Y., Abdel Samad, O., Zhang, L., Duan, B., Tong, Q., Lopes, C., Ji, R.R., Lowell, B.B., Ma, Q., 2010. VGLUT2-dependent glutamate release from nociceptors is required to sense pain and suppress itch. Neuron 68, 543–556.

Lorach, H., Galvez, A., Spagnolo, V., Martel, F., Karakas, S., Intering, N., Vat, M., Faivre, O., Harte, C., Komi, S., Ravier, J., Collin, T., Coquoz, L., Sakr, I., Baaklini, E., Hernandez-Charpak, S.D., Dumont, G., Buschman, R., Buse, N., Denison, T., van Nes, I., Asboth, L., Watrin, A., Struber, L., Sauter-Starace, F., Langar, L., Auboiroux, V., Carda, S., Chabardes, S., Aksenova, T., Demesmaeker, R., Charvet, G., Bloch, J., Courtine, G., 2023. Walking naturally after spinal cord injury using a brain-spine interface. Nature 618, 126–133.

Lovely, R.G., Gregor, R.J., Roy, R.R., Edgerton, V.R., 1986. Effects of training on the recovery of full-weight-bearing stepping in the adult spinal cat. Exp Neurol 92, 421–435.

Lucas-Osma, A.M., Li, Y., Lin, S., Black, S., Singla, R., Fouad, K., Fenrich, K.K., Bennett, D.J., 2018. Extrasynaptic α5GABAA receptors on proprioceptive afferents produce a tonic depolarization that modulates sodium channel function in the rat spinal cord. J Neurophysiol 120, 2953–2974.

Lundström, U., Wahman, K., Seiger, Å., Gray, D.B., Isaksson, G., Lilja, M., 2017. Participation in activities and secondary health complications among persons aging with traumatic spinal cord injury. Spinal Cord 55, 367–372.

Marcantoni, M., Fuchs, A., Löw, P., Bartsch, D., Kiehn, O., Bellardita, C., 2020. Early delivery and prolonged treatment with nimodipine prevents the development of spasticity after spinal cord injury in mice. Sci Transl Med 12.

Marcantoni, M., Fuchs, A., Löw, P., Kiehn, O., Bellardita, C., 2019. Nimodipine prevents the development of spasticity after spinal cord injury. bioRxiv 639211.

Martin, J.H., 2016. Harnessing neural activity to promote repair of the damaged corticospinal system after spinal cord injury. Neural Regen Res 11, 1389–1391.

Martinez, M., Brezun, J.-M., Zennou-Azogui, Y., Baril, N., Xerri, C., 2009. Sensorimotor training promotes functional recovery and somatosensory cortical map reactivation following cervical spinal cord injury. European Journal of Neuroscience 30, 2356–2367.

Martinez, M., Rossignol, S., 2013. A dual spinal cord lesion paradigm to study spinal locomotor plasticity in the cat. Ann N Y Acad Sci 1279, 127–134.

Mathis, A., Mamidanna, P., Cury, K.M., Abe, T., Murthy, V.N., Mathis, M.W., Bethge, M., 2018. DeepLabCut: markerless pose estimation of user-defined body parts with deep learning. Nat Neurosci 21, 1281–1289.

Mathur, N., Jain, S., Kumar, N., Srivastava, A., Purohit, N., Patni, A., 2014. Spinal Cord Injury: Scenario in an Indian State. Spinal Cord 2015 53:5 53, 349–352.

May, Z., Fenrich, K.K., Dahlby, J., Batty, N.J., Torres-Espín, A., Fouad, K., 2017. Following Spinal Cord Injury Transected Reticulospinal Tract Axons Develop New Collateral Inputs to Spinal Interneurons in Parallel with Locomotor Recovery. Neural Plast 2017, 1932875.

Maynard, F.M., Karunas, R.S., Waring, W.P., 1990. Epidemiology of spasticity following traumatic spinal cord injury. Arch Phys Med Rehabil 71, 566–569.

Mazzocchio, R., Rossi, A., 1997. Involvement of spinal recurrent inhibition in spasticity. Further insight into the regulation of Renshaw cell activity. Brain 120.

Meisner, J.G., Marsh, A.D., Marsh, D.R., 2010. Loss of GABAergic interneurons in laminae I-III of the spinal cord dorsal horn contributes to reduced GABAergic tone and neuropathic pain after spinal cord injury. J Neurotrauma 27, 729–737.

Mende, M., Fletcher, E. v., Belluardo, J.L., Pierce, J.P., Bommareddy, P.K., Weinrich, J.A., Kabir, Z.D., Schierberl, K.C., Pagiazitis, J.G., Mendelsohn, A.I., Francesconi, A., Edwards, R.H., Milner, T.A., Rajadhyaksha, A.M., van Roessel, P.J., Mentis, G.Z., Kaltschmidt, J.A., 2016. Sensory-Derived Glutamate Regulates Presynaptic Inhibitory Terminals in Mouse Spinal Cord. Neuron 90, 1189–1202.

Metz, K., Matos, I. C., Li, Y., Afsharipour, B., Thompson, C. K., Negro, F., Quinlan, K. A., Bennett, D. J., & Gorassini, M. A. (2023). Facilitation of sensory transmission to motoneurons during cortical or sensory-evoked primary afferent depolarization (PAD) in humans. *Journal of Physiology*, *601*(10), 1897–1924. https://doi.org/10.1113/JP284275

Michael, F.M., Patel, S.P., Rabchevsky, A.G., 2019. Intraspinal Plasticity Associated With the Development of Autonomic Dysreflexia After Complete Spinal Cord Injury. Front Cell Neurosci 13.

Miller, R.J., Jung, H., Bhangoo, S.K., White, F.A., 2009. Cytokine and Chemokine Regulation of Sensory Neuron Function. Handb Exp Pharmacol 194, 417.

Mills, C.D., Hulsebosch, C.E., 2002. Increased expression of metabotropic glutamate receptor subtype 1 on spinothalamic tract neurons following spinal cord injury in the rat. Neurosci Lett 319, 59–62.

Mizuguchi, R., Kriks, S., Cordes, R., Gossler, A., Ma, Q., Goulding, M., 2006. Ascl1 and Gsh1/2 control inhibitory and excitatory cell fate in spinal sensory interneurons.

Mogil, J.S., 2012. Sex differences in pain and pain inhibition: multiple explanations of a controversial phenomenon. Nat Rev Neurosci 13, 859–866.

Morris, J.L., Ko¨nig, P., Ko¨nig, K., Shimizu, T., Jobling, P., Gibbins, I.L., 2005. Most Peptide-Containing Sensory Neurons Lack Proteins for Exocytotic Release and Vesicular Transport of Glutamate. J. Comp. Neurol 483, 1–16.

Müller, T., Brohmann, H., Pierani, A., Heppenstall, P.A., Lewin, G.R., Jessell, T.M., Birchmeier, C., 2002. The homeodomain factor Lbx1 distinguishes two major programs of neuronal differentiation in the dorsal spinal cord. Neuron 34, 551–562.

Munson, J.B., Foehring, R.C., Lofton, S.A., Zengel, J.E., Sypert, G.W., 1986. Plasticity of medial gastrocnemius motor units following cordotomy in the cat. J Neurophysiol 55, 619–634.

Murray, K.C., Nakae, A., Stephens, M.J., Rank, M., D'Amico, J., Harvey, P.J., Li, X., Harris, R.L.W., Ballou, E.W., Anelli, R., Heckman, C.J., Mashimo, T., Vavrek, R., Sanelli, L., Gorassini, M.A., Bennett, D.J., Fouad, K., 2010. Recovery of motoneuron and locomotor function after spinal cord injury depends on constitutive activity in 5-HT2C receptors. Nat Med 16, 694–700.

Nakajima, H., Uchida, K., Yayama, T., Kobayashi, S., Guerrero, A.R., Furukawa, S., Baba, H., 2010. Targeted retrograde gene delivery of brain-derived neurotrophic factor suppresses apoptosis of neurons and oligodendroglia after spinal cord injury in rats. Spine (Phila Pa 1976) 35, 497–504.

Nam, K.Y., Kim, H.J., Kwon, B.S., Park, J.W., Lee, H.J., Yoo, A., 2017. Robot-assisted gait training (Lokomat) improves walking function and activity in people with spinal cord injury: a systematic review. J Neuroeng Rehabil 14, 1–13.

Nas, K., Yazmalar, L., Şah, V., Aydin, A., Öneş, K., 2015. Rehabilitation of spinal cord injuries. World J Orthop 6, 8.

Neumann, S., Skinner, K., Basbaum, A.D., 2005. Sustaining intrinsic growth capacity of adult neurons promotes spinal cord regeneration. Proc Natl Acad Sci U S A 102, 16848–16852.

Neve, R.L., Finch, E.A., Bird, E.D., Benowitz, L.I., 1988. Growth-associated protein GAP-43 is expressed selectively in associative regions of the adult human brain. Proc Natl Acad Sci U S A 85, 3638–3642.

Nielsen, J., Petersen, N., Crone, C., 1995. Changes in transmission across synapses of, Brain.

Oliveira, A.L.R., Hydling, F., Olsson, E., Shi, T., Edwards, R.H., Fujiyama, F., Kaneko, T., Hökfelt, T., Cullheim, S., Meister, B., 2003. Cellular localization of three vesicular glutamate transporter mRNAs and proteins in rat spinal cord and dorsal root ganglia. Synapse 50, 117–129.

Ondarza, A.B., Ye, Z., Hulsebosch, C.E., 2003. Direct evidence of primary afferent sprouting in distant segments following spinal cord injury in the rat: Colocalization of GAP-43 and CGRP. Exp Neurol 184.

Pandyan, A.D., Gregoric, M., Barnes, M.P., Wood, D., Van Wijck, F., Burridge, J., Hermens, H., Johnson, G.R., 2005. Spasticity: Clinical perceptions, neurological realities and meaningful measurement. Disabil Rehabil 27, 2–6.

Pearson, K.G., 2008. Role of sensory feedback in the control of stance duration in walking cats. Brain Res Rev 57, 222–227.

Persson, S., Boulland, J.L., Aspling, M., Larsson, M., Fremeau, R.T., Edwards, R.H., Storm-Mathisen, J., Chaudhry, F.A., Broman, J., 2006. Distribution of vesicular glutamate transporters 1 and 2 in the rat spinal cord, with a note on the spinocervical tract. Journal of Comparative Neurology 497, 683–701.

Pfaff, S.L., Mendelsohn, M., 1996. Requirement for LIM Homeobox Gene Isl1 in Motor Neuron Generation Reveals a Motor Neuron-Dependent Step in Interneuron Differentiation. Cell 84, 309–320.

Pivetta, C., Esposito, M.S., Sigrist, M., Arber, S., 2014. Motor-circuit communication matrix from spinal cord to brainstem neurons revealed by developmental origin. Cell 156, 537–548.

Plantier, V., Sanchez-Brualla, I., Dingu, N., Brocard, C., Liabeuf, S., Gackière, F., Brocard, F., 2019. Calpain fosters the hyperexcitability of motoneurons after spinal cord injury and leads to spasticity. Elife 8.

Pocratsky, A.M., Shepard, C.T., Morehouse, J.R., Burke, D.A., Riegler, A.S., Hardin, J.T., Beare, J.E., Hainline, C., States, G.J.R., Brown, B.L., Whittemore, S.R., Magnuson, D.S.K., 2020. Long ascending propriospinal neurons provide flexible, context-specific control of interlimb coordination. Elife 9, 1–24.

Qian, Y., Shirasawa, S., Chen, C.L., Cheng, L., Qiufu, M., 2002. Proper development of relay somatic sensory neurons and D2/D4 interneurons requires homeobox genes Rnx/Tlx-3 and Tlx-1. Genes Dev 16, 1220–1233.

R. Eid, S., 2011. Therapeutic Targeting of TRP Channels - The TR(i)P to Pain Relief. Curr Top Med Chem 11, 2118–2130.

Rank, M.M., Flynn, J.R., Galea, M.P., Callister, R., Callister, R.J., 2015. Electrophysiological characterization of spontaneous recovery in deep dorsal horn interneurons after incomplete spinal cord injury. Exp Neurol 271, 468–478.

Reggie Edgerton, V., Courtine, G., Gerasimenko, Y.P., Lavrov, I., Ichiyama, R.M., Fong, A.J., Cai, L.L., Otoshi, C.K., Tillakaratne, N.J.K., Burdick, J.W., Roy, R.R., 2007. doi:10.1016/j.brainresrev.2007.09.002.

Rexed, B., 1952. The cytoarchitectonic organization of the spinal cord in the cat. J Comp Neurol 96, 415–495.

Rexed, B., 1954. A cytoarchitectonic atlas of the spinal cord in the cat. J Comp Neurol 100, 297–379.

Rosen, S., Ham, B., Mogil, J.S., 2017. Sex differences in neuroimmunity and pain. J Neurosci Res 95, 500–508.

Rosenzweig, E.S., Courtine, G., Jindrich, D.L., Brock, J.H., Ferguson, A.R., Strand, S.C., Nout, Y.S., Roy, R.R., Miller, D.M., Beattie, M.S., Havton, L.A., Bresnahan, J.C., Edgerton, V.R., Tuszynski, M.H., 2010. Extensive spontaneous plasticity of corticospinal projections after primate spinal cord injury. Nat Neurosci 13, 1505–1512.

Rossignol, S., 2006. Plasticity of connections underlying locomotor recovery after central and/or peripheral lesions in the adult mammals. Philosophical Transactions of the Royal Society B: Biological Sciences 361, 1647.

Rossignol, S., Frigon, A., 2011. Recovery of Locomotion After Spinal Cord Injury: Some Facts and Mechanisms. Annu Rev Neurosci 34, 413–440.

Rowald, A., Komi, S., Demesmaeker, R., Baaklini, E., Hernandez-Charpak, S.D., Paoles, E., Montanaro, H., Cassara, A., Becce, F., Lloyd, B., Newton, T., Ravier, J., Kinany, N., D'Ercole, M., Paley, A., Hankov, N., Varescon, C., McCracken, L., Vat, M., Caban, M., Watrin, A., Jacquet, C., Bole-Feysot, L., Harte, C., Lorach, H., Galvez, A., Tschopp, M., Herrmann, N., Wacker, M., Geernaert, L., Fodor, I., Radevich, V., Van Den Keybus, K., Eberle, G., Pralong, E., Roulet, M., Ledoux, J.B., Fornari, E., Mandija, S., Mattera, L., Martuzzi, R., Nazarian, B., Benkler, S., Callegari, S., Greiner, N., Fuhrer, B., Froeling, M., Buse, N., Denison, T., Buschman, R., Wende, C., Ganty, D., Bakker, J., Delattre, V.,

Lambert, H., Minassian, K., van den Berg, C.A.T., Kavounoudias, A., Micera, S., Van De Ville, D., Barraud, Q., Kurt, E., Kuster, N., Neufeld, E., Capogrosso, M., Asboth, L., Wagner, F.B., Bloch, J., Courtine, G., 2022. Activity-dependent spinal cord neuromodulation rapidly restores trunk and leg motor functions after complete paralysis. Nat Med 28, 260–271.

Roy, A., Francius, C., Rousso, D.L., Seuntjens, E., Debruyn, J., Luxenhofer, G., Huber, A.B., Huylebroeck, D., Novitch, B.G., Clotman, F., 2012. Onecut transcription factors act upstream of Isl1 to regulate spinal motoneuron diversification. Development 139, 3109–3119.

Roy, F.D., Yang, J.F., Gorassini, M.A., 2010. Afferent regulation of leg motor cortex excitability after incomplete spinal cord injury. J Neurophysiol 103, 2222–2233.

Roy, R.R., Harkema, S.J., Edgerton, V.R., 2012. Basic concepts of activity-based interventions for improved recovery of motor function after spinal cord injury. Arch Phys Med Rehabil 93, 1487–1497.

Rudomin, P., 1999. Presynaptic selection of afferent inflow in the spinal cord. J Physiol Paris 93, 329–347.

Rudomin, P., 2009. In search of lost presynaptic inhibition. Exp Brain Res 196, 139–151.

Rudomin, P., Jimenez, I., Solodkin, M., Duenas, S., 1983. Sites of action of segmental and descending control of transmission on pathways mediating PAD of Ia- and Ib-afferent fibers in cat spinal cord. https://doi.org/10.1152/jn.1983.50.4.743 50, 743–769.

Rudomin, P., Schmidt, R.F., 1999. Presynaptic inhibition in the vertebrate spinal cord revisited. Exp Brain Res 129, 1–37.

Sadlaoud, K., Khalki, L., Brocard, F., Vinay, L., Boulenguez, P., Bras, H., 2020. Alteration of glycinergic receptor expression in lumbar spinal motoneurons is involved in the mechanisms underlying spasticity after spinal cord injury.

Scherrer, G., Low, S.A., Wang, X., Zhang, J., Yamanaka, H., Urban, R., Solorzano, C., Harper, B., Hnaskod, T.S., Edwards, R.H., Basbaum, A.I., 2010. VGLUT2 expression in primary afferent neurons is essential for normal acute pain and injury-induced heat hypersensitivity. Proc Natl Acad Sci U S A 107, 22296–22301.

Shah, P.K., Garcia-Alias, G., Choe, J., Gad, P., Gerasimenko, Y., Tillakaratne, N., Zhong, H., Roy, R.R., Edgerton, V.R., 2013. Use of quadrupedal step training to re-engage spinal interneuronal networks and improve locomotor function after spinal cord injury. Brain 136, 3362–3377.

Sharif-Alhoseini, M., Khormali, M., Rezaei, M., Safdarian, M., Hajighadery, A., Khalatbari, M.M., Safdarian, M., Meknatkhah, S., Rezvan, M., Chalangari, M., Derakhshan, P., Rahimi-Movaghar, V., 2017. Animal models of spinal cord injury: a systematic review. Spinal Cord 55, 714–721.

Sherrington, C.S., Laslett, E.E., 1903. Observations on some spinal reflexes and the interconnection of spinal segments. J Physiol 29, 58.

Shiers, S., Klein, R.M., Price, T.J., 2020. Quantitative differences in neuronal subpopulations between mouse and human dorsal root ganglia demonstrated with RNAscope in situ hybridization. Pain 161, 2410–2424.

Shimizu-Okabe, C., Kobayashi, S., Kim, J., Kosaka, Y., Sunagawa, M., Okabe, A., Takayama, C., 2022. Developmental Formation of the GABAergic and Glycinergic Networks in the Mouse Spinal Cord. International Journal of Molecular Sciences 2022, Vol. 23, Page 834 23, 834.

Shuba, Y.M., 2021. Beyond Neuronal Heat Sensing: Diversity of TRPV1 Heat-Capsaicin Receptor-Channel Functions. Front Cell Neurosci 14, 612480.

Sławińska, U., Majczyński, H., Dai, Y., Jordan, L.M., 2012. The upright posture improves plantar stepping and alters responses to serotonergic drugs in spinal rats. J Physiol 590, 1721–36.

Sławińska, U., Majczyński, H., Dai, Y., Jordan, L.M., 2012c. The upright posture improves plantar stepping and alters responses to serotonergic drugs in spinal rats. J Physiol 590, 1721–1736.

Smith, H.S., Barton, A.E., 2000. Tizanidine in the management of spasticity and musculoskeletal complaints in the palliative care population. Am J Hosp Palliat Care 17, 50–58.

Smith, J.S., Anderson, R., Pham, T., Bhatia, N., Steward, O., Gupta, R., 2010. Role of early surgical decompression of the intradural space after cervical spinal cord injury in an animal model. Journal of Bone and Joint Surgery 92, 1206–1214.

Stepien, A.E., Tripodi, M., Arber, S., 2010. Monosynaptic rabies virus reveals premotor network organization and synaptic specificity of cholinergic partition cells. Neuron 68, 456–472.

Szentágothai, J., 1964. NEURONAL AND SYNAPTIC ARRANGEMENT IN THE SUBSTANTIA GELATINOSA ROLANDI. J Comp Neurol 122, 219–239.

Taccola, G., Sayenko, D., Gad, P., Gerasimenko, Y., Edgerton, V.R., 2018. And yet it moves: Recovery of volitional control after spinal cord injury. Prog Neurobiol 160, 64–81.

Takeoka, A., 2020. Proprioception: Bottom-up directive for motor recovery after spinal cord injury. Neurosci Res 154, 1–8.

Takeoka, A., Arber, S., 2019. Functional Local Proprioceptive Feedback Circuits Initiate and Maintain Locomotor Recovery after Spinal Cord Injury. Cell Rep 27, 71-85.e3.

Takeoka, A., Vollenweider, I., Courtine, G., Arber, S., 2014. Muscle spindle feedback directs locomotor recovery and circuit reorganization after spinal cord injury. Cell 159, 1626–1639.

Thallmair, M., Metz, G.A.S., Z'Graggen, W.J., Raineteau, O., Kartje, G.L., Schwab, M.E., 1998. Neurite growth inhibitors restrict plasticity and functional recovery following corticospinal tract lesions. Nat. Neurosci. 1, 124–131.

Thaweerattanasinp, T., Birch, D., Jiang, M. C., Tresch, M. C., Bennett, D. J., Heckman, C. J., & Tysseling, V. M. (2020). Bursting interneurons in the deep dorsal horn develop increased excitability and sensitivity to serotonin after chronic spinal injury. *J Neurophysiol*, *123*, 1657–1670. https://doi.org/10.1152/jn.00701.2019.

Theiss, R.D., Kuo, J.J., Heckman, C.J., 2007. Persistent inward currents in rat ventral horn neurones. Journal of Physiology 580, 507–522.

Thor, K.B., Roppolo, J.R., Kawatani, M., Erdman, S., deGroat, W.C., 1994. Plasticity in spinal opioid control of lower urinary tract function in paraplegic cats. Neuroreport 5, 1673–1678.

Tillakaratne, N.J.K., De Leon, R.D., Hoang, T.X., Roy, R.R., Edgerton, V.R., Tobin, A.J., 2002. Use-Dependent Modulation of Inhibitory Capacity in the Feline Lumbar Spinal Cord. Journal of Neuroscience 22, 3130–3143.

Tillakaratne, N.J.K., Mouria, M., Ziv, N.B., Roy, R.R., Edgerton, V.R., Tobin, A.J., 2000. Increased expression of glutamate decarboxylase (GAD67) in feline lumbar spinal cord after complete thoracic spinal cord transection. J Neurosci Res 60, 219–230.

Todd, A.J., Hughes, D.I., Polgár, E., Nagy, G.G., Mackie, M., Ottersen, O.P., Maxwell, D.J., 2003. The expression of vesicular glutamate transporters VGLUT1 and VGLUT2 in neurochemically defined axonal populations in the rat spinal cord with emphasis on the dorsal horn. Eur J Neurosci 17, 13–27.

Tong, Q., Ma, J., Kirchgessner, A.L., 2001. Vesicular glutamate transporter 2 in the brain-gut axis. Neuroreport 12, 3929–3934.

Torres-Espín, A., Beaudry, E., Fenrich, K., Fouad, K., 2018. Rehabilitative Training in Animal Models of Spinal Cord Injury. J Neurotrauma 35, 1970–1985.

Valtschanoff, J.G., Phend, K.D., Bernardi, P.S., Weinberg, R.J., Rustioni, A., 1994. Amino acid immunocytochemistry of primary afferent terminals in the rat dorsal horn. J Comp Neurol 346, 237–252.

van den Brand, R., Heutschi, J., Barraud, Q., DiGiovanna, J., Bartholdi, K., Huerlimann, M., Friedli, L., Vollenweider, I., Moraud, E.M., Duis, S., Dominici, N., Micera, S., Musienko, P., Courtine, G., 2012. Restoring voluntary control of locomotion after paralyzing spinal cord injury. Science 336, 1182–5.

Vavrek, R., Girgis, J., Tetzlaff, W., Hiebert, G.W., Fouad, K., 2006. BDNF promotes connections of corticospinal neurons onto spared descending interneurons in spinal cord injured rats. Brain 129, 1534–45.

Wagner, F.B., Mignardot, J.B., Le Goff-Mignardot, C.G., Demesmaeker, R., Komi, S., Capogrosso, M., Rowald, A., Seáñez, I., Caban, M., Pirondini, E., Vat, M., McCracken, L.A., Heimgartner, R., Fodor, I., Watrin, A., Seguin, P., Paoles, E., Van Den Keybus, K., Eberle, G., Schurch, B., Pralong, E., Becce, F., Prior, J., Buse, N., Buschman, R., Neufeld, E., Kuster, N., Carda, S., von Zitzewitz, J., Delattre, V., Denison, T., Lambert, H., Minassian, K., Bloch, J., Courtine, G., 2018. Targeted neurotechnology restores walking in humans with spinal cord injury. Nature 563, 65–93.

Wagstaff, A.J., Bryson, H.M., 1997. Tizanidine. A review of its pharmacology, clinical efficacy and tolerability in the management of spasticity associated with cerebral and spinal disorders. Drugs 53, 435–452.

Walder, R.Y., Radhakrishnan, R., Loo, L., Rasmussen, L.A., Mohapatra, D.P., Wilson, S.P., Sluka, K.A., 2012. TRPV1 is important for mechanical and heat sensitivity in uninjured animals and development of heat hypersensitivity after muscle inflammation. Pain 153, 1664.

Wanaka, A., Shiotani, Y., Kiyama, H., Matsuyama, T., Kamada, T., Shiosaka, S., Tohyama, M., 1987. Glutamate-like immunoreactive structures in primary sensory neurons in the rat detected by a specific antiserum against glutamate. Exp Brain Res 65, 691–694.

Ward, A.B., Aguilar, M., De Beyl, Z., Gedin, S., Kanovsky, P., Molteni, F., Wissel, J., Yakovleff, A., 2003. Use of botulinum toxin type A in management of adult spasticity--a European consensus statement. J Rehabil Med 35, 98–99.

Watkins, J.C., 2000. l-Glutamate as a Central Neurotransmitter: Looking Back. Biochem Soc Trans 28, 297–310.

Weaver, L.C., Verghese, P., Bruce, J.C., Fehlings, M.G., Krenz, N.R., Marsh, D.R., 2001. Autonomic dysreflexia and primary afferent sprouting after clip-compression injury of the rat spinal cord. J Neurotrauma 18, 1107–1119.

Widerstrom-Noga, E.G., Felipe-Cuervo, E., Yezierski, R.P., 2001. Chronic pain after spinal injury: Interference with sleep and daily activities. Arch Phys Med Rehabil 82, 1571–1577.

Willis, W.;Coggeshall, R., 1991. Sensory Mechanisms of the Spinal Cord: Volume 1 Primary Afferent Neurons and ... - William D. Willis Jr., Richard E. Coggeshall - Google Books [WWW Document]. URL https://books.google.ca/books?hl=en&lr=&id=JP_2BwAAQBAJ&oi=fnd&pg=PA1&ots=hOBNaIVUsm&sig=ZWfuZs_3Jd60HvfGtyp4fvNnvwc&redir_esc=y#v=onepage&q&f=false (accessed 4.29.21).

Willis, W.D., Coggeshall, R.E., 2004. Sensory Mechanisms of the Spinal Cord. Sensory Mechanisms of the Spinal Cord.

Windhorst, U., 2007. Muscle proprioceptive feedback and spinal networks. Brain Res Bull 73, 155–202.

Wolpaw, J.R., 2010. What can the spinal cord teach us about learning and memory? Neuroscientist 16, 532–549.

Wu, H., Petitpré, C., Fontanet, P., Sharma, A., Bellardita, C., Quadros, R.M., Jannig, P.R., Wang, Y., Heimel, J.A., Cheung, K.K.Y., Wanderoy, S., Xuan, Y., Meletis, K., Ruas, J., Gurumurthy, C.B., Kiehn, O., Hadjab, S., Lallemend, F., 2021. Distinct subtypes of proprioceptive dorsal root ganglion neurons regulate adaptive proprioception in mice. Nature Communications 2021 12:1 12, 1–13.

Xu, Y., Lopes, C., Qian, Y., Liu, Y., Cheng, L., Goulding, M., Turner, E.E., Lima, D., Ma, Q., 2008. Tlx1 and Tlx3 Coordinate Specification of Dorsal Horn Pain-Modulatory Peptidergic Neurons. Journal of Neuroscience 28, 4037–4046.

Yates, C., Charlesworth, A., Allen, S.R., Reese, N.B., Skinner, R.D., Garcia-Rill, E., 2008. The onset of hyperreflexia in the rat following complete spinal cord transection. Spinal Cord 46, 798–803.

Yates, C., Garrison, K., Reese, N.B., Charlesworth, A., Garcia-Rill, E., 2011. Novel mechanism for hyperreflexia and spasticity. In: Progress in Brain Research. Elsevier B.V., pp. 167–180.

Yelnik, A.P., Simon, O., Bensmail, D., Chaleat-Valayer, E., Decq, P., Dehail, P., Quentin, V., Marque, P., Parratte, B., Pellas, F., Rousseaux, M., Trocello, J.M., Uzzan, M., Dumarcet, N., 2009. Drug treatments for spasticity. Ann Phys Rehabil Med 52, 746–756.

Ying, Z., Roy, R.R., Edgerton, V.R., Gómez-Pinilla, F., 2005. Exercise restores levels of neurotrophins and synaptic plasticity following spinal cord injury. Exp Neurol 193, 411–419.

Yoshimura, M., Jessell, T., 1990. Amino acid-mediated EPSPs at primary afferent synapses with substantia gelatinosa neurones in the rat spinal cord. J Physiol 430, 315–335.

Yoshizaki, S., Yokota, K., Kubota, K., Saito, T., Tanaka, M., Konno, D. jiro, Maeda, T., Matsumoto, Y., Nakashima, Y., Okada, S., 2020. The beneficial aspects of spasticity in relation to ambulatory ability in mice with spinal cord injury. Spinal Cord 58, 537–543.

Yu, L.C., Hansson, P., Lundeberg, T., 1994. The calcitonin gene-related peptide antagonist CGRP8-37 increases the latency to withdrawal responses in rats. Brain Res 653, 223–230.

Zhang, H., Liu, Yaping, Zhou, K., Wei, W., Liu, Yaobo, 2021. Restoring Sensorimotor Function Through Neuromodulation After Spinal Cord Injury: Progress and Remaining Challenges. Front Neurosci 15.

Zhang, Y., Narayan, S., Geiman, E., Lanuza, G.M., Velasquez, T., Shanks, B., Akay, T., Dyck, J., Pearson, K., Gosgnach, S., Fan, C.M., Goulding, M., 2008. V3 spinal neurons establish a robust and balanced locomotor rhythm during walking. Neuron 60, 84–96.

Zholudeva, L. V., Abraira, V.E., Satkunendrarajah, K., McDevitt, T.C., Goulding, M.D., Magnuson, D.S.K., Lane, M.A., 2021. Spinal Interneurons as Gatekeepers to Neuroplasticity after Injury or Disease. The Journal of Neuroscience 41, 845.

Zhou, L., Baumgartner, B.J., Hill-Felberg, S.J., McGowen, L.R., Shine, H.D., 2003. Neurotrophin-3 Expressed In Situ Induces Axonal Plasticity in the Adult Injured Spinal Cord. Journal of Neuroscience 23, 1424–1431.

Ziemlińska, E., Kügler, S., Schachner, M., Wewiór, I., Czarkowska-Bauch, J., Skup, M., 2014. Overexpression of BDNF increases excitability of the lumbar spinal network and leads to robust early locomotor recovery in completely spinalized rats. PLoS One 9.

Zimmerman, Amanda L, Kovatsis, E.M., Poszgai, R.Y., Tasnim, A., Zhang, Q., Ginty, D.D., 2019. Distinct modes of presynaptic inhibition of cutaneous afferents and their functions in behavior HHS Public Access. Neuron 102, 420–434.

Živković, V., Nikolić, S., 2014. Head injuries in falls from a standing height: do fractures of the orbital roof matter? A prospective autopsy study. Forensic Sci Med Pathol 10, 483–486.

Zörner, B., Bachmann, L.C., Filli, L., Kapitza, S., Gullo, M., Bolliger, M., Starkey, M.L., Röthlisberger, M., Gonzenbach, R.R., Schwab, M.E., 2014. Chasing central nervous system plasticity: the brainstem's contribution to locomotor recovery in rats with spinal cord injury. Brain 137, 1716–1732.